

# The Wildland Firefighter Respiratory Protection Device

## *First Respire Team*

Jack Adema  
Manufacturing Engineering

Payton Mayer  
Electrical Engineering

Tommy Ozawa  
General Engineering

Oliver Pilon  
Biomedical Engineering

Xaviera Pons  
Electrical Engineering

Calder Wood  
Mechanical Engineering

## **Advisor**

Dr. iian Black  
Biomedical Engineering  
[iiblack@calpoly.edu](mailto:iiblack@calpoly.edu)

## **Sponsors**

Dr. Lily Laiho  
Biomedical Engineering

Dr. Matthew Zoerb  
Chemistry and Biochemistry  
[mzoerb@calpoly.edu](mailto:mzoerb@calpoly.edu)

## **Funding**

The Wildland Urban Interface (WUI) FIRE Institute at Cal Poly



### **Statement of Disclaimer**

Since this project is a result of a class assignment, it has been graded and accepted as fulfillment of the course requirements. Acceptance does not imply technical accuracy or reliability. Any use of information in this report is done at the risk of the user. These risks may include catastrophic failure of the device or infringement of patent or copyright laws. California Polytechnic State University at San Luis Obispo and its staff cannot be held liable for any use or misuse of the project.



## Table of Contents

<b>Statement of Disclaimer</b>	<b>2</b>
<b>Table of Contents</b>	<b>3</b>
<b>List of Tables</b>	<b>5</b>
<b>List of Figures</b>	<b>6</b>
<b>List of Nomenclature</b>	<b>8</b>
<b>Executive Summary</b>	<b>9</b>
<b>1. Introduction</b>	<b>10</b>
1.1. Objectives	11
<b>2. Background</b>	<b>14</b>
<b>3. Design Development</b>	<b>18</b>
3.2 Concept Selection	22
3.2.1 Air Filter Subsystem	22
3.2.2 Air Delivery Subsystem	23
3.2.3 Power Source	24
3.3. Proof of Concept Analysis	24
3.4. Selected Concept Prototyping	32
3.4.1 Air Delivery Prototyping	32
3.4.2 Filter Prototyping	35
3.4.3 Battery Prototyping	36
<b>4. Description of Final Design</b>	<b>36</b>
4.1. Filter Design	41
4.2. Electrical Design	42
4.3. Mechanical Design	45
4.4. Analysis Results	46
4.5. Cost Breakdown	49
4.6. Safety, Maintenance, and Repair Considerations	49
4.6.1. Safety	50
4.6.2. Maintenance and Repair	51
4.6.3 Sustainability	52
<b>5. Product Realization</b>	<b>54</b>
5.1. Manufacturing Process	54
5.1.1. Air Curtain Assembly	55
5.1.2. Filter Assembly	58
5.1.3. Fan Assembly	59
5.2. Future Manufacturing Recommendations	59
5.3. Cost Estimation for Future Production	60
<b>6. Design Verification and Testing</b>	<b>61</b>
6.1. Test Stand for Filtration Testing	61
6.1.1. Sensor Configuration in Test Stand	63
6.1.2. Sensor Data Utilization in Test Stand	64
6.2 Test Procedure	64



6.2.1 CFM Testing	65
6.2.2 Weight Testing	67
6.2.3 Testing Duration of Use	68
6.2.4 Heat Resistance Testing	69
6.2.5 Donning/Doffing Time Testing	70
6.2.6 Testing for Adjustable Sizing	71
6.2.7 Communication Interference Testing	71
6.2.8 Field of View (FOV) Testing	72
6.2.9 Range of Motion (ROM) Testing	72
6.2.10 Air Cooling Test	73
6.2.11 Filtration Quality Testing	74
6.2.12 Fire Simulation Test	79
6.2.13 Gear Compatibility Test	83
<b>7. Conclusions and Recommendations</b>	<b>86</b>
<b>8. Acknowledgements</b>	<b>90</b>
<b>Appendix A – References</b>	<b>91</b>
<b>Appendix B – Contact Information</b>	<b>94</b>
<b>Appendix C - QFD: House of Quality</b>	<b>95</b>
<b>Appendix D - Pugh Matrices</b>	<b>96</b>
<b>Appendix E - Customer Requirements</b>	<b>99</b>
<b>Appendix F - Technical Specifications</b>	<b>100</b>
<b>Appendix G – Final Drawings</b>	<b>102</b>
<b>Appendix H – Vendor Supplied Specifications and Datasheets</b>	<b>133</b>
<b>Appendix I – Air Curtain Calculations Excel</b>	<b>135</b>
<b>Appendix J – Gantt Chart</b>	<b>137</b>
<b>Appendix K – Safety Checklist</b>	<b>138</b>
<b>Appendix K – SGP30 Sensor Code for Fire Simulation Test</b>	<b>138</b>
<b>Appendix L – SCD-40 Sensor Code for Fire Simulation Test</b>	<b>141</b>

## **List of Tables**

Table 1: Table 8.11.4 From NFPA 1984

Table 2: Values for airflow calculations.

Table 3. Cost Analysis

Table 4a. Test Description, Standards, and Expected Results

Table 4b. Requirements Testing Record

## List of Figures

- Figure 1: From NFPA 1984: Fig 8.1.4.1 Non-Conductive Head Form
- Figure 2: A wildland firefighter from CAL FIRE with standard engine crew equipment
- Figure 3: Rate of particulate matter after going through the respiratory protection device.
- Figure 4: Concentrations of (a) major and (b) minor gases downstream of the respiratory protection device.
- Figure 5: Parker Pumper Helmet Co. device.
- Figure 6: (a) Diagram of Air Curtain from RU2407567C1 showing a basic idea of how to supply air to protect the user's face. (3. Fans, 7. Air Flow, 8. Attachment) (b) Diagram of a smoke proof helmet from CN209915110U showing the filter and pump system.
- Figure 7: Image showing the difference between an Axial and Centrifugal fan.
- Figure 8: Face shield measurements.
- Figure 9.1: Air curtain strength hand calculations.
- Figure 9.2: Air curtain strength hand calculations.
- Figure 9.3: Air curtain strength hand calculations.
- Figure 10: Required magnet strength hand calculations.
- Figure 11 & 12: SOLIDWORKS air curtain assembly model and junction model. First Prototype
- Figure 13: SOLIDWORKS air curtain assembly model. Second Prototype
- Figure 14: SOLIDWORKS air curtain assembly model. Third Prototype
- Figure 15: SOLIDWORKS air curtain assembly model. No Cooling Prototype
- Figure 16: HEPA filter design
- Figure 17: Initial Sketches of Final Air Curtain Design Concept
- Figure 18: Final CAD model of air curtain portion.
- Figure 19: CAD model for magnetic attachment system.
- Figure 20: (a) Initial sketch of full assembly final design concept and (b) finalized CAD model of design.
- Figure 21: 3M Versaflo Heavy Duty Breathing Tube
- Figure 22: 3D printed PAPR hose ends.
- Figure 23: PUREBURG B-D02H Filter with activated charcoal cloth liner.
- Figure 24: Electrical Circuit of Fan Motor Connected to Full System
- Figure 25: Full Assembly Spread Out
- Figure 26: SCD-40 Sensor Measuring Temperature and Humidity
- Figure 26: SOLIDWORKS model of the air curtain design (minus the air holes and magnetic attachment).
- Figure 27: SOLIDWORKS model of air curtain helmet attachment showing inside of junction
- Figure 28: Ametek Microjammer testing
- Figure 29: Minimum air curtain flowrate as a function of wind speed and total outlet area.
- Figure 30: 3D printer used for various components of air curtain assembly
- Figure 31: Air curtain assembly attached to helmet with magnetic attachment system.
- Figure 32: Exploded view of assembly of components K through O.
- Figure 33: Exploded view of magnetic attachment system assembly of components A through E.
- Figure 34: Helmet attachment pieces bolted on with nylon hardware.
- Figure 35: Heat shield attached to air curtain using zip ties.
- Figure 36: Showing the final filter assembly, with the filter cap printed white PLA, and the fan cap printed blue PLA, on either side of the filter combination.
- Figure 37: Scaled Cost Simulation (500 units)

- Figure 38. Picture of the test assembly
- Figure 39: Schematic diagram of the filtration test setup showing the placement of SGP30 and SCD40 sensors on the inlet and outlet sides of the filter for measuring initial gas concentrations.
- Figure 40: Picture of fan testing set up, showing the single nozzle outlet for the 2-person fan.
- Figure 41 & 42 Left: Full final assembly weight testing. Right: Final hose weight testing.
- Figure 43. Temperature Difference During The Cooling Test with Test Subject in Resting Position
- Figure 44. Temperature Difference During The Cooling Test with Test Subject Running
- Figure 45: Picture of the test stand set up for the second test with the bandana, with the Filter Standin in place to hold the bandana in place for testing.
- Figure 46: TVOC Concentration in parts per billion over the duration of the test, with a normalizing period before and after the exposure of each gas.
- Figure 47: eCO<sub>2</sub> Concentration during filter test with a normalized portion before and after gas exposure.
- Figure 48: CO<sub>2</sub> Concentration dissipation data from SCD40 sensor
- Figure 49: CO<sub>2</sub> Concentration accumulation data from SCD40 sensor
- Figure 50: Test Equipment: Channel, Head Form, Tape, and Test Stand
- Figure 51: TVOC and eCO<sub>2</sub> Exposure Levels with No Face Protection Worn
- Figure 52: TVOC and eCO<sub>2</sub> Levels with Double Tube Design
- Figure 53 : eCO<sub>2</sub> Levels with Double Tube Design
- Figure 54 : TVOC and eCO<sub>2</sub> Levels for Bottom Bar Only with Big Holes Design
- Figure 55 : TVOC and eCO<sub>2</sub> Levels with Bottom Bar Only with Small Holes Design



## List of Nomenclature

PAPR (Powered Air-Purifying Respirator): A type of personal protective equipment (PPE) that uses a battery-powered blower to pull air through attached filters, purifying the air before it is inhaled by the user.

HEPA (High-Efficiency Particulate Air) Filter: A type of filter that can trap a large amount of very small particles that other types of filters would simply recirculate back into the air.

CFM (Cubic Feet per Minute): A measure of the volume of air moved per minute, used to quantify airflow in ventilation systems.

TVOC (Total Volatile Organic Compounds): A measure of the total concentration of volatile organic compounds in the air, which are significant air pollutants.

eCO<sub>2</sub> (Equivalent Carbon Dioxide): A metric that reflects the concentration of CO<sub>2</sub> in the air, adjusted to account for the presence of other gases that affect CO<sub>2</sub> sensor readings.

SCD-40 Sensor: A sensor used for measuring temperature and humidity, often included in air quality monitoring setups.

PUREBURG B-D02H Filter: A specific model of filter equipped with an activated charcoal cloth liner for enhanced filtration of gases and particulates.

3M Versaflo Heavy Duty Breathing Tube: A component used in PAPR systems to deliver filtered air to the user's breathing zone.

Axial Fan: A type of fan that moves air parallel to the axis of rotation, commonly used in various ventilation and cooling applications.

Centrifugal Fan: A type of fan that moves air perpendicular to the axis of rotation, used in systems requiring higher pressure airflow.

NFPA 1984: A standard published by the National Fire Protection Association covering respirators for wildland firefighting operations.

Air Curtain: A stream of air directed downward or across an opening to prevent contaminants from passing through, used in the design to protect the firefighter's face.

Magnetic Attachment System: A method used in the design for attaching components securely using magnets, allowing for easy assembly and disassembly.

## Executive Summary

This paper presents the development of First Respire and their design of a powered air-purifying respirator (PAPR) specifically curated for wildland firefighter while simultaneously addressing the critical absence of respiratory protection for wildland firefighters operating in the challenging wildland-urban interface (WUI) environments. Current respiratory protection options, such as bandanas and N95 masks, fall short in providing adequate defense against toxic particulate matter and gases, exposing firefighters to increased risks of health complications, including cancers and respiratory diseases. Through collaborative efforts of the Wildfire Conservancy, the WUI Fire Institute at Cal Poly, and CAL FIRE, First Respire aims to create a durable, NFPA 1984-compliant device that offers effective respiratory protection while considering the specific needs and challenges faced by wildland firefighters. This paper outlines the significant objectives, drawing from stakeholder discussions and numerical specifications outlined in NFPA 1984 standards. The design focuses on addressing key challenges such as respiratory resistance, weight distribution, duration of use, heat resistance, donning/doffing time, and communication interference. The device integrates two subsystems, air filter and air delivery, ensuring the interdependence of these subsystems for optimal performance. Consideration is given to the comfort, adjustability, and compatibility with existing gear to encourage widespread adoption.

## 1. Introduction

Over the past fifteen years, the Wildfire Conservancy has addressed some of the most significant challenges encountered by wildland-urban interface (WUI) and wildland firefighters. One of the most glaring absences though, has been and remains the lack of respiratory protection for wildland firefighters, protection which they desperately need to minimize exposure on the job to smoke and other toxic materials that have life-threatening consequences. A mortality study of nearly 30,000 career urban firefighters by the National Institute for Occupational Safety & Health (NIOSH) found that the firefighters had higher mortality rates for all cancers compared to the general population in the United States. Furthermore, it was found that there were positive exposure-response relationships, indicating that greater exposure to firefighting conditions was directly correlated to increased mortality, for deaths from lung cancer, leukemia, and chronic obstructive pulmonary disease (COPD). Another study estimated that, across a range of exposure scenarios (49 to 98 fire days per year) and career durations (5 to 25 years), wildland firefighters were at an 8-43% increased risk of lung cancer and a 16-30% increased risk of cardiovascular disease.

Although manufacturers have attempted to create respiratory protection devices for wildland firefighters, none have been certified under the National Fire Protection Association (NFPA) 1984 Standard on Respirators for Wildland Firefighting and Wildland Urban Interface Operation. As a result, federal wildland agencies don't require firefighters to use any respirators because none meet the necessary standards. As of right now, the only devices that wildland firefighters frequently use for respiratory protection are bandanas and N95 masks. N95 masks can filter 95% of smoke particles down to 0.3 micrometers but are ineffective against oil mists, gases, and vapors. Bandanas are the most worn form of respiratory protection but offer markedly less protection than the already deficient N95 masks. More effective existing respirators face a very difficult fight to achieve widespread adoption both because of their often poor functionality under wildland firefighting conditions and the decades of wildland firefighting traditions that have instilled, in many wildland firefighters, a willing acceptance of the occupational hazards. There is an apprehension about the changes that widespread introduction of respirators could bring.

A field test hosted by Cal/OSHA and the Los Angeles County Fire Department that included respirators made by big firms like 3M, MSA Safety Inc., and Ventus Respiratory Technologies highlighted some of these exact hurdles. In the hills outside of Los Angeles, firefighters took turns carrying out various tasks they might perform during a shift fighting a real wildfire while trying out different masks "... and plenty broke. Hoses popped out of sockets. Straps snapped. Masks slid down sweating faces. Filters became dislodged." The responses of the firefighters ranged from "I can't imagine wearing that for an hour" to "it's better than nothing" to "I'd rather take nothing". Leadership, however, remains committed to persevering



through the "technological and cultural challenges" to find a solution because wildland firefighters' lives are at stake .

To continue moving toward an effective wildland firefighting respirator, the WUI Fire Institute at Cal Poly and CAL FIRE, via the Wildfire Conservancy, is providing funding for this project aimed at creating a new respiratory device that meets both the NFPA 1984 standards and the expectations of the wildland firefighters on the front lines. First Respire aims to create a long-lasting air-respirator device that protects wildland firefighters from harmful particulates and gases, all while providing constant airflow and being a reliable product.

## **1.1. Objectives**

Throughout discussions with project stakeholders Frank Frievalt, Matt Rahn, and Kelcey Stricker, a range of customer requirements were identified, relying on NFPA 1984 requirements for most numerical specification objectives. The remaining objectives are operational requirements verified by available public data as well as input from Captain Jason Pratt and his crew from Station 1 in San Luis Obispo. Refer to the requirements table in Appendix B for a concise numerical representation of project requirements.

### **1. Respiratory Resistance**

Currently available designs limit the available air for the user, disqualifying such devices for standard use in WUI (Wildland-Urban Interface) settings. Firefighters cannot use respiration equipment if breathing is impeded, the maximum tolerated resistance is 25mmH<sub>2</sub>O for exhalation and 80mmH<sub>2</sub>O for inhalation in equivalent pressure .

### **2. Weight**

With daily required equipment ranging from 30-45 pounds, WUI firefighters will not carry any unneeded additional weight that exceeds 10 pounds. Firefighters have stated that along with the device being lightweight on the head, it is also integral that the weight is distributed throughout the body, rather than concentrated in one place. This constraint applies to the entire respirator, filter, and pump assembly. Weight: With daily required equipment ranging from 30-45 pounds, WUI firefighters will not carry any unneeded additional weight that exceeds 10 pounds. Firefighters have stated that along with the device being lightweight on the head, it is also integral that the weight is distributed throughout the body, rather than concentrated in one place. This constraint applies to the entire respirator, filter, and pump assembly.

### **3. Duration of Use**

A standard shift while working on a wildland fire can range from 8 to 12 hours, in which the device is required to operate for a minimum of 3 hours without intervention. During this time the assembly



must power itself, operate within specifications. The power source must operate for a minimum of 8 hours so replacement filters or batteries may be administered as needed.

#### 4. Heat Resistance

During a wildfire, operators experience a wide variety of temperatures. Any standard product must not change in composition or overall shape and must not fail to meet other requirements when exposed to temperatures up to 175 °C (350 °F). Failure to survive extreme conditions severely reduces equipment effectiveness .

#### 5. Donning/Doffing Time

Firefighters will need to put on (don) and remove the assembly (doff) at least once every shift. Donning must be under 120 seconds and doffing cannot exceed 10 seconds. The assembly is worn throughout the entire shift thus donning time is less crucial. However, in the case of an emergency the assembly may need to be removed quickly (with the backpack), constraining doffing time .

#### 6. Comfortable/Adjustable Sizing

The device needs to operate within specification when worn by a variety of firefighters. Based on *Figure 1: NFPA Fig. 1.8.4.1* , the team determined a minimum 100mm (approx. 4 inches) bilateral adjustable range for all radial points of fit. Respirators must fit onto firefighters of differing head sizes, hair, and other facial proportions.

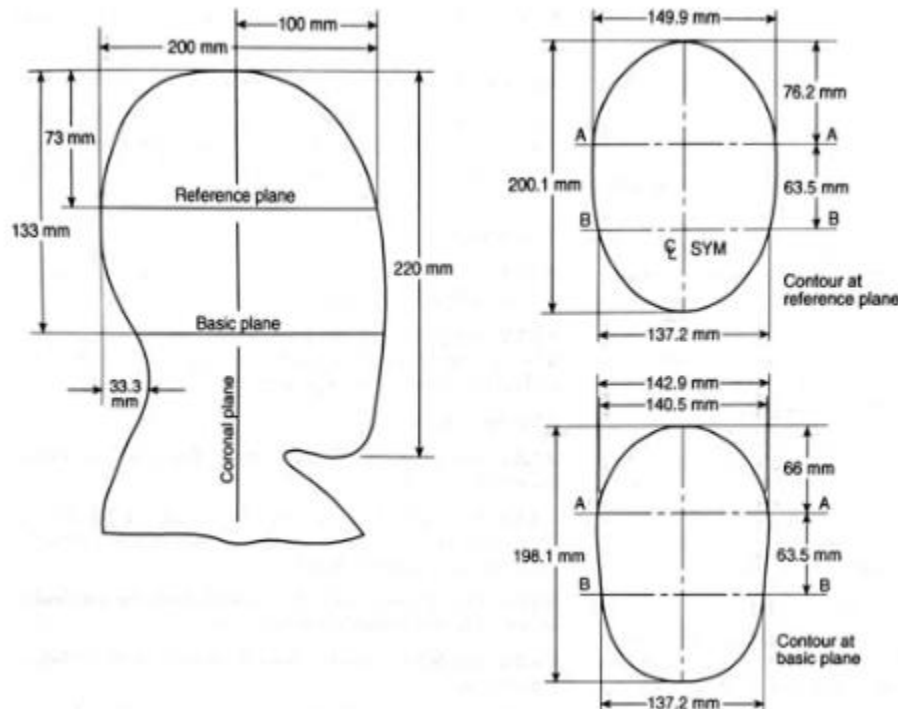


Figure 1. From NFPA 1984: Fig 8.1.4.1 Non-Conductive Head Form



## 7. Communication Interference

The device must not impede verbal communication between WUI firefighters in the field. A communication effectiveness test outlined in Section 7.1.8 will ensure the assembly allows users to communicate within a range of 1.5 meters in loud conditions. Without the ability to communicate, firefighters lose cohesion, reliability, and safety.

## 8. Field of View

Firefighter's vision just not be substantially impaired when the device is in use. Based on a central fixation point, the human field of view extends approximately 100° laterally. Maintaining this wide FOV unimpeded while wearing the assembly is necessary for use.

## 9. Motion Inhibition

The device is required to allow sufficient head movement during use. Firefighters must have an up and down range of 130° (total) up and down and 77° (each) left and right. Center of movement range measured when the head is in upright, resting position. Arm and leg movement and rotation must not be inhibited if the device is housed along limbs, waist, or torso.

## 10. Air Cooling

As air is provided by the device, the exiting vapor's temperature will be 1-3°F cooler than the air entering the system. This effect is a naturally occurring phenomenon dependent on the groups target exiting CFM (equation: CFM = (3.16 x Watts) / dT) This reduces the possibility of heat-related injuries; it's important to ensure the firefighter's temperature does not increase from operating the respirator.

## 11. Filtration Quality

The filtration ability of the assembly is vital; carbon monoxide, and volatile organic chemicals (VOCs) are the most important particles to remove from the air before supply. The assembly will aim to perform to the standard outlined in Table 1 .

*Table 1. Table 8.11.4 From NFPA 1984*



Protection	Test Temp. (°C)	Test RH (%)	Gas/ Vapor	Challenge Concentration (ppm)	Flow rate <sup>a</sup> (lpm)	Penetration (ppm)	Minimum Service Time (min)
Carbon monoxide <sup>b</sup>	25	92	CO	200	115 / 170	25 ppm averaged over a rolling 5-min time frame	480
Carbon monoxide Intermittent use <sup>b</sup>	25	92	CO	200	115 / 170	25 ppm averaged over a rolling 5-min time frame	240, storage for 20 hours, 240
Carbon monoxide <sup>b</sup>	25	92	CO	1200	115 / 170	200 ppm averaged over a rolling 5-min time frame & 1380 / 2040 mL cumulative	480
Carbon monoxide inspiration temperature <sup>b</sup>	25	92	CO	1200	40 cyclic at 24 rpm	200 ppm averaged over a rolling 5-min time frame & 60 mL cumulative <sup>c</sup>	60
Organic vapors	25	80	C <sub>6</sub> H <sub>12</sub>	300	115 / 170	10	20
Organic vapors	25	25	C <sub>6</sub> H <sub>12</sub>	300	115 / 170	10	20
Sulfur dioxide	25	80	SO <sub>2</sub>	50	115 / 170	200	30
Sulfur dioxide	25	25	SO <sub>2</sub>	50	115 / 170	200	30
Nitrogen dioxide	25	80	NO <sub>2</sub>	25	115 / 170	1 ppm NO <sub>2</sub> or 25 ppm NO	30
Nitrogen dioxide	25	25	NO <sub>2</sub>	25	115 / 170	1 ppm NO <sub>2</sub> or 25 ppm NO	30
Formaldehyde	25	80	HCHO	50	115 / 170	1	30
Formaldehyde	25	25	HCHO	50	115 / 170	1	30
Acrolein	25	80	C <sub>3</sub> H <sub>4</sub> O	10	115 / 170	0.1	20
Acrolein	25	25	C <sub>3</sub> H <sub>4</sub> O	10	115 / 170	0.1	20
Hydrogen fluoride <sup>d</sup>	25	80	HF	70	115 / 170	3	20
Hydrogen fluoride <sup>d</sup>	25	25	HF	70	115 / 170	3	20
Hydrogen cyanide <sup>d</sup>	25	80	HCN	1000	115 / 170	5	20
Hydrogen cyanide <sup>d</sup>	25	25	HCN	1000	115 / 170	5	20

## 12. Gear Compatibility

Design will not impede the storage, use, or effectiveness of existing tools and equipment. This specific objective will be verified by firefighters testing prototype compatibility and feasibility through mock use.

## 13. Unit Cost

The cost of lifesaving equipment affects its availability. To ensure the required budget increase to outfit firefighters is not overwhelming, the design will aim to provide a manufacturability cost of \$400 per unit. This price would be less than a usual radio or pair of boots meant for the same conditions.

## 2. Background

Wildland firefighters are away from base camp for extended periods of time during their shift, usually within a range of 8-12 hours. Wildland firefighters must first hike into the wilderness for several miles until reaching their target area. While on shift, wildland firefighters are outfitted with a wide variety of equipment, which can weigh between 15-20 kg (35-45 lbs) as shown in *Figure 2*. Conditions only worsen in the wildland-urban interface as smoke from artificial structure fires can expose wildland firefighters to a



whole new array of toxic substances. Out on the line, firefighters can experience extreme temperatures, high winds, and exposure to toxic carcinogenic particulates and gases including ash, carbon monoxide, sulfur dioxide, nitrogen dioxide, formaldehyde, acrolein, benzene, hydrogen cyanide, and ozone .



Figure 2. A wildland firefighter from CAL FIRE with standard engine crew equipment

Bandanas and N95 masks are the most common types of respiratory protection currently employed by wildland firefighters, but neither is effective at filtering out both the toxic particulate matter and the toxic gases they are exposed to daily on the job. A study examined the relative effectiveness of a handful of different respiratory protection devices by passing smoke from smoldering Douglas Fir needles through different respiratory protection device materials and measuring the concentration of particulate matter and gases on the other side . *Figure 3* and *Figure 4* below provide a summary of the study's findings.

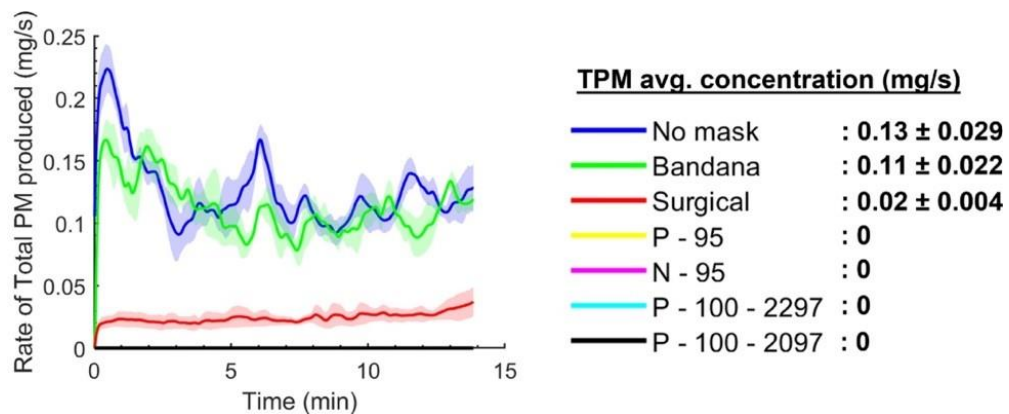


Figure 3. Rate of particulate matter after going through the respiratory protection device.

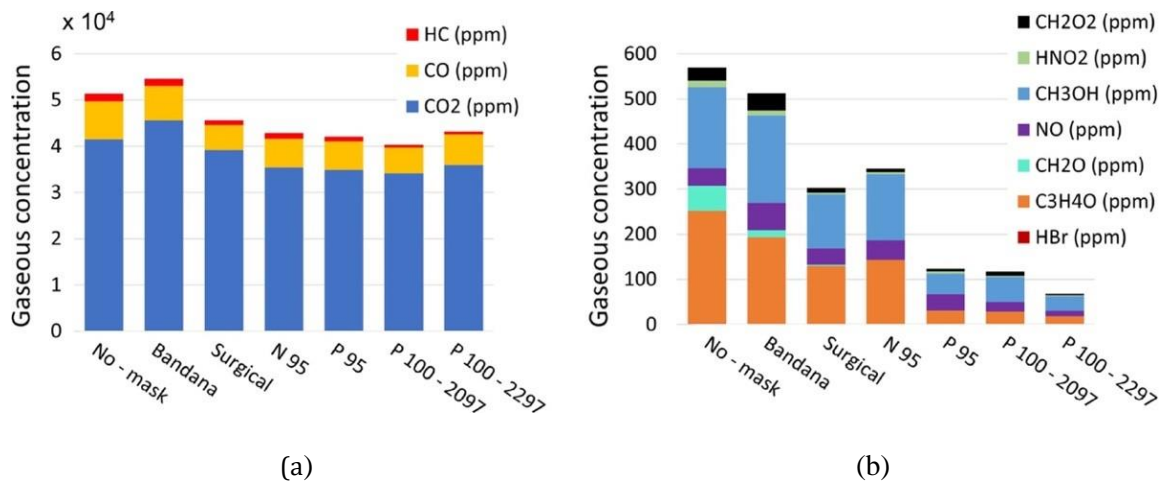


Figure 4. Concentrations of (a) major and (b) minor gases downstream of the respiratory protection device.

The bandana was almost entirely ineffective and performed similarly to having no mask at all in most cases. The bandana even resulted in an increased concentration of CO<sub>2</sub> compared to having no mask. Aside from blocking very large particulate matter and offering a potentially psychologically reassuring sense of protection, the bandana does not provide any meaningful protection for wildland firefighters against toxic gases. On the other hand, the N95 did improve the particulate matter concentration, but did little to filter out the major gases, carbon monoxide, carbon dioxide, and hydrogen cyanide. Additionally, N95 masks can clog up and restrict breathing fairly quickly, a problem noted by wildland firefighters who experienced it firsthand.

Currently, urban firefighters use a device called a power air-purifying respirator (PAPR) when entering a building, which provides urban firefighters with around 30 minutes of clean air. A wildland firefighter would have less than 30 minutes of clean air with the conditions they are in. PAPRs, however, have a time limit based on battery discharge. They can be expensive and lose airflow based on battery life and filtration, which can ultimately harm the individual wearing the device. Other companies have released products that accomplish only some of the needs of the firefighters, but said devices have all failed during product testing due to the products either breaking down during standard use or being so difficult to use that the firefighters would never use them to begin with. Since wildland firefighters do not have the ability to easily replace broken equipment when miles away from base camp, it is critical that all their equipment is durable and compact as possible on top of being able to effectively filter out carcinogenic gases.

One of the designs First Respire investigated is the helmet air pump designed by a local company called Rugged Radios shown in figure 5. This device is an air pump used to pump clean air into the helmets of



drivers for recreational off-road vehicle (ROV) racing. This device vacuums the air from outside the vehicle through a pre-filter and dust filter. The air is then pumped through a vacuum tube into the top of the driver's helmet. A voltage control device controls the motor and either increases or decreases the amount of air being pumped into the helmet. The motor and fan are encased in plastic, and the vacuum tube is flexible and extendable. It is powered and grounded to the battery of the vehicle lasting as long as the car runs. It can withstand temperatures of 100+ degrees Fahrenheit, along with rocks and debris. Another device very similar to the Rugged Radios helmet air pump is the Parker Pumper Helmet Co. device, which works the same way and delivers air at a constant 138 CFM, weighs approximately 1.5 lbs with a single speed running at 2.7 amps for their smallest device.



*Figure 5. Parker Pumper Helmet Co. device.*

Alongside an air pump, the idea of air curtains was also explored. The two patents that the group found were patents RU2407567C1 and CN209915110U . Patent RU2407567C1 discusses a device that uses two DC pumps that can be adjusted to go around the individual's head, over their eyes, or hook over the individual's ears and pump air over their mouth. When the pumps are over the mouth, they face each other, pumping air against each other "connecting" the air, creating a barrier, and prohibiting particles from being inhaled by the individual. When the pumps are above the individual's eyes, the pumps both face



down, run at a higher speed, and block particles from going into their eyes. Patent CN209915110U claims to have a smoke-proof helmet. This device uses a micro-exhaust filter that vacuums the smoke-contaminated air and pumps it into a filter box as shown in Figure 6. The filter box contains active carbon and cotton filters. The filtered air then gets sent through a jet pipe that runs along the brim of the firefighter's helmet; holes are punched into the bottom of the pipe, and the air is blown over the face of the firefighter. First Respire's goal is to design a powered air-purifying respirator (PAPR) for wildland firefighters.

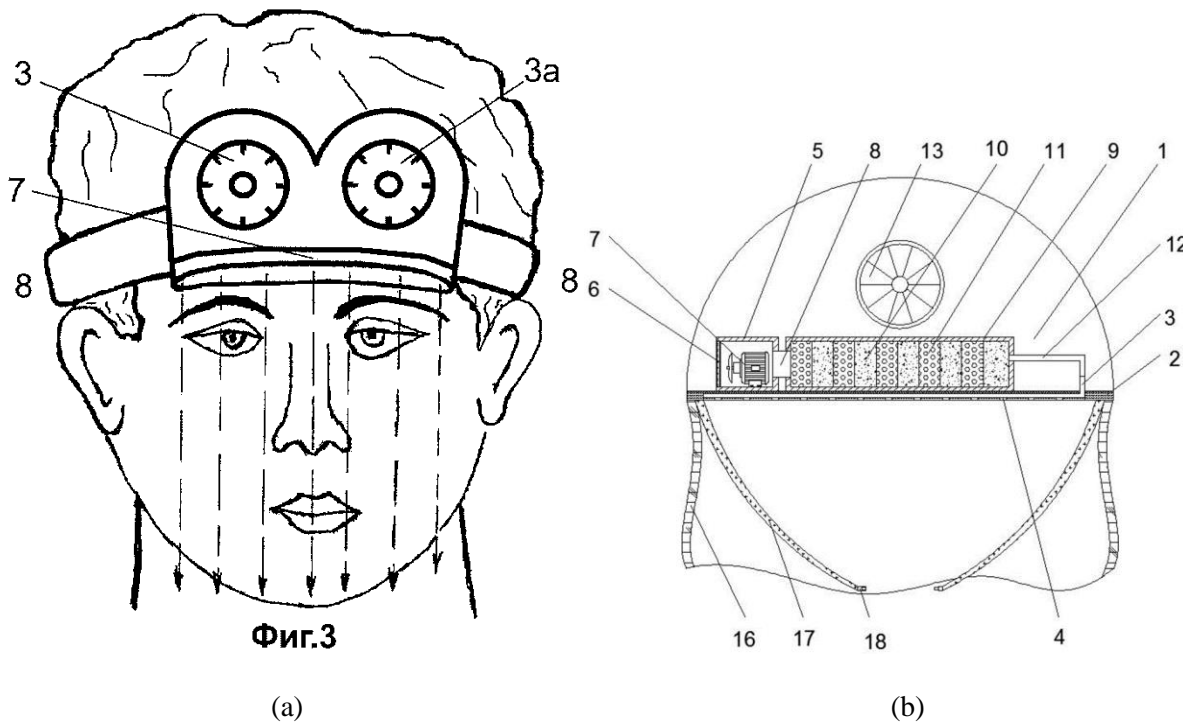


Figure 6. (a) Diagram of Air Curtain from RU2407567C1 showing a basic idea of how to supply air to protect the user's face. (3. Fans, 7. Air Flow, 8. Attachment) (b) Diagram of a smoke proof helmet from CN209915110U showing the filter and pump system.

### 3. Design Development

Currently, wildland firefighters do not have access to viable breathing protection against smoke, gas, and particle emissions when deployed to wildfires. Many use bandanas or similar contraptions intermittently to protect themselves from large particulates as there are no available respiratory devices deemed capable of performing at the required standards. Some major flaws in designs included heaviness, insufficient air supply, and ineffective filtration. First Respire's air respirator design improves air quality before air delivery and provides ample respiratory support. While aiming to meet standard requirements, a large improvement in air quality compared to non-suited equipment, such as a bandana, is also considered a success. The device does not inhibit an operator's ability to perform duties, communicate with their team,



or significantly limit their field of view. The final assembly is compatible with existing equipment and easily deployable and removable, as well as remaining aesthetically appealing to firefighters.

The device was split into two different subsystems: air filter and air delivery. Although at first the overall device was to be split into two different projects, air filter and air delivery, the final chosen concept integrates the two instead. Each subsystem of the final concept was tested to ensure device effectiveness. It is crucial that each subsystem does their job to ensure successful integration and efficiency.

In addition to the device being split into two subsystems, the device also has a variety of features to be considered, such as comfortability, donning/doffing time, and duration of use as stated in the objectives. These features include considering the way the device must be worn on the body and face, such as deciding whether to use masks, bandanas, helmet, gaiters, etc. First Respire deduced that the duration of the device was confined by the following features: weight, carrying capacity, accessibility, cost, and voltage. When speaking with local firefighters, First Respire learned that wildland firefighters carry batteries on hand for other devices. Since wildland firefighters are out in the field for an average of 8-12 hours per shift, it became apparent that it would be necessary to use batteries as the power source of the device. Thus, the design development for the power source came down to deciding how many batteries would be used.

## 3.1. Top Concepts

With all the objectives at hand, the top concepts for design development are split into air filter, air delivery, and power source to keep a sense of clarity on concept generation. However, it is important to note that the power source is not its own subsystem as it will be powering the entire device, since the air filter and air delivery subsystems will be integrated in the final design.

### 3.1.1. Air Filter Subsystem

#### A. VOC Filtration (HEPA)

VOC filtration was the most difficult obstacle for preliminary filter design due to their high variety and small size. The options were narrowed by the passive filter Pugh matrix (Appendix D) after researching VOC characteristics and available methods of control. The highly popular HEPA filter is considered due to its ability to filter well for a long period with relatively low air resistance. This is under the assumption that the filter will not be entirely exposed to wildfire environments during its usage.

#### B. Ash Filtration (Mesh Filter)

To combat large particles of ash and debris, another passive filter is considered to be included, covering the rest of the filters. The high porosity, low resistance mesh fluid filter has the single purpose of extending the usable lifespan of the filters beneath it in the stack. By removing large



contaminants, the passive and active filters underneath will take longer to clog in the same conditions.

### C. CO Filtration (Activated Charcoal Block)

Carbon Monoxide is the most important aspect of the proposed filtration process. CO is a poison and is thus an acute hazard. Guarded in the same way as the HEPA filter (underneath a mesh), the design is free to use the best filtration method with less regard for immediate clogging. Activated carbon filters, or charcoal filters, are perfectly suited for removing CO from a fluid, proving that the charcoal filters will be substantial in removing CO in a variety of concentrations. This filter is an active filter, meaning that the filtration method is primarily chemical.

### D. Mixed Stack

The final filter stack consists of a mixture of the three filter types, covering the bases for effective filtration and long-lasting use. All filters chosen are relatively cheap, replaceable, and size-customizable.

## 3.1.2 Air Delivery Subsystem

### A. Air Distribution Interface

#### 1. Face Air Respirator with Clear Mask

This concept consists of a clear face mask that the firefighters would wear with clean filtered air blowing into the face mask that they can breathe in. There would be a one-way filter to ensure CO<sub>2</sub> would leave the mask when the firefighters exhale. Although ideally this concept would work, the tubes delivering air would be placed in front of the firefighters, which could impede their movement and get in the way of them being able to for their job. A mask like that would also be hot and would potentially be ineffective or uncomfortable for firefighters with facial hair.

#### 2. Helmet Air Curtain

Using the helmet itself to form a wall of air to keep the debris from wildfire out and keep clean air surrounding the firefighter was also an option to consider. The idea behind a design like this is that it would run along the brim of the firefighter's helmet, and blow air directly straight down protect the firefighters face. The biggest downside would be the required CFM to blow a consistent curtain of air to block out particulates. This concept is like the patent discussed in the background; however, the patent was only designed to cover the eyes of the firefighters. Power required to create that much CFM is too high and the air curtain being created would likely be too turbulent and inconsistent to be effective.

#### 3. Face Shield Air Curtain



Another similar concept to the helmet air curtain but using a face shield as additional protection along with possibly channeling the air more effectively. With its design, the face shield can be used to protect the firefighters' eyes while supporting two pathways for air to be delivered, creating two separate air curtains. This can then lower the required CFM necessary to cover the entire face of the firefighter and instead, only must be a CFM high enough to cover a portion of their face.

## B. Fan System

### 1. Axial Fan

Axial fans provide a high volume of air flow at low pressure. A common example is a box fan.

### 2. Centrifugal Fan

Centrifugal fans provide high pressure air flow at low volume (compared to axial fans). An example can be seen in *Figure 7*.

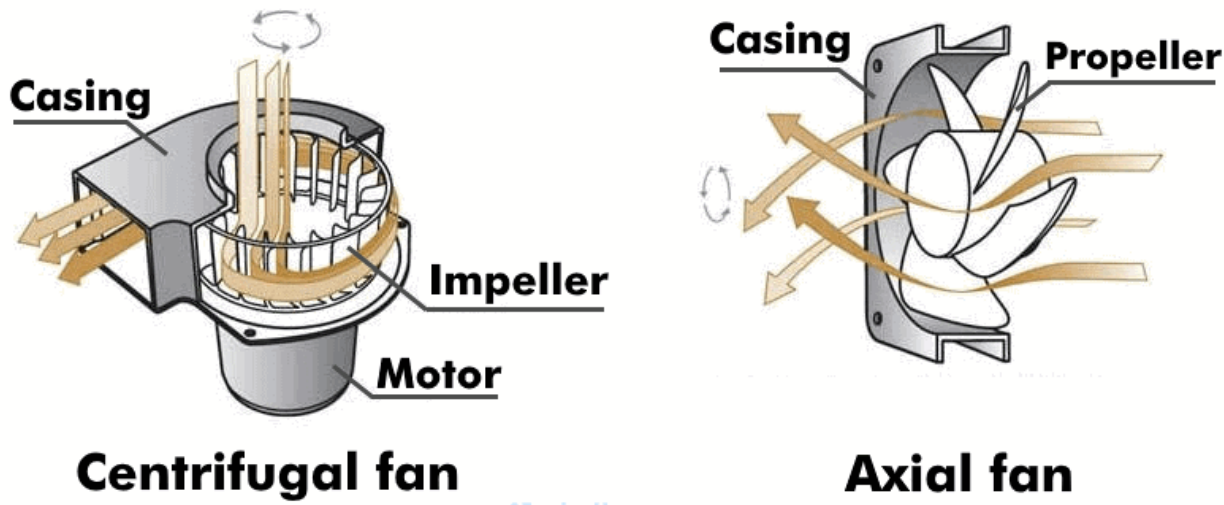


*Figure 7.* Image showing the difference between an Axial and Centrifugal fan.

### 3. Mixed Flow Fan

Mixed flow fans combine the properties of axial and centrifugal fans to develop air flow at a greater volume than centrifugal fans and a greater pressure than axial fans, an efficient and economical compromise if it meets your requirements.



### 3.1.3 Power Source

#### A. 9VDC from 6 AA batteries

AA batteries are commonly used by firefighters currently. The air delivery subsystem will need at least 12V to be powered successfully. Therefore, utilizing 6 AA batteries, and using a converter to step up the voltage to create a 12VDC output will meet that requirement. If using a brushless DC blower (a power-hungry device), a boost converter is needed to step up from the 9VDC to 12VDC to conserve battery life. If it can be implemented successfully, the 6 AA batteries will have about a longer lifespan when used as at 12VDC.

#### B. 3M PAPR Battery

The 3M PAPR Battery is specifically designed for the “Large 3M Powerflow Face-Mounted Powered Air Purifying Respirator.” It has a battery life of 8 hours, is rechargeable, and attaches specifically to the 3M PAPR device. Although this is what is currently available to firefighters, this device is only really useful for structural firefighters, not wildland firefighters.

#### C. Power Bank Solar Charger

The Power Bank Solar Charger combines portability of a power bank with solar charging capability, ideal for outdoor tasks and situations with limited access to power that wildland firefighters face. This device is 5V/3.1A capable and supposed to be heat-resistant. Although the main benefit from this device is that it is rechargeable with the power of the sun, its voltage capability is lower than desired, and cannot be used to power the whole device for long.

## 3.2 Concept Selection

The selection of the final design considered what's available on the market, what's currently being used, and what is preferred by wildland firefighters.

### 3.2.1 Air Filter Subsystem

The final filter design involves a strategic combination of various filter types to address specific requirements. The inclusion of a HEPA 13 filter ensures the removal of 99.95% of particles measuring at least 0.2 microns in diameter, effectively eliminating particulates and many VOCs. To safeguard the HEPA filter from larger particulate that may lead to quick clogging, an outer layer of standard mesh filter is applied. On the opposite side of the HEPA filter, an activated charcoal filter is positioned. Through this comprehensive combination of HEPA, mesh, and activated charcoal filters, the filter stack successfully meets the necessary criteria for NFPA 1984 PAPR certification .

In selecting the ultimate filter design, the team prioritized the total surface area to optimize air intake. The primary concern was the volume of air passing through the filter. Enhancing the surface area allows for decreased pressure differential, thereby lessening the fan load while maintaining adequate air supply for



the firefighter. A cylindrical filter was chosen for its superior surface area compared to a disk of the same size. The internal stacking of filter layers in the cylindrical design significantly contributes to this advantage.

### 3.2.2 Air Delivery Subsystem

#### A. Air Distribution Interface

Upon careful consideration, it was determined that the final design would incorporate a face shield integrated with an air curtain. Following discussions with firefighters, it became evident that they appreciated the concept and functionality of an air curtain that would protect the face from debris, filter air, and offer a cooling effect on the head. Consequently, the decision was made to adopt an air curtain as the definitive design element, with the focus shifting to the method of its implementation.

The notion of employing an air curtain that encompasses the entire face presented challenges, as it would necessitate generating a significant CFM output to adequately cover the firefighter's entire face while maintaining sufficient strength to function as an effective air curtain. Leveraging the face shield allows for the division of airflow pathways, thereby reducing the surface area that the air must cover. By partitioning the air curtain, one segment can safeguard the eyes while another segment protects the nose and mouth.

Furthermore, considering that firefighters are required to utilize protective eye equipment during field operations, typically goggles, it has been observed that these often fog up or become too dirty to provide clear vision, leading firefighters to forgo their use. The integration of a face shield offers a practical solution to this issue, enhancing eye protection alongside the functionality of the air curtain system.

#### B. Fan System

In the evaluation of fan systems, the team explored three options before arriving at a definitive choice. Selection centered on a blower featuring an axial fan configuration. Initially, a centrifugal fan was considered due to its capacity to generate high air pressure at low volumes. However, the investigation into centrifugal fans revealed challenges in sourcing models operating at low voltages (12VDC or lower) capable of delivering approximately 25 CFM while remaining lightweight. Consequently, the focus shifted to axial fans, which emerged as the secondary option. Subsequently, the team found a blower capable of generating 139 CFM, operable at 12VDC, and commonly utilized in off-road racing vehicles. In the context of these vehicles, the blower functions by drawing external air through filters and supplying it to the driver's compartment. Upon



recognizing the availability of this blower in the market, it was determined to be the optimal choice for the final design implementation.

### 3.2.3 Power Source

The decision to utilize AA batteries for the power supply stemmed from insightful discussions with firefighters, who articulated their existing practice of carrying a substantial quantity of AA batteries during field operations. Given this established habit, integrating AA batteries as the power source for the device emerged as a logical choice. By leveraging AA batteries, firefighters can promptly replace depleted batteries, facilitating uninterrupted operation of the device.

Considering the inherent limitations of AA batteries in sustaining continuous power output for extended durations, targeting an operational span of approximately 2-3 hours aligns with practicality. Rather than striving for an impractical 8-hour continuous runtime, a more efficient approach involves optimizing the device for a shorter operational window, which can be supplemented by battery interchangeability. This strategy ensures a balance between operational longevity and the practical constraints associated with AA battery usage in powering the blower.

### 3.3. Proof of Concept Analysis

Based on prior discussion with wildland firefighters, the PAPRs used by urban firefighters are not viable because, while they last an urban firefighter an hour, they would only last wildland firefighters around 15 minutes. Each tank has a volume of 87 ft<sup>3</sup> so urban firefighters consume the air at around 1.45 ft<sup>3</sup>/min (CFM) whereas wildland firefighter consumes around 5.8 CFM. When calculating the required air curtain strength, a minimum 5.8 CFM is required to meet the respiratory demand of the firefighters. The CFM provided must also be sufficient to create an air curtain strong enough to maintain integrity in the often-windy ambient environment on the firefighting line so that the air the firefighters are breathing remains clean. To perform any more calculations to determine air curtain details some assumptions will have to be made.

The air curtain will be split into two parts, the upper part that is contained within the face shield and the lower part that will be doing most of the work keeping particulate matter and gases away from the firefighters' mouths and noses. The lower portion of the air curtain is what was chosen to be focused on for most of the calculations as that is the critical portion of the air. Using the NFPA 1984 standard described in *Figure 1*. NFPA Fig 8.1.4.1, the upper portion of the face shield will be projecting air down the face starting at the reference plane or 73 mm from the top of the head. The lower portion will begin 133 mm from the top of the head at the basic plane.

For the lower air curtain, the width is 40 cm (15.748 in) and the height is 30 cm (11.811 in). These values were conservative estimates based on measurements taken where the face shield will attach to the helmet provided. See *Figure 8* below for the initial measurements.

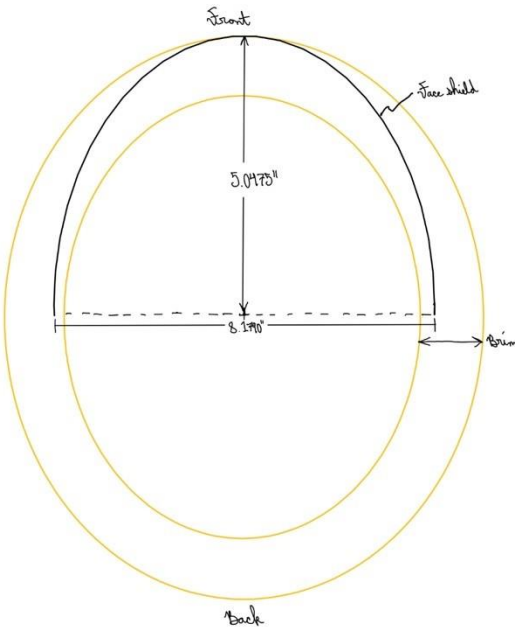


Figure 8. Face shield measurements.

To calculate the airflow of the air curtain, the effects of temperature, pressure, and wind need to be considered. The temperature differential across the air curtain, the pressure differential across the air curtain, and the wind stress on the air curtain all result in air trying to push through the air curtain. The total airflow trying to pass through the air curtain is the sum of temperature, pressure, and wind effects and, along with the dimensions of the air curtain and the density of the air, can be used to determine the required CFM of the air curtain.

To calculate airflow due to the temperature differential the following equation is used,

$$Q_T = \frac{W}{3} \cdot H^{1.5} \cdot C_d \cdot \sqrt{g \cdot \frac{\Delta\rho}{\rho_m}}$$

$Q_T$  represents the airflow due to temperature differential in cubic meters per second ( $\text{m}^3/\text{s}$ ) through an opening.  $W$  and  $H$  refers to the air curtain width and height in meters, which were determined earlier based on the head form.  $C_d$  is the flow coefficient (also called the discharge coefficient), which typically ranges between 0.6 and 0.9, indicating the theoretical efficiency of airflow through the space occupied by the air curtain if the air curtain was not present.  $g$  is the gravity coefficient equal to  $9.81 \text{ m/s}^2$ , accounting for the effects of Earth's gravitational pull on the airflow.  $\Delta\rho$  is the difference in density between the air on each side of the curtain and  $\rho_m$  represents the average density of the two bodies of air.

The airflow due to the pressure differential is calculated with the following equation,

$$Q_P = W \cdot H \cdot \sqrt{\frac{\Delta P \cdot 2}{\rho}} \cdot C_d$$



$Q_p$  is the airflow in  $\text{m}^3/\text{s}$  that results from the pressure differential across the air curtain.  $\Delta P$  is the pressure differential across the air curtain, and  $\rho$  is the density of air (assumed to be the density of the less dense error to make the calculations for the required CFM of the air curtain more conservative).

The airflow due to wind stress,  $Q_v$ , is calculated with the following equation, which assumes uniform distribution across the whole area of the air curtain and a rectangular shape for the air curtain,

$$Q_v = W \cdot H \cdot C_v \cdot v$$

$Q_v$  is the airflow in  $\text{m}^3/\text{s}$  across the air curtain due to wind stress,  $v$  is the wind speed in  $\text{m}/\text{s}$ , and  $C_v$  is the wind direction coefficient, which ranges from 0.5 to 0.6 if the wind load is perpendicular to the air curtain. The wind load was assumed to be perpendicular and a coefficient of 0.6 was used to make the final required CFM more conservative. Especially given the curved nature of the actual air curtain, the wind load is extremely unlikely to be perfectly perpendicular over the whole surface of the air curtain at any time so the  $Q_v$  calculated is almost certainly an overestimate.

The total airflow across the air curtain area,  $Q_{tot}$ , is then calculated in  $\text{m}^3/\text{s}$  using the equation,

$$Q_{tot} = Q_T + Q_P + Q_v$$

To perform the initial calculations to find the estimated total airflow across the air curtain area, the team used the following values given in *Table 2*.

*Table 2.* Values for airflow calculations.

Air curtain width, $W$	0.40 m
Air curtain height, $H$	0.30 m
Flow (discharge) coefficient, $C_d$	0.75
Gravity coefficient, $g$	9.81 $\text{m}/\text{s}^2$
Density of ambient air, $\rho_a$	1.155 $\text{kg}/\text{m}^3$
Density of air curtain air, $\rho_c$	1.165 $\text{kg}/\text{m}^3$
Wind speed, $v$	0 – 30 mph
Wind direction coefficient, $C_v$	0.6

The air curtain width and height were estimated using measurements taken with the firefighting equipment provided to the team and was assumed to be rectangular to simplify calculations. The actual shape of the air curtain is not perfectly rectangular because the distance from the air curtain outlets to the firefighter's body decreases progressively as you move horizontally from the center of the air curtain to its sides so the airflow due to wind stress calculated is more conservative than the actual value.  $g$  is assumed to be 9.81



m/s<sup>2</sup> since variations in Earth's gravity are very small. Under similar conditions, flow coefficients ( $C_d$ ) are typically higher for air compared to other fluids because of the low density of air, but this device is going to be used out in the wilderness in extremely variable conditions and it's very unlikely that the theoretical flow in those variable conditions would be laminar and highly efficient. Given all of that and the fact that it would be difficult to determine a precise  $C_d$  for the device experimentally, a  $C_d$  of 0.75 in the middle of the typical range was used for the air curtain strength calculations. In addition, during the calculations, it became clear that most of  $Q_{Tot}$  is due to  $Q_v$ , so the choice of  $C_d$  had a nearly negligible effect on the calculations. It was assumed that the body of air on either side of the curtain was at atmospheric pressure (i.e. 101.325 kPa) because it is very unlikely the helmet air curtain is going to create a significant pressure differential between the ambient air and the air inside the air curtain. This assumption should be verified using a functional prototype of the device and pressure sensors, but the pressure difference would have to be quite large for a consequential airflow due to pressure differential across the air curtain to occur, especially given the magnitude of the airflow due to wind stress.

The density of the ambient air,  $\rho_a$ , was calculated assuming dry air at atmospheric pressure and a temperature of 32.6°C. Given that warmer air has lower relative humidity and firefighters are often working in hot conditions, the dry air assumption is a safe approximation for the actual conditions. Additionally, assuming dry air means a lower average density term,  $\rho_m$ , in the  $Q_T$  equation, which makes the value of  $Q_T$  greater and ultimately makes the calculation of the required fan CFM more conservative. An ambient temperature of 32.6°C was chosen based on study characterizing the thermal environment of wildland firefighters during live fire suppression. The density of the air curtain air,  $\rho_c$ , was calculated assuming dry air at atmospheric pressure and a temperature of 29.8°C, which corresponds to approximately 5°F of cooling. The 5°F of cooling is based on one of the team's secondary goals to provide some cooling to the firefighters because it was emphasized several times during meetings with sponsors and advisors that providing a device with a cooling effect could be a strong incentive to get wildland firefighters to wear the air curtain respirator.

The cooling effect will likely be due to increased convective cooling as a result of the airflow over the firefighters' faces rather than being due to a lower temperature of air coming from the air curtain outlets, but an actual temperature difference was assumed for the calculations because that is one of the team's stretch goals and it ultimately makes the fan selection more conservative by generating a non-zero value for  $Q_T$ . The CFM required for the air curtain was calculated for wind speeds ranging from 0 to approximately 50 km/h (0 to 30 mph). In discussions with the team's sponsors and advisors that had firefighting experience, it was mentioned that winds on the fire line could get up to 50 mph, but that is the extreme end of wind conditions that the team cannot feasibly design for with the air curtain solution. Based on a wildland fire study simulating the fire environment with wind speeds ranging from 0 m/s to 10 m/s (36



km/h or ~22.4 mph), the range of 0 mph to 30 mph was chosen to both underestimate and overestimate the required strength of the air curtain given that First Respire's goal is to have the air curtain retain integrity in winds reaching speeds of up to 20 mph. The initial hand calculations can be seen below in *Figure 9.*

Example calculation of required air curtain strength:

Known:

- $T_a = 25^\circ\text{C}$ , temperature of ambient air
- $V_a = 40 \text{ km/h}$ , wind speed
- $T_c = 22.2^\circ\text{C}$ , temperature of air curtain air (equates to approx. 5°F of cooling)
- $H = 30 \text{ cm}$ , air curtain height
- $W = 40 \text{ cm}$ , air curtain width
- $g = 9.81 \text{ m/s}^2$

Assumptions:

- ①  $C_d = 0.75$ , flow coefficient (discharge coefficient) \* values typically range from 0.6 to 0.9 w/ higher values typical for gases and vapors. [Discharge Coefficient Info](#)
- ② Wind is directed perpendicular to the air curtain ( $C_v = 0.6$ )
- ③ Atmospheric pressure on either side of air curtain (noisy assumption with testing)  
⇒  $\Delta p$  due purely to  $\Delta T$
- ④ Forces due to gravity on air are negligible (given low density of air)
- ⑤ Uniform distribution of temperature and wind stress on air curtain surfaces
- ⑥ Steady flow

Solution/Analysis:

Airflow due to temperature differential across air curtain,

$$Q_T = \frac{W}{3} \cdot H^{3/2} \cdot C_d \cdot \left( g \cdot \frac{\Delta T}{f_m} \right)^{1/2}$$

$$f_0 = 1.195 \text{ kg/m}^3 \text{ at } T_c = 22.2^\circ\text{C}, P_0 = 1 \text{ atm}$$

$$f_a = 1.184 \text{ kg/m}^3 \text{ at } T_a = 25^\circ\text{C}, P_a = 1 \text{ atm}$$

$$Q_T = \left( \frac{0.40 \text{ m}}{3} \right) \left( 0.30 \text{ m} \right)^{3/2} (0.75) \left[ (9.81 \text{ m/s}^2) \left( \frac{(1.195 - 1.184) \text{ kg/m}^3}{2} \right) \right]^{1/2}$$

$$Q_T = 0.00494 \dots \text{ m}^3/\text{s}$$

\*  $\text{m} \cdot \text{m}^{3/2} \cdot \text{m}^2 \cdot \text{s}^{-1} = \text{m}^3/\text{s}$

*Figure 9.1.* Air curtain strength hand calculations.



Airflow due to wind stress,

$$Q_v = W \cdot H \cdot C_v \cdot V_a$$

$$Q_v = (0.40m)(0.30m)(0.6)(40 \frac{km/h}{1km})\left(\frac{1000m}{1km}\right)\left(\frac{1m}{3600s}\right)$$

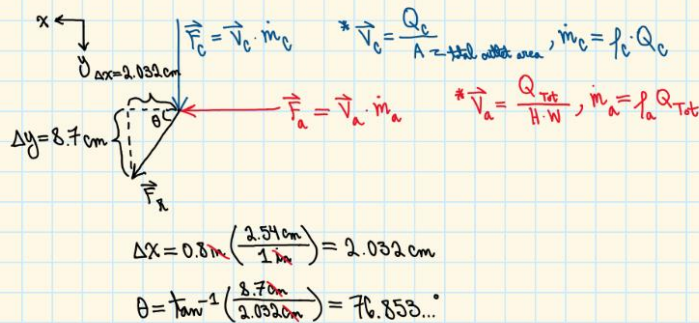
$$Q_v = 0.8 \frac{m^3}{s}$$

Total airflow,

$$Q_{Tot} = Q_T + Q_v$$

$$Q_{Tot} = 0.00499 \dots \frac{m^3}{s} + 0.8 \frac{m^3}{s}$$

$$Q_{Tot} = 0.804 \dots \frac{m^3}{s}$$



For a fixed  $W$ ,

$$\sum \vec{F} = \cancel{\int_C} \vec{V} dt + \int_{CS} \vec{V} (\vec{V} \cdot \vec{n}) dA$$

$$\sum \vec{F} = \int_{CS} \vec{V} (\vec{V} \cdot \vec{n}) dA$$

$$\vec{F}_R = m_c \vec{V}_c + m_a \vec{V}_a$$

$$\vec{F}_R = m_c V_c \hat{j} + f_a Q_{Tot} \left( \frac{Q_{Tot}}{H \cdot W} \right) \hat{i}$$

$$F_{Rx} = f_a Q_{Tot} \left( \frac{Q_{Tot}}{H \cdot W} \right)$$

$$F_{Ry} = m_c V_c$$

$$\tan \theta = \frac{F_{Ry}}{F_{Rx}}$$

$$\frac{8.7 \text{ cm}}{2.032 \text{ cm}} = \frac{F_{Ry}}{F_{Rx}}$$

$$F_{Ry} = 4.281 \dots F_{Rx}$$

$$m_c V_c = 4.281 \dots f_a Q_{Tot} \left( \frac{Q_{Tot}}{H \cdot W} \right)$$

$$(f_c Q_c) V_c = 4.281 \dots f_a Q_{Tot} \left( \frac{Q_{Tot}}{H \cdot W} \right)$$

$$(f_c V_c A) V_c = 4.281 \dots f_a Q_{Tot} \left( \frac{Q_{Tot}}{H \cdot W} \right)$$

Figure 9.2. Air curtain strength hand calculations.



$$V_c^2 = 4.281 \dots \left( \frac{f_a Q_{Tot}^2}{f_c \cdot H \cdot W \cdot A} \right) \quad \text{Unknowns}$$

$$V_c = \sqrt{4.281 \dots \frac{f_a Q_{Tot}^2}{f_c \cdot H \cdot W} \cdot A^{-1/2}}$$

For example, if we are going to use 20 holes each with a diameter of  $d = 1\text{ cm}$ ,

$$A = 20 \cdot \pi \cdot \left(\frac{1\text{ cm}}{2}\right)^2 \left(\frac{1\text{ m}}{1000\text{ cm}}\right)^2$$

$$A = 1.570 \dots \times 10^{-3} \text{ m}^2$$

$$\rightarrow V_c = \left( 4.281 \dots \frac{(1.184 \dots \text{m}^2)(0.804 \dots \text{m}^3/\text{s})^2}{(1.115 \dots \text{m}^3)(0.30\text{m})(0.40\text{m})} \right)^{1/2} \left( 1.570 \dots \times 10^{-3} \text{ m}^2 \right)^{-1/2}$$

$$\Rightarrow V_c = 120.755 \dots \text{m/s}$$

$$V_c = 97.353 \dots \text{m/s} \text{ for } V_a = 32.2 \text{ km/h} (\approx 20 \text{ mph})$$

$$Q_c = V_c \cdot A$$

$$\Rightarrow Q_c = 324.023 \dots \text{CFM}$$

$$Q_c = (120.755 \dots \text{m/s})(1.570 \dots \times 10^{-3} \text{ m}^2)$$

$$Q_c = 0.1896 \dots \text{m}^3/\text{s} \left( \frac{1\text{ ft}}{0.3048\text{ m}} \right)^3 \left( \frac{60\text{s}}{1\text{min}} \right)$$

$$Q_c = 401.914 \dots \text{CFM}$$

Figure 9.3. Air curtain strength hand calculations.

Initially, the ambient temperature used was 25°C and the air curtain temperature was 22.2°C, which is why some of the values used in the hand calculations are different than those provided in *Table 2*. For calculations with the updated values, refer to Appendix I - Air Curtain Calculations Excel. For a discussion of the results of the Excel analysis, refer to the 4.4. Analysis Results section. While the values in the hand calculations are slightly different than in the Excel calculations, the process remains the same. Looking at *Figure 9.3*, the airflows due to temperature differential and due to wind stress were calculated using the previously mentioned values and assumptions, at which point it became clear that the wind stress was by far the most significant contributor to the total airflow trying to force its way through the air curtain. For the hand calculations,  $Q_v$  accounted for 99.4% of  $Q_{Tot}$ . Using the calculated value for  $Q_{Tot}$ , the forces exerted by the air trying to push across the air curtain and the forces exerted by the air coming from the air curtain outlets were both modeled as point force vectors, which requires assuming that the mass flow rate and velocity is uniform for the air trying to push across the air curtain and the air coming from the air curtain. This assumption will not be entirely true in real life, but it allows for a simplification of the math to get a ballpark estimate of the CFM required from the fan the team selects. Based on the position of the face shield



on the provided firefighting helmet (see *Figure 10*), the team had one team member wear the helmet and took measurements to estimate the horizontal distance from the tip of the nose to the air curtain outlets and the vertical distance from the air curtain outlets to the bottom of the chin. The direction of the resultant force vector,  $\vec{F}_R$ , of the force exerted on the air curtain by the wind and temperature differential,  $\vec{F}_a$ , and the force of the air curtain air itself,  $\vec{F}_c$ , had to be directed at a minimum angle,  $\theta$ , from the horizontal to ensure that the air curtain would not be pushed into the firefighter's chin and lose integrity. Knowing that  $\vec{F}_R = \vec{F}_a + \vec{F}_c$ , the resultant force was broken into  $x$ - and  $y$ -components,  $F_{R_x}$  and  $F_{R_y}$  respectively. The minimum angle,  $\theta$ , of the resultant force was used to figure out  $F_{R_y}$  in terms of  $F_{R_x}$ . Because the system was modeled with the air curtain flow coming down vertically and the ambient air trying to disrupt the air curtain coming in horizontally,  $F_{R_x} = F_a$  and  $F_{R_y} = F_c$  so  $F_{R_y}$  in terms of  $F_{R_x}$  is also the magnitude of  $\vec{F}_c$  in terms of  $\vec{F}_a$ . That relationship can then be used to solve for the minimum required velocity of the flow from the air curtain outlets,  $V_c$  as a function of the total air curtain outlet area,  $A$ , by expanding  $F_{R_y}$  and  $F_{R_x}$  and solving for  $V_c$  on one side of the relationship. The CFM needed for that  $V_c$  and  $A$  can then be found by multiplying the two together since flow rate is given by the equation,  $Q = V \cdot A$ . Some conversion factors are needed to change from  $\frac{m^3}{s}$  to CFM (i.e.  $\frac{ft^3}{min}$ ). This CFM gives a ballpark estimate of the CFM that the air delivery system needs to provide that can be used to assess the viability of different fan options, though the CFM calculated will likely be an underestimate because it does not account for the air diverted to the upper portion of the air curtain design and assumes all the CFM is diverted to the tubing along the bottom edge of the face shield that is being used to produce the air curtain. For a discussion of the results in the context of the mechanical design, see section 4.4 Analysis Results.

The other somewhat novel portion of the mechanical design whose feasibility needed to be verified was the use of magnets to allow for easy attachment and removal of the face shield and air curtain assembly to and from the helmet. The shape of the face shield and air curtain assembly attached to the helmet was approximated as a semi-circular arc and it was assumed it all will have a maximum weight of 3 pounds, which will likely be more than the actual weight of the assembly attached to the helmet because the firefighters do not want any significant weight added to the helmet so the team is focused on minimizing the weight of that portion of the design in particular. Based on those assumptions and a maximum rotational head velocity of 25.0 rad/s in the horizontal plane (swiveling side to side), the approximate centrifugal force that the magnetic attachment system needs to withstand was calculated to be approximately 18.6 lbf. The exact calculations can be seen below in *Figure 10*. For a discussion of the magnet strength analysis in the context of the mechanical design, see section 4.4 Analysis Results.

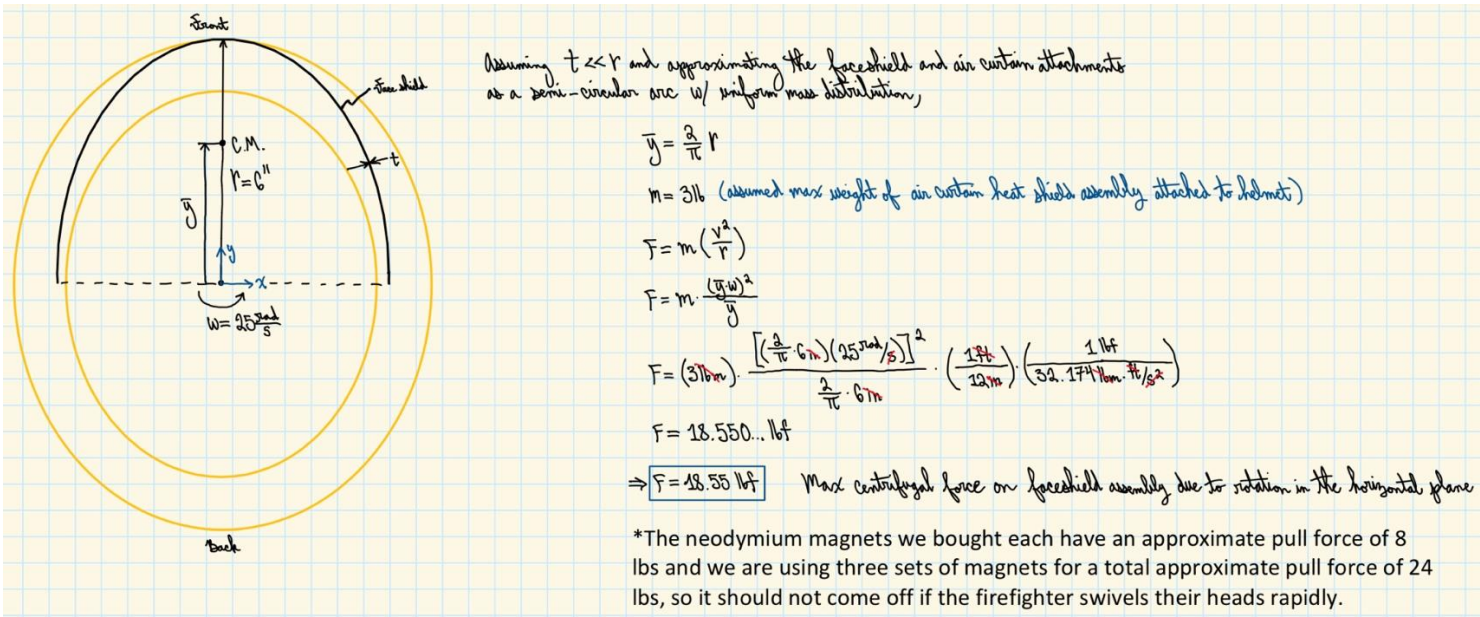


Figure 10. Required magnet strength hand calculations.

### 3.4. Selected Concept Prototyping

#### 3.4.1 Air Delivery Prototyping

When designing the prototypes for the air curtains, careful measurements of the helmet's arc were taken to inform the shape and length of the air curtain tubes. This precise measurement process was crucial, as it ensured that the air curtain would fit seamlessly with the helmet and function as intended.

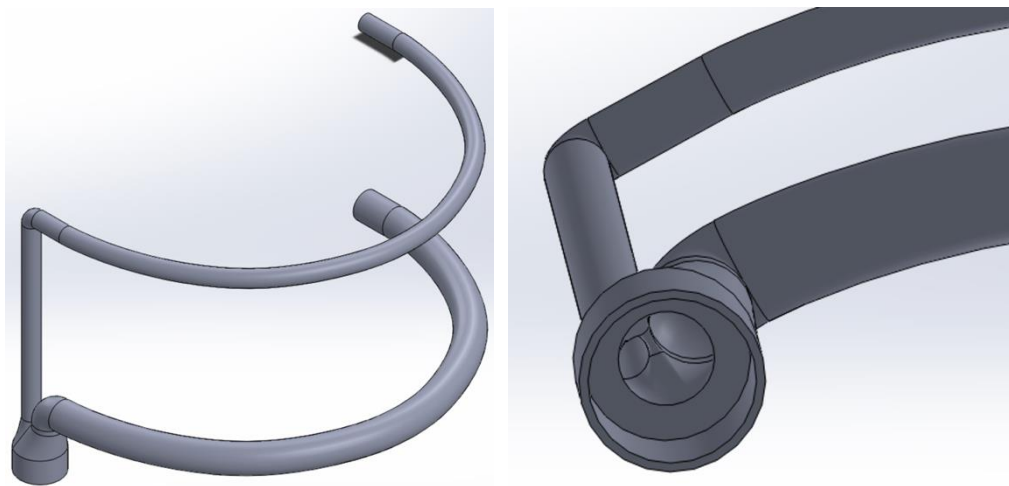
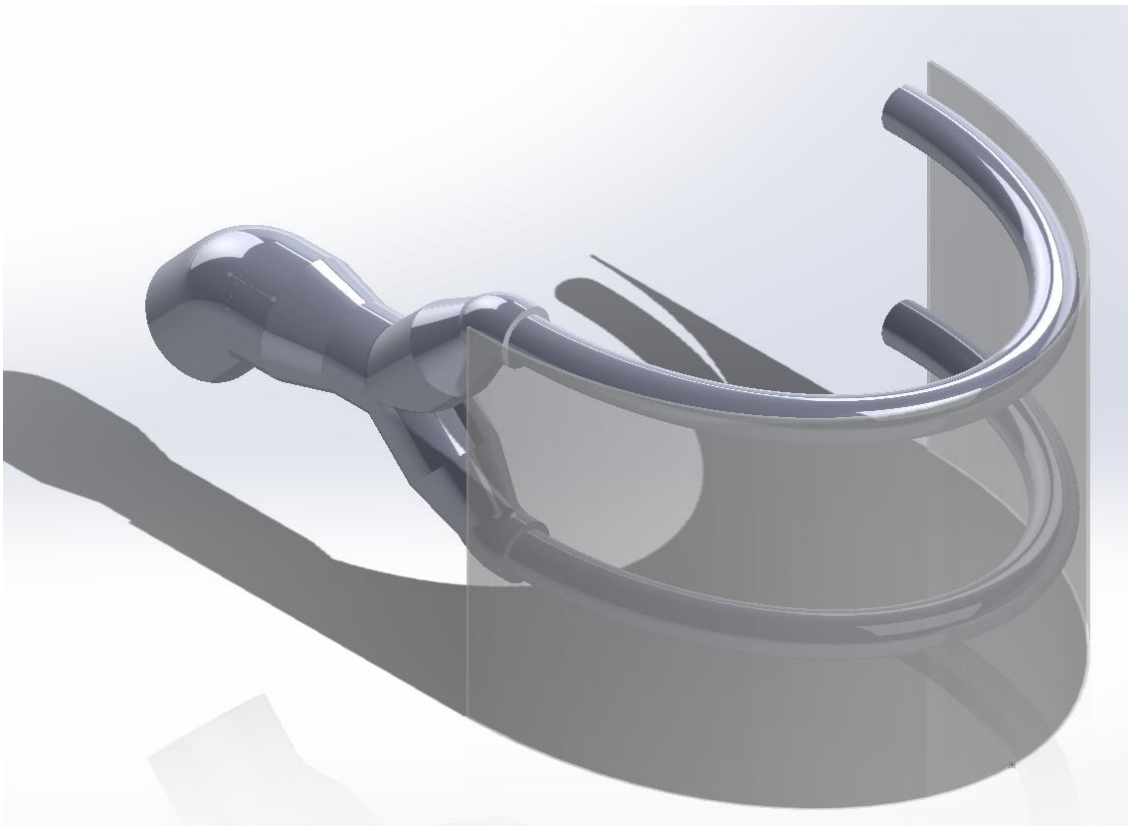


Figure 11 & 12. SOLIDWORKS air curtain assembly model and junction model. First Prototype.



CAL POLY



*Figure 13.* SOLIDWORKS air curtain assembly model. Second Prototype

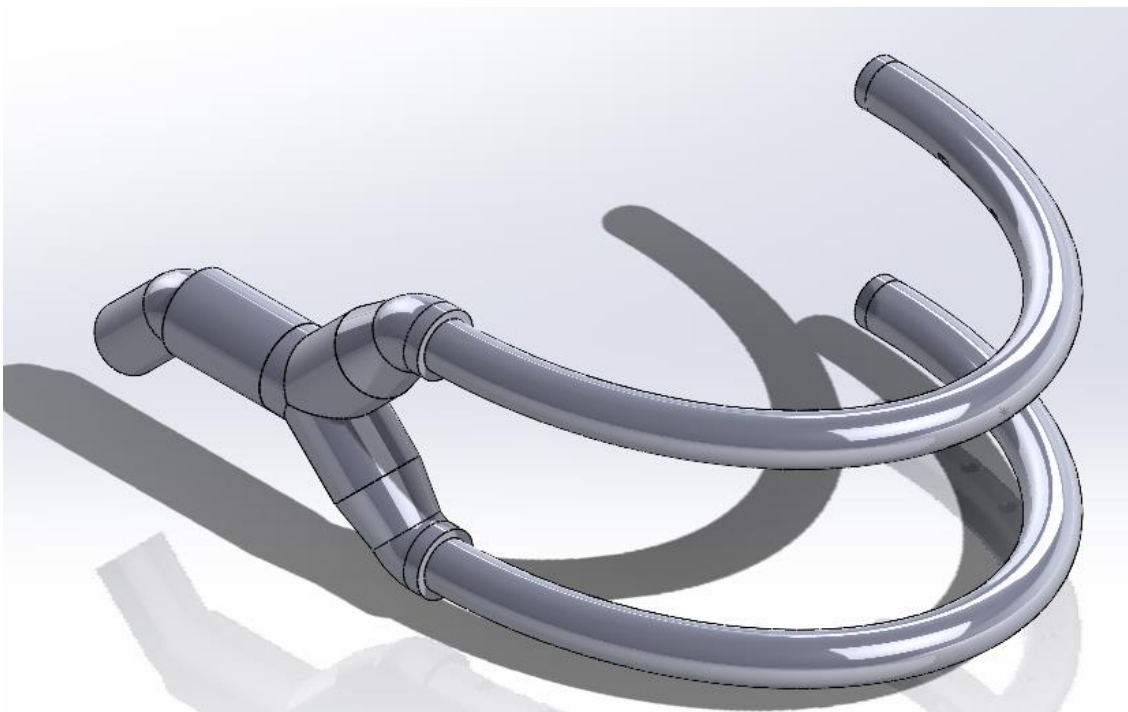


*Figure 14.* SOLIDWORKS air curtain assembly model. Third Prototype

In the development of the second iteration of the tubes, several improvements were made, including enhancements to the arc path, length, outer diameter, and inner diameter of the tubes. Notably, while the tube's wall thickness remained constant at 0.0625 inches, the outer diameter was increased to 0.750 inches, and the inner diameter was expanded to 0.625 inches. These changes allowed for a larger internal volume within the tubes, enabling greater airflow and significantly enhancing the cubic feet per minute (CFM) potential compared to the initial prototype. Additionally, the tube size became identical for the upper and lower parts of the system. By changing the parts to be the same, air flow will be evenly directed when the tubing splits. To achieve even distribution, the system incorporated a y-split junction. Controlling the air flow allows for better adjustments and modifications to increase the effectiveness of the air curtain.

The third prototype introduced an experimental approach by testing different hole shapes, specifically circles and rectangles, to determine their impact on the effectiveness of the air curtain. Each tube in this version contained 15 holes, strategically placed to maximize airflow distribution. After thorough testing, it was found that the shape of the holes had minimal impact on the system's overall performance. As a result, circular holes were selected for the final design, primarily because they were easier to manufacture using a 3D printer, thereby simplifying the production process.

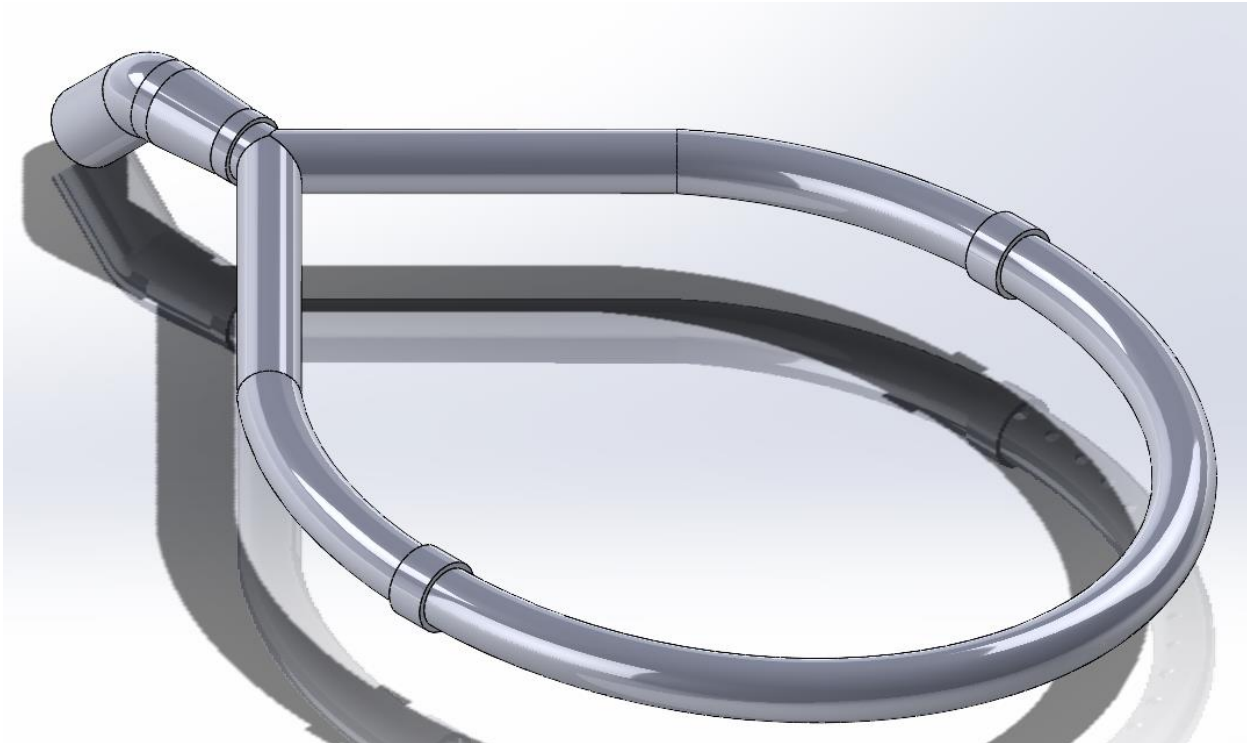


*Figure 15. SOLIDWORKS air curtain assembly model. No Cooling Prototype*



Furthermore, two distinct models were created to evaluate whether incorporating a cooling function in the air curtain would be beneficial or detrimental. The primary concept behind one of these models was to direct the fan's airflow exclusively into the air curtain, thereby creating a stronger and more effective barrier. However, the cooling function was also considered valuable because it helped clear the firefighter's vision. This dual functionality raised the question of whether the cooling effect might detract from the potential airflow that could otherwise enhance the air curtain. By testing both models, critical factors could be evaluated, including visibility, the uniformity of the air curtain, and the overall CFM.

### 3.4.2 Filter Prototyping

During filter design, 3 main hazards were identified, later downsized to two. Initially, the project followed NFPA guidelines while deciding on device requirements; this led to VOC (Volatile Organic Chemicals), CO (Carbon Monoxide), and CO<sub>2</sub> (Carbon Dioxide) filtration to be the driving considerations. CO<sub>2</sub> was later downgraded in importance as the former two compounds are poisonous and/or carcinogenic. The team purchased raw, pelletized carbon, HEPA filters (some with interior carbon layers), and a variety of industrial vapor filters. Designed to cover industrial stacks or outlets and washed for reuse, the industrial filters were purchased to envelop the filter assembly and expand filter lifespan. However, it was found that the added resistance was constraining air curtain effectiveness, air speed, and battery lifespan. For future iterations a removable filter cover could be a useful component, but due to project complexity, i.e. because so many integrated subsystems are being designed simultaneously, the overall design could not afford to support a filter cover without complete redesign. This was also the case for the raw carbon, seen as another potential 'replaceable' and 'reusable' filter method, the OTS (off the shelf) filters were consistent, dependable, and compatible with our motors. When purchasing motor and hose components, filters were included in the injection molded and machined housings of motor assemblies. It was clear that one of the OTS housings would be used in the final design, and prototyping shifted finally to testing, the final stage of filtration design. Design then focused on outfitting the previous project's testing equipment, taking inventory of materials, and manufacturing mating components to fix the new filters onto the equipment. Filter Design sections and filter testing outline the next steps in more detail.



*Figure 16: HEPA filter design*

### **3.4.3 Battery Prototyping**

For the power source, the initial design involved using a boost converter to step up the voltage from 9VDC, generated by 6 AA batteries, to 12VDC. The team procured several off-the-shelf boost converters to evaluate their effectiveness. Testing revealed that the boost converter could successfully step up the voltage from the power pack to 12VDC and power the fan. However, when the variable speed controller (VSC) was turned past half speed, the power draw increased significantly, causing the input voltage to the boost converter to drop to 7VDC, and it continued to decrease as the speed increased. Consequently, with the boost converter, the power source could only operate the fan at half speed or less, as the input voltage was insufficient to consistently step up to 12VDC.

Given these limitations, the team decided to reconsider the power source and examined the performance with just the batteries powering the fan. To achieve 12VDC, the team used 8 AA batteries, which successfully powered the fan at all speeds. Although the team considered using a buck converter, it was deemed inefficient. Buck converters step down the input voltage at the output. To generate a voltage higher than that required to power the fan, the team would need to connect the power packs in series. Using two power packs, each holding 8 AA batteries, in series would produce 24VDC, which a buck converter could step down to 12VDC, meeting the maximum current requirement of 3A. However, this approach was impractical, as it would require firefighters to dispose of 16 batteries at a time to continue powering the air curtain, which was excessive and inefficient. Therefore, the team concluded that using a single 8 AA battery power pack to run the fan was the most practical solution.

## **4. Description of Final Design**



For the final concept, the design ultimately chosen incorporated the best elements as determined by the Pugh matrices (see Appendix B). The input voltage will be 12VDC from 8 AA batteries idea was chosen as the final concept to power the air delivery subsystem. In section 6.2.3, the team tested the battery pack and observed that it could run for 2.5-3 hours in one run at various speeds. This meets the power requirements necessary to run the fan. Although, in theory, this power source concept proved to have about a 1-hour lifespan, it proved to be longer once effectively tested. Another reason why this power source concept was chosen was so that it integrates well with the lifespan of the air filter, which is about 3 hours. The battery is required to endure the lifespan of the air filter since the battery is powering the air delivery subsystem. The two subsystems are integrated together, meaning that if the battery dies or drops below the voltage threshold to power the blower, then the whole device will shut down. Furthermore, if the air delivery subsystem does not function at its full capacity with the battery power source, then the air filter won't either. The filters in the air filter subsystem will be replaced about every 3 hours to ensure peak performance. Therefore, the battery must be able to keep up with the lifespan of the replaceable filters.



Figure 17. Initial Sketches of Final Air Curtain Design Concept

An initial sketch of the final design concept for the air curtain portion of the assembly can be seen in Figure 17 and a finalized CAD model of the air curtain assembly can be seen below in Figure 18.



*Figure 18.* Final CAD model of air curtain portion.

The air curtain attachment to the helmet is printed out of ABS plastic in five separate parts that are fixed together using super glue (see the Product Realization section for more in-depth information on the manufacturing process and an exploded view).

The heat shield is made from polycarbonate.

The magnetic attachment system uses six Neodymium N40SH disc magnets for a total of three points of attachment (one point at the front of the arc of the 3D printed face shield and one more on each of the sides of the arc). Each magnet has an approximate pull force of  $8 \text{ lbf}$  (see Appendix H for the magnet information from the seller) for a total of  $24 \text{ lbf}$  that is sufficient to keep the face shield and air curtain assembly firmly in place on the firefighters' helmets based on the hand calculations at the end of 3.3 Proof of Concept Analysis. The magnetic attachment system is made up of nine components printed from ABS plastic shown in Figure 19 below. One half of the system bolts onto the helmet using nylon fasteners and the other half clamps around the printed air curtain tubing shown in Figure 19 (see Manufacturing Process section).

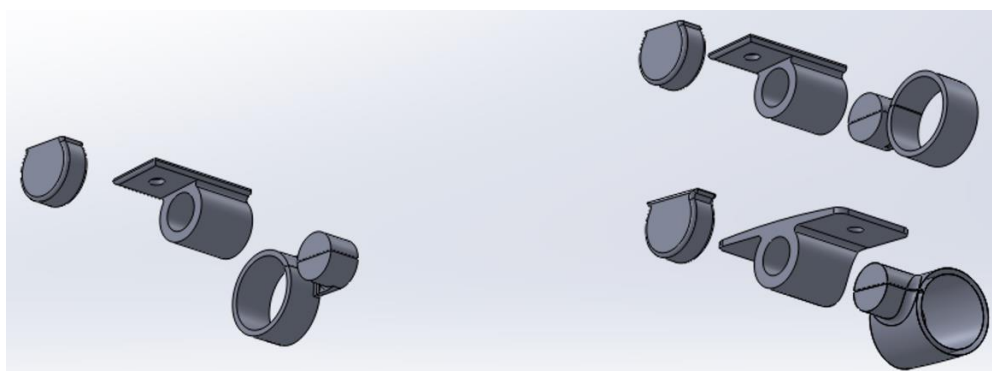


*Figure 19.* CAD model for magnetic attachment system.



The air delivery is provided by the MAC Air Pumper from Rugged Radios. The initial plan was to use a centrifugal fan because centrifugal fans are more capable of supporting the higher static pressures the team expects the air delivery system to generate, but some simple experimentation and hand calculations (described in 4.4 Analysis Results) made it clear that the centrifugal fans commercially available, that were small enough and light enough to be used in the air delivery assembly, were significantly under powered. The MAC Air Pumper delivers nearly 8 times the CFM provided by the Ametek Microjammer used by one of the previous teams. Unfortunately, the AA battery pack used to power the system can not sustain enough current to run the fan at full power for 2 hours straight, so the design cannot utilize all the CFM the MAC Air Pumper can provide for an entire run time. However, discussions with the team's sponsors suggested that getting proof of concept, even if the air curtain is ultimately underpowered, is the primary goal. Creating a custom centrifugal fan and power source to address this issue is now a future goal for the next team to take on this challenge.

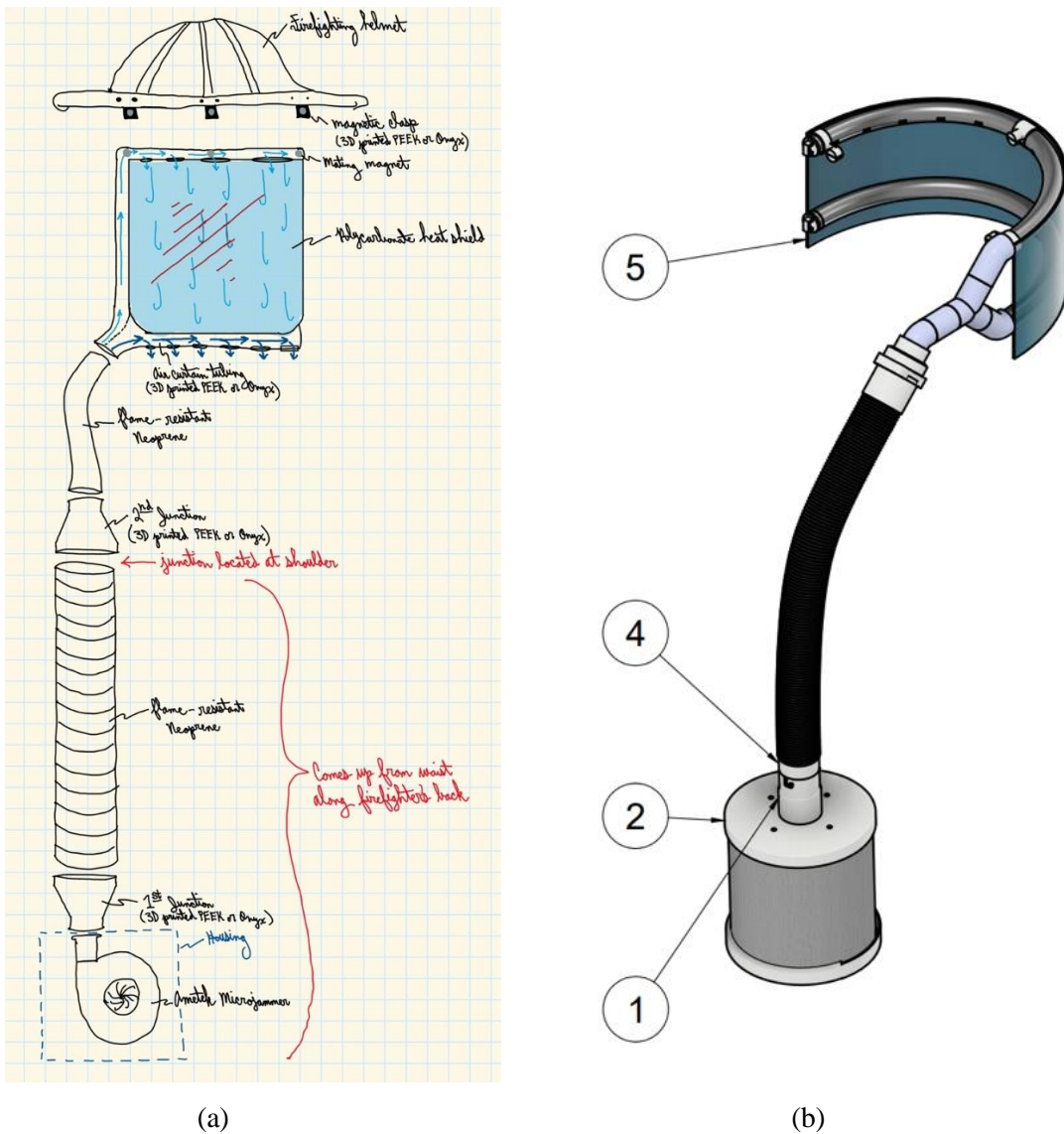


Figure 20. (a) Initial sketch of full assembly final design concept and (b) finalized CAD model of design.

Figure 20 shows an initial sketch of the final design concept for the full assembly compared with the finalized CAD model of the design (see Appendix G for the fully labeled final assembly drawing). The initial sketch was made before it became clear the Ametek Microjammer fan would be insufficient. The actual final assembly has been designed to use the MAC Air Pumper. The assembly begins with the filter and fan system contained within the 3D printed housing (see Appendix G for detail drawings of the housing).



Figure 21. 3M Versaflo Heavy Duty Breathing Tube

The filter and fan housing is connected to a junction secured at the shoulder on the firefighters' packs by a 3M heavy duty neoprene rubber PAPR hose, shown above in Figure 21, with junctions on either end to mate to the fan housing and air curtain that are 3D printed with ABS plastic, shown below in Figure 22.

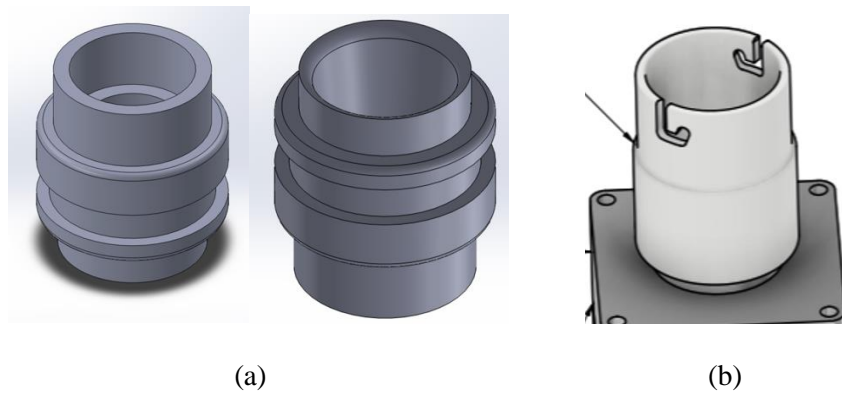


Figure 22. 3D printed (a) squeeze-end junction and (b) twist-end junction for PAPR hose.

#### 4.1. Filter Design

The filter is made of a triple stack of three different types of filters, a course outer mesh filter, a HEPA-13 filter and an inner activated charcoal filter. The filter stack is set up in this order to filter largest to smallest as the particles travel farther into the system. The mesh will capture large particulate that will more quickly clog or block the HEPA filter. The team decided to begin testing and designing around the PUREBURG B-D02H-Replacement shown in Figure 11 as it has many of the features that are needed with minimal modifications, such as already being integrated with a coarse mesh and activated charcoal filter in the appropriate spots, that will make modification and replacement of those two parts much easier. An addition activated charcoal filter will be added to the inside of the HEPA filter made from an activated charcoal cloth allowing for easy installation while still providing a large surface area to volume ratio.



*Figure 23.* PUREBURG B-D02H Filter with activated charcoal cloth liner.

As discussed in Section 3.2A, a cylindrical design for the filter was chosen. Since the inlet for the fan used in the design is 3 inches, a circular filter efficiently covering the fan inlet would have a surface area of  $28.27 \text{ in}^2$ . Whereas by using the cylindrical filter with a length of 5 inches, it has a surface area of  $82.40 \text{ in}^2$  for both the mesh filter and the HEPA filter.

#### **4.2. Electrical Design**

Originally, the team contemplated employing a buck converter due to its typical function of stepping down voltage from a higher level to a lower one, commonly utilized for power management purposes. However, while researching different brushless blowers capable of generating high CFM, it was found that the majority operate at 12VDC or higher. The team decided it was impractical to require firefighters to carry a 24V power pack only to step it down to 12V.

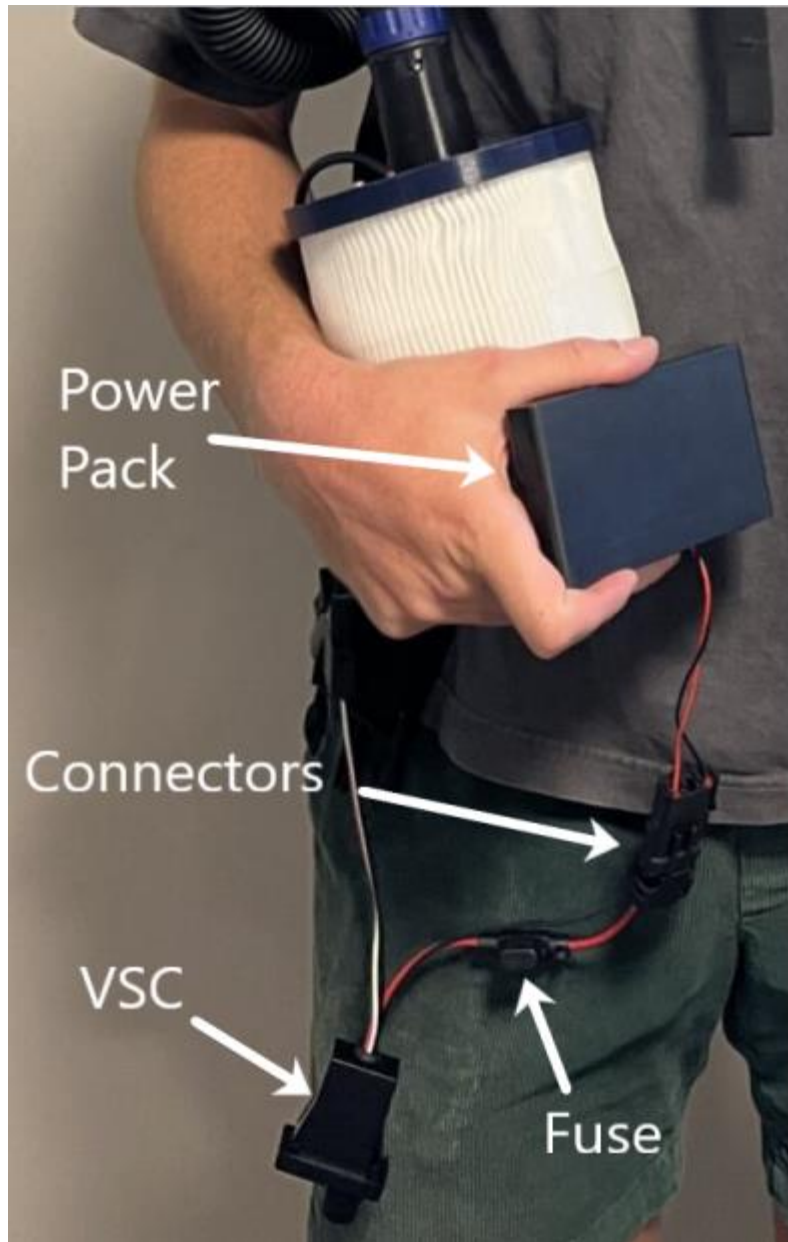


Figure 24. Electrical Circuit of Fan Motor Connected to Full System

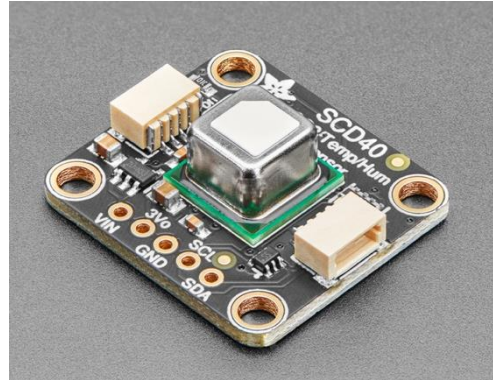
To circumvent this issue, the team then considered using a boost converter that would modestly elevate the voltage, maintain efficiency, and marginally extend battery life. However, when testing the boost converter configuration, the power draw was so large it wouldn't allow the fan to get past half speed and would drain the battery considerably due to power loss through the converter. Figure 24 above displays the current configuration involves utilizing a 12V AA battery holder interfaced with the variable speed controller (VSC).



Figure 25. Full Assembly Spread Out

Using a battery pack to power the fan offers significant advantages in terms of compactness and reliability. The small and easily storable power pack effectively powers the fan at all speeds without the substantial power loss observed with the converter. This point will be further elaborated in Section 6.2.3. While the team acknowledges the potential benefits of using a converter, for our specific requirements, the battery pack has proven to be the most effective, reliable, and compact solution for the prototype.

One of the last major electrical design components being utilized in the air respirator design by First Respire is the use of Adafruit SGP30 Air Quality Sensors and Adafruit SCD-40 Temperature and Humidity Sensor. The toxic gases that must be filtered out by the air filter subsystem are VOCs and CO. The SGP30 Air Quality Sensor was selected for its ability to provide readings of Total Volatile Organic Compound (TVOC) as opposed to other sensors on the market that only indicate the presence of VOCs. The SGP30 provides detailed measurements of the actual concentration of total VOCs (TVOCs) that can then be analyzed to determine air filter quality and efficiency. Additionally, the SGP30 Air Quality Sensor was chosen for its capability to measure equivalent CO<sub>2</sub> (eCO<sub>2</sub>) levels. Unfortunately, there are no compact, CO-specific sensors available on the market that fit within the test stand configuration, as seen in Section 6. The team's research determined that there are no CO-specific sensors that can be easily connected to an Arduino Uno or that provide CO level readings. The only readily available CO-specific sensors are household carbon monoxide detectors, which do not output CO level readings but merely detect the presence of CO. Similarly, the few Arduino-compatible CO-specific sensors only detect CO presence without providing level measurements, which is insufficient for the team's needs as we require precise CO level data. While eCO<sub>2</sub> is not a direct measurement of CO, environments with elevated eCO<sub>2</sub> levels can sometimes correlate with higher CO levels, especially in poorly ventilated spaces where various gases accumulate together. Therefore, using a SGP30 Air Quality Sensor is the next best option to ensure we get valuable data on air quality as it measures both TVOCs and eCO<sub>2</sub>, as further described in Section 6.1.1 and Section 6.2.12.



*Figure 26. SCD-40 Sensor Measuring Temperature and Humidity*

Similarly, the SCD-40 Temperature and Humidity Sensor was selected for its accuracy in temperature readings. The significance of the SCD-40 sensor lies in its ability to detect temperature variations before and after the fan motor circulates air through the filter. This capability is crucial because it ensures that the air filtered by the device remains cool, preventing firefighters from overheating during their shifts when wearing the device. The cooling aspect of the air respirator is a key selling point for wildland firefighters, making it essential to ensure the device effectively provides this functionality. The sensors mentioned are shown below.

### **4.3. Mechanical Design**

The mechanical design encompasses most of the respiratory protection device assembly from all the housing and tubing to the fan and the magnetic attachment system. Much of the mechanical design was discussed in 4. Description of Final Design, but some more detail is provided here.

A closer examination of Figure 21 shows, the 3M Versaflo tubing uses a twist junction at one end (corresponding to mating junction (b) in Figure 22) and a ring that must be squeezed open to connect and disconnect on the other end (corresponding to mating junction (a) in Figure 22). The connection between the filter and fan housing and the Versaflo tubing will use the twist junction so that the squeeze end is located at the firefighter's shoulder and will be easier for them to manipulate with one hand.

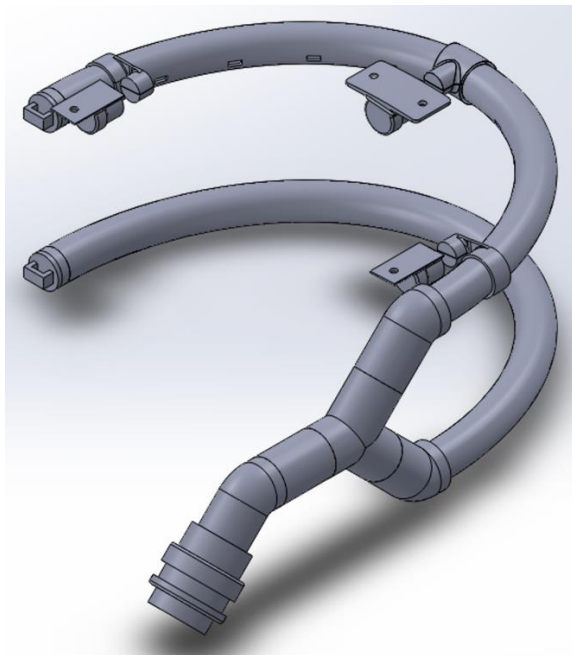


Figure 26. SOLIDWORKS model of the air curtain design with magnetic attachment system.

The use of the magnetic attachment system was chosen because it provided a way to quickly don and doff the air curtain assembly (see 6.2.5. Donning/Doffing Time Test).

#### 4.4. Analysis Results

One of the most critical components of the air delivery system that needed to be selected was the fan system. There was the option of using a centrifugal fan, an axial fan, or a mixed flow fan. The primary trade-off was between high volume air flow and high-pressure air flow. Axial flow fans can provide a lot of volume but are incapable of supporting a lot of back pressure unless multiple axial flow fans are placed in series, which isn't a great option for a device that needs to reduce weight and size to a minimum. Centrifugal fans lie on the opposite end of the spectrum, providing high pressure air flow, but at a low volume compared to axial fans. For this project, which will require a fan capable of producing high pressure differences to be able to pull air through an increasingly clogged filtration system and generate the high velocity flow needed to create the air curtain, the centrifugal fan seemed intuitively to be the best option and the totals in the team's Pugh matrix (see Appendix D) supported that theory. However, once the team did some simple testing using the 119350-51 Ametek Microjammer brushless blower that the Greater Respirator group utilized in their air curtain design, it became clear that the centrifugal fan option might not be the best way to go in practice. The team used a power source in an EE student project lab to run the fan while covering the blower intake with part of the modular filter assembly used by the Greater Respirator group and then with an N95 mask (*Figure 28*).



*Figure 28. Ametek Microjammer testing*

Even based on this simple testing, the air flow from the fan was significantly reduced. Attaching a short piece of hose to the fan outlet without any sort of filter over the fan inlet also resulted in a large decrease in airflow speed from one end of the hose to the other. In combination with the calculations in 3.3 Proof of Concept Analysis, this made it clear that the small Ametek centrifugal fans available were not sufficiently powerful for our application and no other company seemed to offer stronger small centrifugal fans than what Ametek offers.

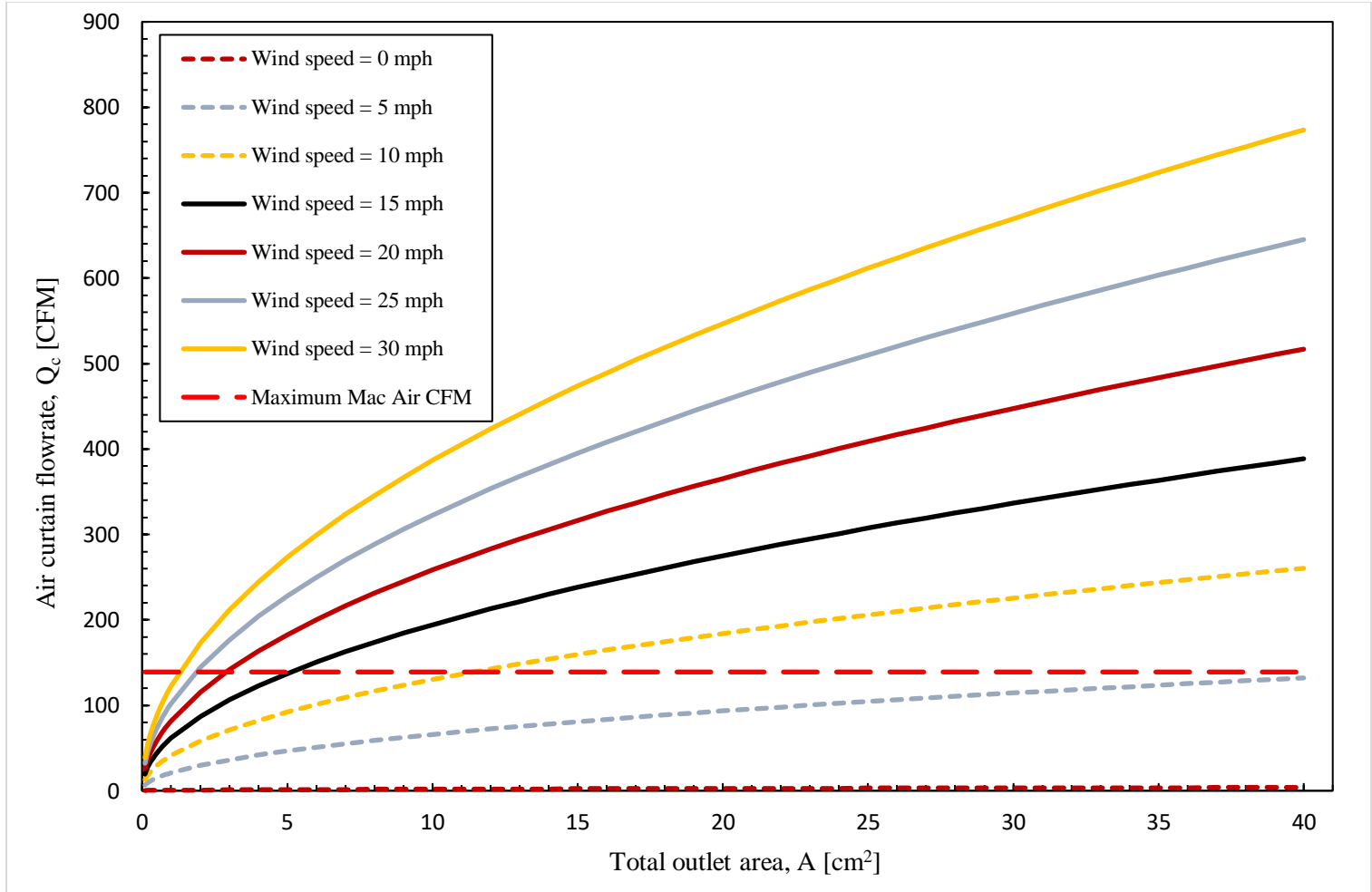


Figure 29. Minimum air curtain flowrate as a function of wind speed and total outlet area.

Figure 29 shows the results of the calculations discussed in 3.3 Proof of Concept Analysis. The plot gives the air curtain flow rate required to maintain the integrity of the air curtain (and by extension, the quality of the air delivered to the firefighters) as a function of the total outlet area on the 3D printed air curtain (Figure 29) for different wind speeds. The maximum CFM that the MAC Air Pumper can deliver is also plotted for reference. Very precise values from the plot do not have a great degree of value because of the many assumptions involved in the analysis, but the general behavior is a helpful guide for fan selection and design of the air curtain outlets. It is immediately clear that a lot more CFM was needed than the 19 CFM that the Ametek Microjammer could supply, which is why the switch was made to the MAC Air Pumper with a maximum output of 139 CFM. Based the plot, it is also clear that, for the air curtain to be potentially strong enough to withstand any sort of wind, the total outlet area must be very small. Both of these realizations have helped save valuable time in the prototyping process and shaped the design of the 3D printed air curtain.



#### 4.5. Cost Breakdown

The respirator's materials are split into the three sub-assemblies: air delivery assembly, filter assembly, and electronics. Each sub-assembly has a breakdown of components used, quantity purchased, vendor, price, and date delivered.

*Table 3. Cost Analysis*

Air Delivery				
Component	Quantity	Vendor Information	Price	Date Delivered
Helmet Air Pumper Bundle	1	Rugged Radios	394.82	13-Feb-24
800cc Onyx FR-A Spool	1	Markforged	260	26-Jan-24
3M Versaflo Heavy Duty Neoprene Rubber Breathing Tube BT-40	1	3M	78	N/A (from previous project)
Weather-Pack Connectors kit	1	Amazon	21.98	99-Feb-24
Ucreative High Temperature Reinforced Silicone Vacuum Tubing	1	Amazon	13.99	29-Feb-24
Polycarbonate Sheets	3	Amazon	29.85	13-Feb-24
Neodymium Magnets	7	Magnets4Less	24.06	27-Feb-24
Foam	1	Amazon	15.43	27-Feb-24

Electronics				
Component	Quantity	Vendor Information	Price	Date Delivered
Arduino/USB	1	Arduino	41.69	9-Feb-24
SCD-40	1	Adafruit	202.15	13-Feb-24
SGP30	4	Adafruit	20	27-Feb-24
AA Batteries	28	Amazon	20	Continuous

Filter				
Component	Quantity	Vendor Information	Price	Date Delivered
Activated Charcoal	1	Delta Absorbants	20.99	20-Feb-24
Micron Filters	1	USPlastics	8.81	26-Jan-24

#### 4.6. Safety, Maintenance, and Repair Considerations

Firefighter safety is among the top priorities for First Respire. Safety regulations have guided the design parameters over project conception, research, requirements, and now prototyping and testing. To ensure the device will remain reliable once in use, methods of maintenance and repair must now also be considered.



First Respire has evaluated various safety, maintenance, and repair considerations. The following sections will describe the most prominent considerations in the prototyping, testing, and next steps.

### 4.6.1. Safety

In terms of safety, the following objectives were considered and coupled with design requirements: respiratory resistance, duration of use, heat resistance, communication interference, donning/doffing, motion or vision inhibition, air cooling, and filtration quality. A major consideration spanning every component in the design is material selection. The temperatures and wind speeds experienced in the field by WUI firefighters not only pose risks to the operator directly, but also to the integrity of the equipment experiencing these conditions. To confirm proper material selection and device design, no visible deformations or evidence of combustion should appear during heat resistance testing. Changes to the chemical composition of components could lead to numerous exposure hazards such as smoke, hot surfaces, or dripping; changes to the structure or shape of components could lead to loss in efficiency, malfunction, or failure. All other comparable wildland firefighter equipment requires these outcomes to be mitigated [14]. By selecting component materials, filter media, and electronics suited for the described environments, testing will verify they meet project specifications and clear them for use in the device design.

Along with the respirator, the face shield will be utilized for more effectiveness and safety. Debris and particles in extreme weather conditions batter the firefighters. Most firefighters use glasses, goggles, or lens apparatus that are durable enough to withstand the flying particles that damage and obscure vision. The standards of vision defined in the NFPA 8.5.5.1 for lenses will apply to the face shield since the face shield is transparent, yet durable. The standard field of view, 100° laterally, and range of motion the firefighters deal with will be considered and applied to face shield visibility. Once the face shield becomes worn out and visibility is hindered due to scratches from particulates and dust accumulation over months of use, firefighters have the option to replace the face shield. As a temporary solution, firefighters can wipe off dust from the face shield when build up occurs.

Another safety risk that was heavily considered by First Respire was the use of lithium batteries as a power source for the device as lithium batteries pose a significant fire risk when exposed to high temperatures or flames. In the early design stages, various power sources were evaluated based on lifespan, flammability, size, weight, and compatibility referred to in the power design Pugh matrix seen in Appendix B. Rechargeable non-lithium-based batteries were the front runner for the power source of the device until speaking with Frank Frievalt, the current WUI FIRE Institute Director at Cal Poly. With over 40 years of experience in roles from firefighter to Fire Chief, Frank Frievalt's input is highly valuable and heeded. Frievalt stated that wildland firefighters typically carry AA batteries in their backpacks during shifts, therefore having to carry an additional type of battery exclusively for the air respirator device was deemed



impractical and burdensome, potentially reducing the device's adoption among firefighters. Consequently, First Respire opted against using rechargeable batteries and instead designed the device to operate on AA batteries.

Another critical set of safety aspects to evaluate pertains to the device's ergonomics. Addressing how the utilization of the device can affect factors such as range of motion, field of view, air temperature, donning and doffing time, sizing and weight of device, and respiratory resistance is key in ensuring firefighter operations are not limited, but instead heightened. This device is designed to improve firefighters' breathing without interfering with their other tasks and operations.

This is a safety concern for two main reasons. The first is if the operator feels uncomfortable wearing the device, they are less likely to use it. The second is that decreasing efficiency of other equipment or general motion poses an immediate risk. Clearly, the more important of the two, the second reason mentioned was examined more heavily in the early stages of the design. Requirements such as adjustable sizing, field of view, and don/doff time are (comparably) easy to conform downstream in the design process.

The most limiting ergonomic factors based in safety include air temperature, range of motion, and respiratory resistance. Luckily, air cooling is built into the air delivery system; by utilizing volumetric flow and outlet size, air traveling through the assembly will be cooled upon exiting the small hose openings as pressure is reduced dramatically. When meeting with the team, Frank Frievalt also stressed the importance of air cooling, primarily for two reasons: comfort and heat injury mitigation. Air cooling, to the best of Frank's knowledge, would drastically increase the number of firefighters who would choose to wear the device. Beyond the main goal of providing clean air to the operator, cool air may encourage firefighters to use the device regardless of inherent added weight, sound, and complexity. Constant reduction of thermal energy will add a uniquely comfortable experience for the wearer. This is coupled with Frank's second consideration: reducing heat injuries. More specifically, when in operation, the design will decrease temperature in face and head, reducing risks such as heat stroke or delaying the other effects such as dehydration.

### **4.6.2. Maintenance and Repair**

Repair from a critical failure will be rare often impossible to fix in the field in wildfire conditions, however, failures will be highly unlikely as the maintenance regiment will control the most venerable product components. By selecting materials and fastenings well, maintenance instead becomes a primary concern.

Sensors will be implemented in various locations on the device post-prototyping. The group intends on creating analog outputs from integrated sensors so an HMI (Human-machine interface) may be developed in the future. These sensors will include airflow, battery-life, and filter status; The first, airflow, will be



measured near outlet; Battery-life will be measured by using available information used by the boost converter; filter status will compare battery output to outlet speed and determine if the filter's resistance has increased due to use.

A more pressing maintenance concern is the prototype's ability to replace the filter components and don/doff hastily. Filter stacks are designed to easily insert and lock, as well as detach when necessary. The team suspects additional filter stacks and batteries will be the only extra equipment needed with the prototype; these will mitigate most common maintenance concerns. Another aspect of maintenance being addressed at design meetings is the dust removal from the face-shield. Over time, all surfaces collect dust and debris, in a wildland fire, environments will be experienced where this effect is nearly instantaneous. Designing with these environments in mind will ensure this concern is mitigated.

### 4.6.3 Sustainability

Cal Poly defines sustainability as the ability of the Natural and Social Systems to survive and thrive together to meet current and future needs . The three spheres of sustainability consist of environmental, economic, and social factors. Although in theory other routes can be used to make the air respirator device more sustainable, the most important aspect to consider when designing the device is the firefighter's needs. Thus, First Respire prioritizes meeting the requirements of the firefighters over absolute sustainability. That said, First Respire still aims to create a device designed for energy efficiency, refurbishment, and disassembly.

To enhance sustainability, First Respire considered utilizing rechargeable batteries to power the fan motor of the air respirator device to significantly reduce the consumption of disposable batteries used by firefighters. However, after speaking with Frank Frievalt, WUI FIRE Institute Director, he stated he thought it best to not use rechargeable batteries since firefighters already carry around AA batteries for their other required daily equipment, meaning they would be opposed to having to carry a different set of batteries on top of that. Moreover, he emphasized that wildland firefighters typically spend around 8-12 hours away from base camp, suggesting that rechargeable batteries may not be practical for their needs. Once again, given that Frank Frievalt is a retired Fire Chief and firefighter with over 40 years of experience, First Respire decided to choose AA batteries instead. Since batteries are consumables and not inherently environmentally friendly, First Respire is striving to develop an efficient circuit design that aims to extend battery life, reducing the frequency of battery consumption, and thereby mitigating environmental impact to the best of their ability.

From a sustainability standpoint, refurbishment involves repairing, renovating, or restoring a product. By upgrading or modernizing older products, refurbishment aids in prolonging the lifespan of products.



First Respire is prioritizing sustainability by designing an air respirator that seamlessly integrates with the helmets already in use by wildland firefighters, eliminating their need to purchase or utilize new helmets. This approach embodies refurbishment principles as it extends the lifespan of existing equipment and enhances the functionality of current helmets. In addition, using magnets to attach the air respirator device to the regular wildland firefighter helmet satisfies the need to keep the air respirator device as close to current equipment that firefighters already use, increasing their likelihood to wear the device. The fan motor is also ideally supposed to be long-lasting and durable in terms of material and lifespan. Refurbishment and disassembly go hand in hand when it comes to extending product lifespan.

Designing for disassembly is a sustainability-oriented approach that involves creating products to simplify their disassembly and recycling at the end of their life cycle. First Respire is purposely designing the air respirator device to be easily disassembled as possible while still having structural integrity. The intention is to make the device easy to take off and put on for firefighters while on the job. The device is considered to have an easy disassembly since the shield portion of the device is attached to the helmet with intensely strong magnets that guarantee the device stays in place but can still be taken off without an unusual amount of force if needed. In addition, First Respire is also considering different ways of cleaning dust buildup off said shield to keep max visibility for firefighters while working on the line. Therefore, making the shield detachable also enables firefighters to conveniently clean it as necessary throughout their shift, ensuring the shield's reusability. Another component considered for easy disassembly and replaceability was the air filters, as they are being designed to be relatively small and light, yet functional, to be carried by the firefighters in their backpacks. In addition, First Respire has designed the air filter to be attachable as well for relatively quick donning/doffing. For this device, ensuring the creation of easily attachable components is crucial to maintaining firefighter safety during period of poor air quality or when airflow is insufficient for comfortable breathing — especially in scenarios of sudden device malfunction or filter blockage.

## 5. Product Realization

After the CDR, first priority became fabricating our ever-changing iterations of air curtains. CAD, CAM, slicers, and simulation software utilization made it possible for the team to quickly prototype many designs. During manufacturing, designs were often updated, reproduced, or scrapped, changing the style of our design approach and often finalizing small aspects of subsystems or components along the way. This section will briefly describe the manufacturing process used to achieve certain systems, future manufacturing plans and suggestions, as well as a brief cost analysis for a future scaled production of the final product assembly.

The product realization phase encompassed the detailed development and refinement of the air respirator system, translating conceptual designs into a functional prototype. This stage included iterative testing, integration of subsystems, and adjustments based on feedback to ensure the final product met all operational and safety requirements. The focus was on delivering a reliable, user-friendly device that enhances the safety and effectiveness of wildland firefighters.

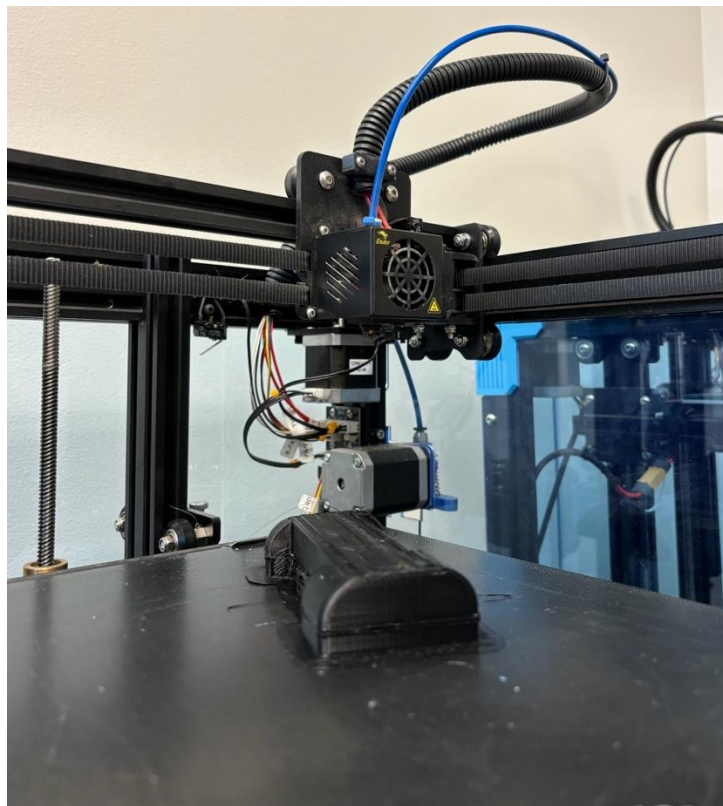


*Figure 30. 3D printer used for various components of air curtain assembly*

### 5.1. Manufacturing Process



This section outlines the manufacturing process, highlighting the key steps involved from initial material selection to final product assembly. It focuses on the methods, techniques, and technologies utilized to ensure efficient production and maintain high-quality standards throughout each stage.

### 5.1.1. Air Curtain Assembly



*Figure 31. Air curtain assembly attached to helmet with magnetic attachment system.*

The air curtain assembly is comprised of everything, pictured above in Figure 31 that attaches directly to the helmet using the magnetic attachment system, including the heat shield and the magnetic attachment system itself. The majority of the air curtain assembly was 3D printed from ABS plastic. The intention was to print using Onyx FR-A filament, but the team discovered, after ordering the spool of material, that there were no printers on campus capable of printing that filament (see the Future Direction/Recommendations section at the end of the report for more information about future manufacturing recommendations related to this issue). Referencing the Appendix G – Final Drawings, the air curtain assembly was composed of components K through V. Components K through O were assembled as shown in Figure 32 below and fixed together using super glue.

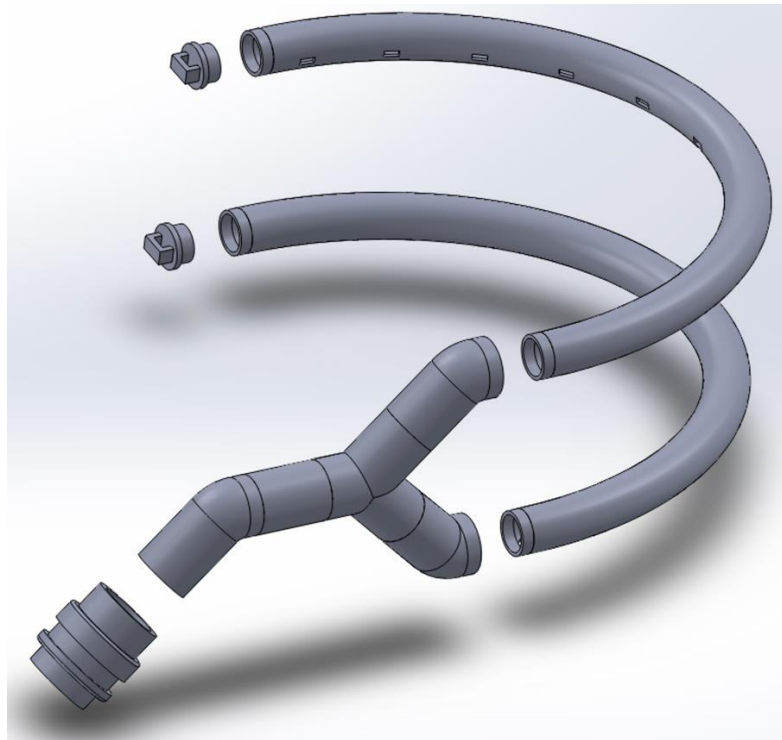


*Figure 32.* Exploded view of assembly of components K through O.

The magnetic attachment system (components P through V) is assembled as shown in Figure 33 below. The curtain attachment pieces (components P, Q, and R) are clamped over the cooling curtain bar (i.e. the top bar) and then each is super glued shut with a neodymium magnet inside.

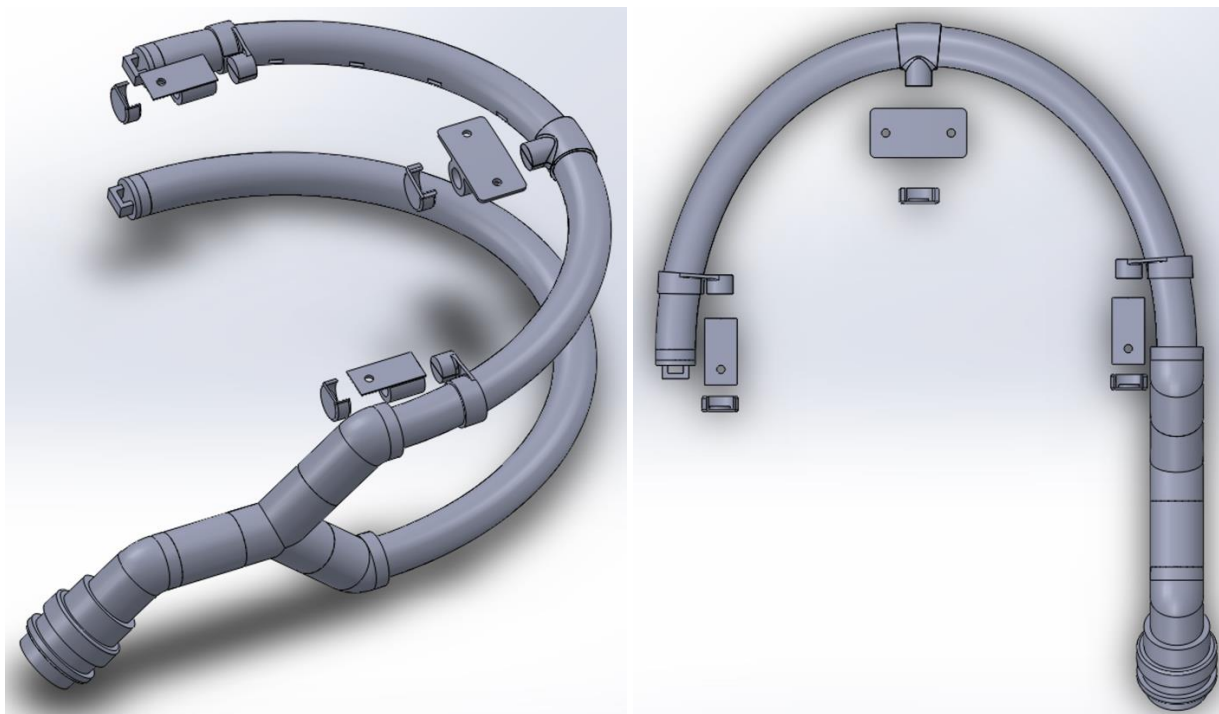


Figure 33. Exploded view of magnetic attachment system assembly of components A through E.

Holes are drilled into the helmet and then the helmet attachment pieces (components S and U) are bolted to the helmet using M4 nylon nuts and bolts, as shown in Figure 34 below. The neodymium magnets are then placed into the helmet attachment pieces and the caps (components T and V) are super glued on.



Figure 34. Helmet attachment pieces bolted on with nylon hardware.

Lastly, the heat shield is cut down to size using a table saw and then holes are drilled along the top and bottom edges so it can be zip tied to the bars of the air curtain assembly as shown in Figure 35 below.



*Figure 35.* Heat shield attached to air curtain using zip ties.

Once the whole air curtain is assembled, super glue is added around the edges of the magnetic attachment system pieces on the helmet and on the 3D printed curtain bars to help keep them from rotating.

### 5.1.2. Filter Assembly

The filter assembly was composed of three main parts, the filter itself, the filter cap on the bottom of the filter, and the fan cap on the top of the filter. The final filter is made of two key parts, a HEPA filter purchased from PUREBURG, and an internal liner made of activated charcoal fabric cut to form a tube that is inserted into the HEPA filter. The caps are both 3D printed from PLA plastic.



*Figure 36:* Showing the final filter assembly, with the filter cap printed white PLA, and the fan cap printed blue PLA, on either side of the filter combination.

### 5.1.3. Fan Assembly

Most parts from the fan assembly came from the MAC-1X Single Person High Output Helmet Air Pumper, which provided the fan, fan reducer, and fan mount for the assembly. The additional join connecting the fan reducer to the PAPR hose is 3D printed from ABS.

The team connected the power pack directly to input of the VCS and the output of the VCS goes to the fan which is housed within the filter. The connectors used to connect each were three pin weather pack connectors.

## 5.2. Future Manufacturing Recommendations

The 3D printed parts in the final design are not heat resistant enough to withstand the extreme environmental conditions that firefighters often encounter due to the ABS material. Exposure to high temperatures, flames, and intense heat can cause these parts to fail. To address this issue, the next iteration of the design will



utilize Onyx FR-A filament, a high-performance material known for its exceptional heat resistance and durability. Onyx FR-A can withstand temperatures up to 145°C (293°F), making it suitable for the harsh conditions firefighters face. This material not only provides the necessary thermal stability but also maintains structural integrity under high stress and heat. By incorporating Onyx FR-A filament into the future design, the components will be more durable, reliable, and capable of withstanding prolonged exposure to extreme temperatures, ensuring the safety and longevity of the equipment for the wearers.

Additionally, the tubing from the fan to the air curtains needs to be more flexible and lightweight. The current tubing, due to its rigidity and weight, imposes a noticeable burden on the wearer's head, even though it does not impede their range of motion. This discomfort is primarily because the inflexible nature of the existing tube causes it to shift and exert unwanted pressure. To address this, a lightweight and flexible alternative tubing material is necessary. This material should be capable of maintaining the necessary airflow without adding significant weight or stiffness, thereby enhancing comfort and usability for the wearer.

Furthermore, the fan's output duration on maximum power depletes the batteries much too quickly. The fan is designed to operate optimally with a 22V car battery; however, when used with 12V batteries, it drains them rapidly, leading to frequent battery changes or recharges that can be impractical in the field. This inefficiency is a significant drawback, as reliable and long-lasting power is crucial for the sustained operation of the air curtain system. Future solutions must consider either implementing a more robust battery system capable of supporting the fan's high-power demands or adopting a different fan that balances energy efficiency with sufficient power output.

### 5.3. Cost Estimation for Future Production

Taking into account the cost of raw and bought materials, labor, equipment, and overhead, the team was able to simulate an estimated scaled production cost analysis, featured below. The highest cost, that of the capable printer, is the initial purchase price (not included in the total cost figure). Instead, maintenance and power costs were calculated (proportional to units simulated of course) and included into the total. The simulation simulated 500 units being manufactured over one year. This amount would merit a single, part-time worker, as well as an occasionally contracted engineer to run quality studies and validate requirements. The second highest cost would be that of a physical facility, an investment that would likely be in CA, and thus very expensive, much like the elevated power cost (\$.21/kWhr). If a remote or free location to set up production was readily available, the project could easily half it's expected cost.



AIR CURTAIN ASSEMBLY SCALED DESIGN COST SIMULATION								
PROCESS	NAME	DESCRIPTION	COST (\$)	QTY	UNITS	TOTAL		
MATERIAL COSTS	Helmet Air Pumper Bundle	Filter, VSC, Motor	\$395.00	1	bundles	\$395.00		
	Onyx FR-A Spool	3D filliment containing carbon fiber	\$0.52	50	grams	\$26.00		
	PolyCarb Faceshield	Heat resistant shielding support mateiral	\$40.00	1	shields	\$40.00		
	Ucreative Tubing	High temp. silicone vacuum tubing	\$14.00	1	tubes	\$14.00		
	Neodymium Magnets	Magnets to fix curtain assembly to helmet	\$12.00	3	magnets	\$36.00		
	Weatherpack Connectors	Connects pumper bundle components	\$22.00	1	connector	\$22.00		
						UNIT MATERIAL COST \$ 533.00		
CAPITAL COSTS	ONYX X3 Printer	Onyx FR-A compatible equipment	\$45,000.00	1	printers	\$45,000.00		
	ONE-TIME EQUIPMENT COST \$ 45,000.00							
	Annual Maintenance	Trouble-shooting, repairs, updates	\$300.00	1	est. cost	\$300.00		
	Unit Power Cost	Cost of power used in sustained production	\$0.21	100	kWhr	\$10,500.00		
LABOR COSTS	Monthly Overhead	Rent, remaining utilities	\$2,500.00	12	monthly	\$30,000.00		
	RECURRING EQUIPMENT AND CAPITAL COST \$ 40,800.00							
	Technician/Assembler	Low wage worker for assembly	\$15.00	750	hours	\$11,250.00		
LABOR REQUIREMENTS	Quality/Mechanical Engineer	Experinced engineer for safety and quality	\$60.00	75	hours	\$4,500.00		
	ANNUAL WAGE COST \$ 15,750.00							
	ASSEMBLY TIME / UNIT	TEST TIME / UNIT	UNITS	500	TOTAL COST			
	1.5	0.15	hours					
	750	75	hours	UNITS SIMULATED				

Fig 37: Scaled Cost Simulation (500 units)

## 6. Design Verification and Testing

The design and verification testing phase focused on developing a comprehensive air respirator system tailored for wildland firefighters. This phase involved creating and integrating air filtration and delivery subsystems, followed by rigorous testing to ensure the device met performance and safety standards. The goal was to verify that the final product effectively improves air quality and supports firefighters in their operational environment.

### 6.1. Test Stand for Filtration Testing

Before finalizing anything with the filtration method, a testing stand has been designed and manufactured to test the filter subsystem. The testing stand will assess the filter's filtration efficiency and compliance with the engineering specifications outlined in earlier sections. Figure 38 shows the full test stand assembly below.



*Figure 38.* Picture of the test assembly

The testing stand is made up of six key components shown in Fig 38, the Test Stand Baseplate, Filter (or Filter Stand In), Sensor Outlet Holder, Test Rig Mount, Arduino Covers/Sensor Holder and Filter Cap. The Test Stand Baseplate (Appendix F) serves as the foundational support for the entire testing rig. Its primary role is to provide stability and ensure that the entire system remains level and secure. Beyond its load-bearing function, the baseplate also plays a crucial role in maintaining an airtight seal around the base of the Filter Enclosure (Appendix F). Constructed from clear acrylic, the Filter Enclosure allows for visual monitoring during experiments. This transparency is critical for observing the filter's performance and any potential issues that may arise during testing. The fan is attached into Test Rig Mount (Appendix F) by sandwiching it between the filter and the outlet it ensures efficient circulation and controlled air movement. Designed with modularity in mind, the housing can be easily removed for maintenance or adjustments between tests. The test rig mount securely holds the filter or test material, using the Filter Stand In (Appendix F) to create a seal with the fan and test rig. Finally, positioned at the open side of the filter, the Arduino Filter Cap (Appendix F) prevents any contaminated air from entering during testing while holding the sensors and Arduinos in the test chamber.



### 6.1.1. Sensor Configuration in Test Stand

To provide a useful metric for the filtration data without requiring extensive sensor system calibration, two sets of sensors were employed. An SGP30 sensor and an SCD40 sensor were attached to the bottom of the filter, with the sensors facing the inside of the test chamber. These two sensors recorded the initial gas concentrations before passing through the filters. An additional set of each sensor was placed on the outlet side of the test stand, after the filter. By comparing the initial concentration readings from the first set of sensors to the readings from the second set, the percent reduction in gas concentration was determined. This comparison provides a reliable metric for assessing filter quality and efficiency.

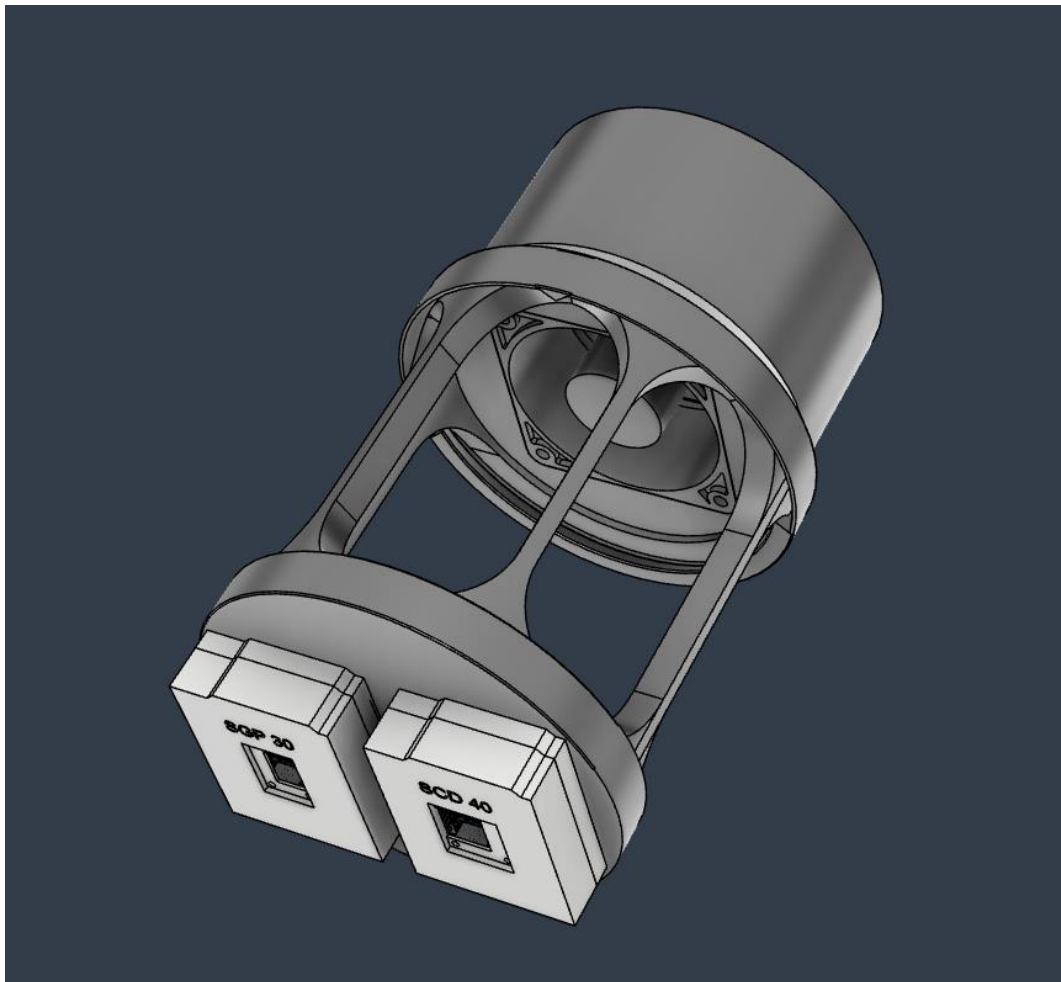


*Figure 39:* Schematic diagram of the filtration test setup showing the placement of SGP30 and SCD40 sensors on the inlet and outlet sides of the filter for measuring initial gas concentrations.



### 6.1.2. Sensor Data Utilization in Test Stand

The SGP30 and the SCD-40 sensors were interfaced with an Arduino Uno as its microcontroller to detect total VOC (TVOC) concentration levels, equivalent CO<sub>2</sub> (eCO<sub>2</sub>) concentration levels, temperature, and humidity of the air after it passes through the filter all contained within the test stand. Positioning of the Arduino Uno was placed close to the sensors to maintain proper wiring. Adafruit provided the software needed to run both sensors and output the concentration level of TVOC, eCO<sub>2</sub> and readings of the temperature and humidity in the test stand. Refer to Appendix L to view the software. The sensors' input and output data were extracted to compare and analyze values to show the filter's effectiveness. By doing so, visual aid graphs were created to see the trends and patterns of the data, which indicate if the filter is working as intended as seen in Section 6.2.11.

## 6.2 Test Procedure

Upon completing the first prototype's construction, three key areas have been identified as crucial factors for the design: power supply, filter efficiency, and air curtain strength. The longevity of the battery life is of paramount importance. Given that wildland firefighters often work shifts lasting at least 16 hours, it's crucial that the device can operate for extended periods without frequent battery replacements. Ideally, the device should be designed so that the batteries need to be replaced only 2-3 times per shift.

To test this, the team will set up a real-world scenario by connecting the batteries to the device as if they are in the field. They will then monitor the device under normal operating conditions and measure how long the batteries last. This will provide a more accurate understanding of the battery lifespan and help identify potential areas for improvement.

The efficiency of the filters is another critical aspect that needs testing. The device must effectively filter out particulate matter (PM) and volatile organic compounds (VOCs) from the air firefighters breathe. To ensure this, sensors will be placed before and after the filter to compare the readings. This will allow for accurate measurement of the filter's effectiveness in real-time. The data collected from these tests will be analyzed to ensure the filters provide the necessary protection. If the filters aren't performing as expected, the team will investigate ways to enhance their efficiency.

In addition to battery life and filter efficiency, the team has identified the strength of the air curtain as a third key specification. The air curtain plays a vital role in protecting firefighters from smoke and other airborne hazards. Therefore, it's essential that it has sufficient strength to provide an effective barrier. To



test this, the team will measure the velocity and volume of the air being expelled by the device. They will also assess how well the air curtain can maintain its strength over time and under different conditions. This will help ensure that the device provides a robust and reliable air curtain.

By following this comprehensive testing procedure, the team can thoroughly evaluate the performance and effectiveness of the respirator. The results will provide valuable insights into how well the respirator can protect firefighters in hazardous environments. This data will also highlight areas where the respirator can be improved to provide better protection. Ultimately, this will help ensure that the respirator is reliable and effective when needed most, contributing to the safety of firefighters working in hazardous conditions.

### **6.2.1 CFM Testing**

The CFM (Cubic Feet per Minute) output of the fan in the prototype must meet the required specifications. Three repetitions of a comprehensive airflow test will be performed, both under loaded and unloaded conditions, and the mean of these three trials will be documented as the numerical CFM value. The power consumption of the fan will also be measured during these tests. The outcome of the test will be categorized as either a pass or fail.

*Additional equipment:*

Hot-wire anemometer (analog output), computer, filter test rig (Figure 13), timer, 12V battery pack, HEPA/Carbon filter

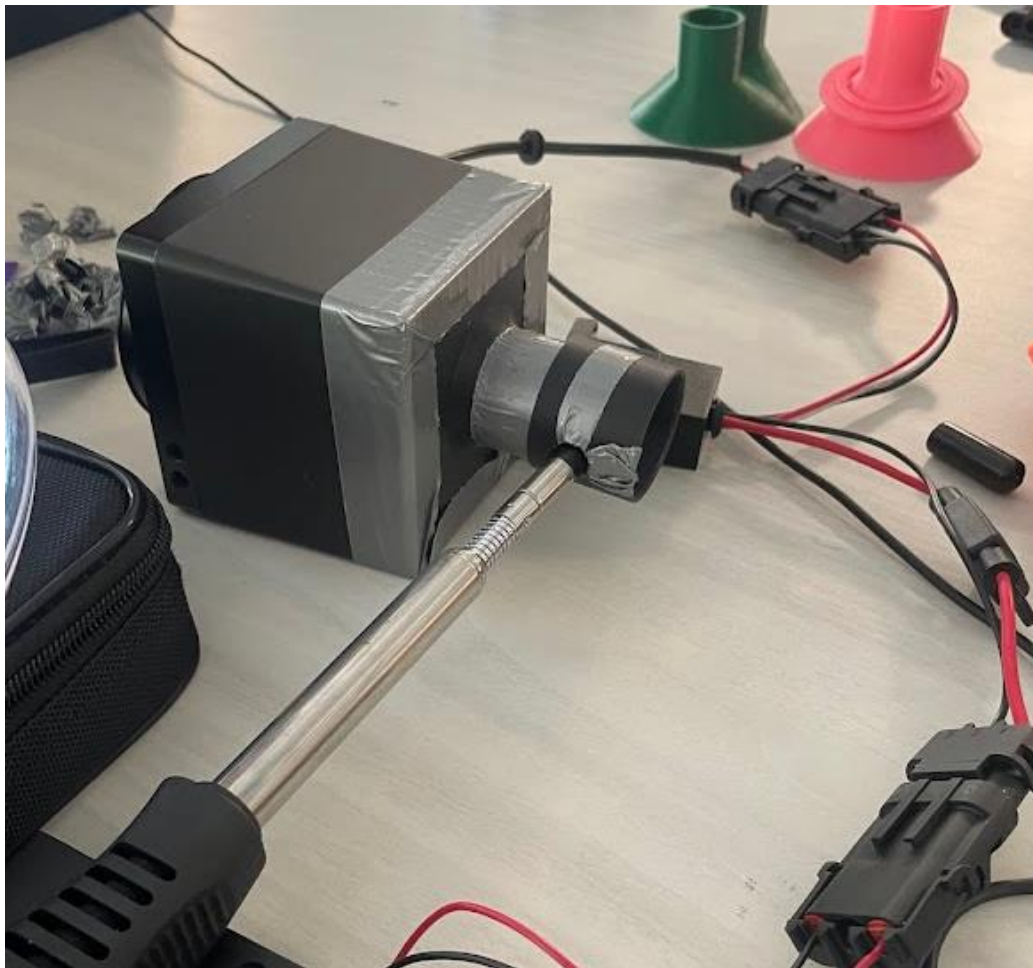


Figure 40: Picture of fan testing set up, showing the single nozzle outlet for the 2-person fan.

The airflow test for the prototype fan was designed to ensure that the Cubic Feet per Minute (CFM) output met the required specifications. This process involved conducting three repetitions of comprehensive airflow tests under both loaded (with a filter) and unloaded (without a filter) conditions. The mean CFM value from these three trials was documented as the representative numerical CFM value for each condition.

Two fans were tested, the MAC-1x Single Person High Output Helmet Air Pumper Fan, and the 2-Person Helmet Air Pumper Fan. The 2- Person Helmet fan was tested first. In the unloaded condition, the fan produced an airflow measured in three trials. The CFM values recorded were 13.49 for the first trial, 14.02 for the second trial, and 13.49 for the third trial. The mean CFM value for the unloaded condition was calculated to be 13.67 CFM. Under the loaded condition, similar tests were conducted to measure the fan's airflow. The test was then repeated with a filter attached to the fan. The mean CFM value for the loaded condition was determined to be 13.4 CFM. During these tests, the power consumption of the fan was also monitored. In the unloaded condition, the average power consumption was 82.4 W, while in the loaded condition it was effectively the same at 82.1 W. While setting up this test two outlet orientations were



tested, a single nozzle, centrally located following the fan, or two nozzles located diagonally from one another. Using the same power, the dual nozzle produced an average of 84 CFM. These tests were completed a second time with the Single Person fan, with a mean CFM of 112 unloaded, and a loaded output of 106 CFM using an average of 83.2 W and 84.1 W respectively, as this fan is considerably smaller than the other, only one outlet was tested.

Based on these results the Single Person Fan was selected as it had a similar power requirement but output higher CFM numbers through a single outlet, which fits our design better.

By the time the airflow reached the air curtain tubes, the change in diameter to the hole sizes caused a reduction in the CFM. The transition from a larger diameter in the main tube to the smaller diameters air curtain tubes and the holes created a bottleneck effect, increasing the resistance to airflow. This increase in resistance led to a higher back pressure within the tube, which in turn reduced the overall volumetric flow rate (CFM) of air exiting through the holes. The trials achieved 4.912, 4.726, and 4.695 CFM from the holes. This means that the fan, back pressure, tube diameter, and holes size interfere with each other.

### 6.2.2 Weight Testing

The mass of the full prototype must be less than 10 lbs. (4.54 kg). Three repetitions of a straightforward scale test will be performed, and the mean of these three trials will be documented as the numerical mass value. The outcome of the test will be categorized as either a pass or fail. The customer specifications primarily influenced by these factors include portability, usability, comfort, and overall compatibility with communication systems and existing personal protective equipment (PPE). Table 4 will be used during design validation to keep record of tests performed and conducted.

*Additional equipment:*

*Calibrated scale, worktable*

The full prototype (motor, filter, hoses, curtain, and electronics) was weighed. This does not include the helmet or backpack that is normally used with the assembly, as the test is meant to constrain added weight, not total carrying weight of the end user. This was a recurring test that measured the weight over multiple iterations of the device, simply ensuring that total weight did not exceed 10 lbs. Each design iteration passed these tests, consistently measuring below 4 lbs. When necessary, individual components were weighed when designs were adjusted to accurately measure net assembly weight. Below are representative images of the project's weight testing, the included figures describe the final assembly design iterations for each subsystem.



Figure 41 & 42 Left: Full final assembly weight testing. Right: Final hose weight testing.

The measurements were taken on a flat, metric scale, utilizing support material as infrequently as possible; creative methods of stacking were often employed to measure the larger subsystems or combined weight tests, as seen above. The final assembly weighed in at 1.618 kilograms, which is equivalent to 3.57 lbs., well below half the pass/fail maximum of 10 lbs.

### 6.2.3 Testing Duration of Use

The prototype power supply is required to maintain operational functionality for at least 2 hours. A series of pass or fail time assessments will be conducted three times to ascertain the prototype's ability to sustain full operational capacity autonomously. It is imperative that the prototype achieves the specified 2-hour minimum runtime without any adjustments to the boost module. Given the presence of a Variable Speed Controller (VSC) in the design, the testing procedure will operate the device at 1/3 of its maximum speed.

During testing, the device will solely power the blower, and the duration of its operation will be measured. This stringent specification is aimed at ensuring that critical systems within the design receive reliable power supply during operation. Additional tests will be conducted at varying speeds to assess any impact on the power supply's performance. Test data will be recorded in Table 4.

*Additional Equipment:*



*12V power supply (VSC pref.), voltmeter (x2), hot-wire anemometer (analog output), computer, timer*

For the power delivery system, the team opted to use 8 AA batteries to supply 12V to the Rugged Radios fan. Initially, the plan was to use 6 AA batteries providing 9V and utilize a boost converter to step up the voltage to 12V. However, testing revealed that the fan's power consumption was so substantial that it would drain the batteries within minutes.

It is important to note that the fans employed by the team are typically used in off-roading vehicles to cool racers, drawing power from the car's battery. Thus, while high-power consumption was anticipated, the extent of the drain, particularly when using the converter, was surprising.

The team acquired two fans from Rugged Radios: a larger fan operating at 12V and 3.8A, and a smaller fan operating at 12V and 2.7A. Tests conducted with both the battery and the converter showed a similar power draw for both fans. Subsequently, the team decided to test the larger fan with just the battery pack, without the converter. The results were promising, as the battery pack could power the fan for approximately 2.5 to 3 hours at various speeds. The speeds tested were full speed, half speed, and one-third speed, chosen because they provided a sufficient air curtain.

At full speed, the fan operated for 45 minutes before hitting its voltage threshold. At half speed, it ran for 80 minutes, and at one-third speed, it lasted for 35 minutes before the batteries were depleted.

Based on these observations, the team decided to power the fan using the battery pack alone, without the converter. This setup met the requirement of sustaining the fan for as long as the filters remained clean. Consequently, when the firefighter replaces their filter, they also swap the batteries for the fan, ensuring continuous operation without the need for separate interventions.

#### **6.2.4 Heat Resistance Testing**

Prototype must endure thermally challenging environments without effecting net shape or material properties. A stable environment of minimum 170 degrees Celsius (°C) will be prepared in an enclosed oven or clave; prototype will be exposed to controlled environment for a minimum of 5 minutes. Once retrieved, a pass or fail visual inspection will determine if “*evidence of ignition, melting, dripping, or [component] separation*” is observed . Indications of such occurrences constitute an immediate failure. Tests will be conducted three times, results and observations recorded in *Table 4*.

*Additional Equipment:*

*Autoclave (or oven and thermocouples (x2)), timer, clean baking-sheet, disposable rags (x6), masks, heat-resistant gloves*



Due to the importance of other design specifications, such as air delivery and filter design, that are project unique and complex, heat resistance in a multi-component assembly generally implies weakest material selection will be the cause of test failure. However, at this point in iterative design, the most strenuous subsystems are already difficult to prototype and test; requiring robust, temperature resistant material is an adjustment that is most easily implemented when design is finalized. Therefore, heat resistant testing was not conducted with the current final design, as material selection was not strictly temperature constrained. This decision is agreed upon by our sponsors and advisors and is instead included as a main suggestion regarding future work in manufacturing and research for this project.

### **6.2.5 Donning/Doffing Time Testing**

Prototype assembly must be quickly applied and removed from an operator in full WUI gear. Pass or fail time tests were performed three times each for donning and doffing following these respective parameters: donning must not exceed 120 seconds and doffing must not exceed 10 seconds. This ensured prototype donning is simple and efficient; removal time is heavily considered to mitigate hazard during a system malfunction or an emergency scenario.

The donning and doffing test was straightforward. A team member, Payton Mayer, was timed while putting on and taking off the full system. The initial goal was to achieve a donning time of 120 seconds and a doffing time of approximately 10 seconds. The test participant was required to don and doff the system three times to ensure redundancy and to observe any improvements in speed with repeated attempts.

*Additional Equipment:*

*Timer, WUI standard required equipment (donned)*

The first test was started with the device attached to a Fireline backpack provided by the project sponsors. The backpack with the device already attached was placed on the floor. Mayer was then instructed to put on the backpack, place the helmet on his head with the face shield already attached, and snap the buckles of the backpack into place as quickly as possible. Another team member, Xaviera Pons, set a timer to measure the donning time. This test was repeated a total of three times. To measure the doffing time, Mayer was asked to repeat the process, but in the opposite order. The results are in Table 4b.

The results show Mayer achieving an average donning time of approximately 13.6 seconds and a doffing time of 5.6 seconds. These results were significantly faster than expected, with donning nearly 100 seconds (about 1 and a half minutes) quicker and doffing taking half the anticipated time.



A separate test focusing on the face shield attachment to the helmet was performed by Calder Wood. Wood was instructed to attach the face shield to the helmet and then detach the face shield from the helmet. Pons timed the process of removing and reattaching the face shield, averaging 1.3 seconds to doff and 3.4 seconds to don the face shield as seen in Table 4b. This simple test demonstrated the effective and efficient design of the facemask attachment system.

These results indicate that the team's design allows for rapid and efficient donning and doffing, surpassing the initial time goals and proving the system's practicality in real-world scenarios.

### **6.2.6 Testing for Adjustable Sizing**

The final design accommodates all firefighters with a range of head sizes, hair lengths, and facial features. The mask and face shield will be adjustable through straps and the system will be flexible and protraction/retract through semi-stretchable material tubing from the fan to the face shield. The system will still be secure and tight enough to not fall or slip from the firefighter's head. Pass/Fail test will determine the effectiveness of the straps.

*Additional Equipment:*

*Adjustable straps, Standard gear*

Using the firefighter standard equipment, the final design utilizes the adjustable sizing already available. By using standardized gear, firefighters know how to use the gear that is familiar to them. All team members donned the gear and were able to adjust all the gear straps to conform to their respective sizes.

### **6.2.7 Communication Interference Testing**

The device must not decrease communication effectiveness when worn; the prototype's fan and air curtain will generate noise and some physical obstructions over the operator's ears and mouth. Test conductor will set the fan speed to 5 increasing levels: 25%, 33%, 50%, 75%, and 100%. The test conductor will measure dB levels of the fan at the 5 different speeds through their dB level reader on their phone. The end result is measured by subtracting the dB level of the fan by the dB level of the outside environment. The average dB level that wildland firefighters are surrounded by in their work environment is well above 85dB, meaning that the device should be lower than that. ". Tests will be conducted five times in a pass or fail format, requiring dB level of the device to be less than the average dB level of a wildland firefighter's environment while working.

*Additional Equipment:*

*Sound level meter*



To conduct the communication interference test, the team set up the full assembly in a room where the baseline noise level was 54.1 decibels (dBA). They tested the fan at various speeds — quarter, one-third, half, three-quarters, and full — and measured the changes in dBA. At quarter speed, the team recorded 61.9 dBA, representing a 7.8 dBA increase from the baseline. At one-third speed, the reading was 72.1 dBA, an 18 dBA increase from the baseline. From one-third speed to half speed, there was a slight variance, with the measurement showing a 19 dBA increase, reaching 73.1 dBA. Finally, at three-quarters and full speeds, the team observed a 25 dBA increase from the baseline, with levels settling at 79.3 dBA.

These results exceeded the team's expectations. However, when a team member wore the device, it became difficult to hear another individual from more than 10 feet away. This issue was not concerning for the team's measurements and expectations because firefighters operate in inherently loud environments. The primary goal, which was achieved, was to avoid significantly increasing the noise level and to design a device that allows the wearer's mouth to remain visible.

### 6.2.8 Field of View (FOV) Testing

The prototype must at least have the same field of view as a firefighter wearing standard goggles or glasses. The face shield will be tested for visibility when worn with full prototype; 100° of lateral vision must be unimpeded (50° from center of test board). Test board will be displayed at a controlled direction and distance from wearer as lateral field of view is measured. Three tests will be performed with pass or fail parameters, and *Table 4* will record their results.

*Additional equipment:*

*Measuring tape, string, construction paper, markers, stool, calculator, camera*

FOV testing was removed from priorities once it was clear that the assembly would not be inhibiting the visual field of the user severely. Additionally, the air curtain design is subject to extreme change in future iterations, and encouraging or discouraging certain designs at this stage, based on FOV, was not sought. The air curtain effectiveness, air cooling, and filter effectiveness are all more vital to meeting project requirements and are likely closer in design to the realization of their final form.

### 6.2.9 Range of Motion (ROM) Testing

A full prototype attached to the head and neck cannot pose obstruction to the physical movements of the firefighter. Operators (fully donned) will undergo an ergonomic pass or fail test meeting the following performance criteria: Operator's nodding motion must have minimum range of 130°, measurements will be taken from tangential perspective using visual indicators to measure vertical (nodding) range. The operator's horizontal shaking motion must have a minimum range of 77° in each direction from 'center'. Exact center positions, upright and forward-facing, will be determined preceding tests and visual indicators



will again be used to determine range. Three tests will be performed in total; results will be recorded in *Table 4*.

*Additional equipment:*

*Measuring tape, string, construction paper, markers, stool, calculator, camera*

Much like the FOV testing considerations, ROM is similarly unimportant when compared to other test focuses. In this case it is even more obvious, as gear compatibility and assembly weight both verify ease of movement in some extent. Due to redundancy and constant donning/doffing of the assembly, this test was omitted; the importance of testing such attributes thoroughly will likely come later in the project's lifespan.

### 6.2.10 Air Cooling Test

The cooling test focused on measuring the temperature of the person's forehead before and after using system. The trials included a baseline control for at rest, meaning the subject was sitting down in the sun, a control for jogging, the system on at rest, and the system on for jogging. The duration of the at-rest tests was 10 min and the person jogged for a duration of 180 seconds, with 45 second integrals for each lap ran. Comparing the tests to their respective baselines, the temperature was 1°F cooler while at rest and 1.3°F cooler after jogging.

*Additional equipment:*

*Timer, 12V battery pack, HEPA/Carbon filter, Fireline backpack, forehead thermometer scanner*

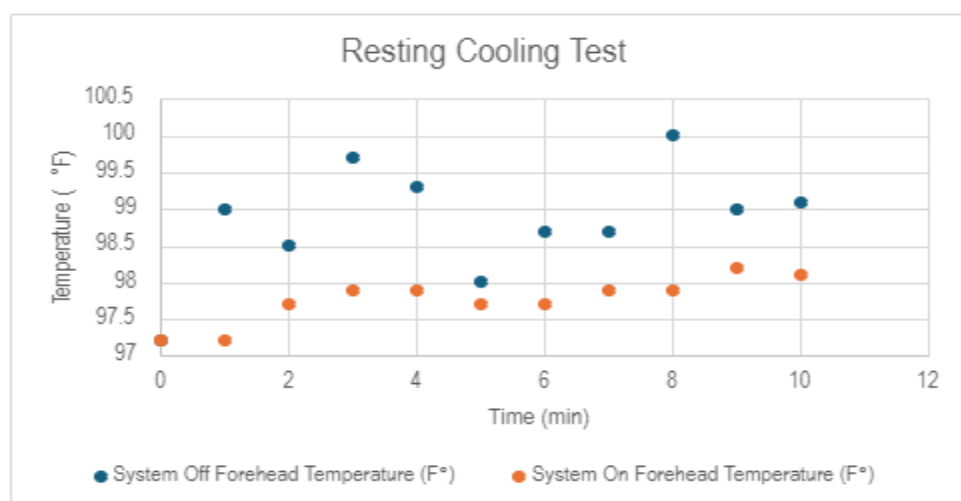


*Figure 43. Temperature Difference During The Cooling Test with Test Subject in Resting Position*

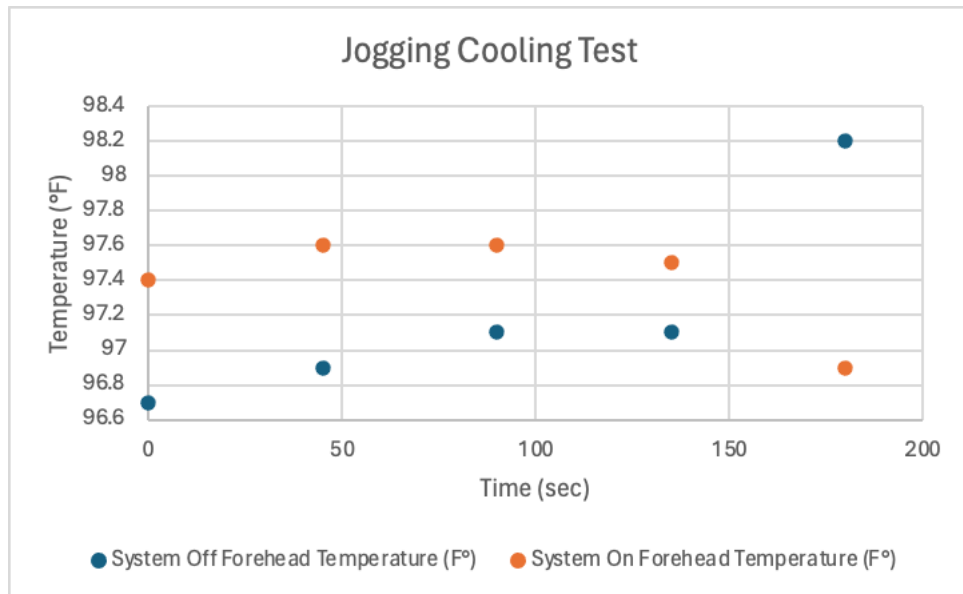


Figure 44. Temperature Difference During The Cooling Test with Test Subject Running

The resting position cooling test gave promising results (Figure 43), but there was a lot of measurement inconsistency with the infrared thermometer during the jogging test that may explain why that data was so poor by comparison.

### 6.2.11 Filtration Quality Testing

The filtration test can be broken into three key components: Particulate, Gasses, and VOC's each have their own properties that affect how the filter is designed. The primary concern with much of this project is filtration, which necessitates its division into subcategories to guarantee a comprehensive examination of all filtration techniques. The mechanical filtration of large and small ash particles, which prevents these particles from being inhaled by firefighters, is one such category. Smaller particles pose a greater risk as they are more difficult to filter out, making them the most significant factor in meeting the customer's need to minimize harmful respiratory exposure to particulates. The reduction limit of VOCs is crucial in reducing dangerous respiratory exposure to chemicals, another customer requirement. The design's filtration efficiency can be tested in-house by constructing a test stand that measures the concentration of pollutants in the air before *and* after it passes through the device.

*Additional equipment:*

*Hot-wire anemometer (analog output) (x2), computer, filter test rig (Figure 15), timer, 12V battery pack, HEPA/Carbon filter*

The filter was tested by isolating the filter in the test rig as described in section 6.1.1 with the sensors described and set up from section 6.1.2. A base level reading of the gasses in the test chamber and at the outlet in order to get a base level to compare against. The gasses, Nitrogen (N<sub>2</sub>), Ethylene (C<sub>2</sub>H<sub>4</sub>) and



Carbon Dioxide (CO<sub>2</sub>) are then pumped into test rig for 10 minutes. Once the gasses have been shut off at 10 minutes, the test stand is allowed to return to baseline. The filter testing was completed in two stages, a primary test of just the filter, exposed to N<sub>2</sub>, C<sub>2</sub>H<sub>4</sub>, and (CO<sub>2</sub>), and a secondary test comparing the filter to an N95 and a bandana at CO<sub>2</sub> filtration. For both tests, the fan was attached to a power supply allowing the test to run without interruption due to air speed decline as batteries ran out of power. The sensors were set up as described above in section 6.1.1.



*Figure 45.* Picture of the test stand set up for the second test with the bandana, with the Filter Standin in place to hold the bandana in place for testing.

The results from our filtration tests provide valuable insights into the effectiveness of different materials in removing particulate matter and gases from the air. The results of our tests illustrate the filtration system's capability in reducing harmful pollutants, particularly Total Volatile Organic Compounds (TVOC) and equivalent Carbon Dioxide (eCO<sub>2</sub>) concentrations. In figure 46, it is evident that the inlet TVOC concentration is significantly higher than the outlet TVOC concentration throughout the test duration. The average percent difference between inlet and outlet TVOC was found to be 70.22%, indicating a substantial reduction in TVOC levels as the air passes through the filter. This significant reduction demonstrates the filter's capacity to effectively remove a large portion of VOCs from the air, addressing the primary concern of protecting against harmful respiratory exposure to chemicals.

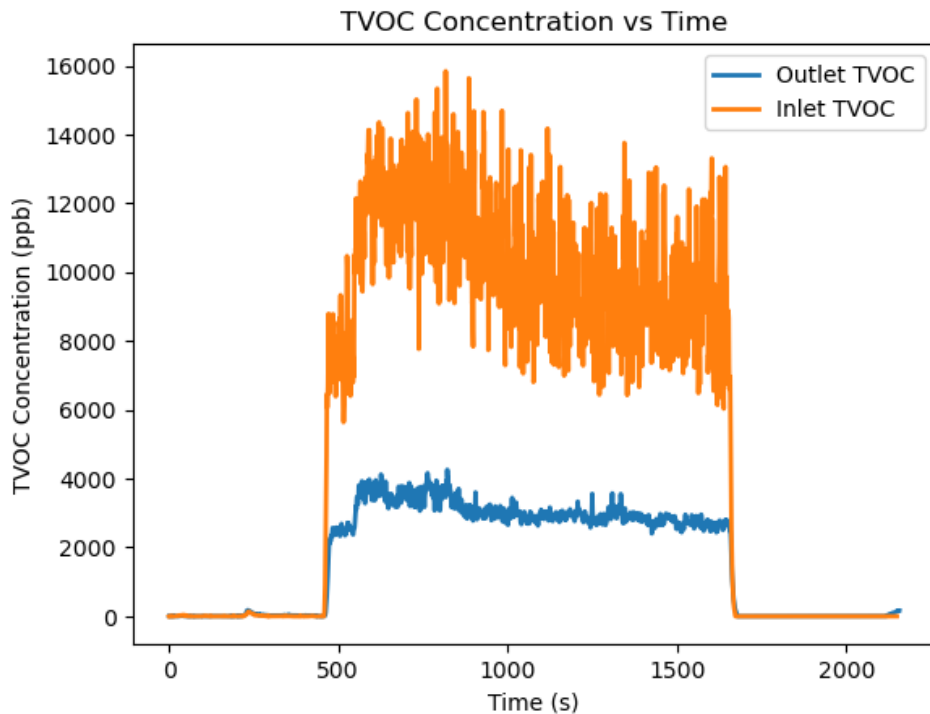


*Figure 46.* TVOC Concentration in parts per billion over the duration of the test, with a normalizing period before and after the exposure of each gas.

Similarly, figure 47 shows the inlet and outlet eCO<sub>2</sub> concentrations over time. The inlet eCO<sub>2</sub> levels peak much higher than the outlet eCO<sub>2</sub> levels, with an average percent difference of 66.24%. This consistent reduction in eCO<sub>2</sub> concentrations highlights the filter's efficiency in reducing CO<sub>2</sub> levels, an important factor for ensuring breathable air quality. Notably, the sharp decrease in both TVOC and eCO<sub>2</sub> concentrations after the initial peak periods further validates the filter's performance in maintaining lower pollutant levels throughout the test. Additionally, the average percent difference between outlet and inlet CO<sub>2</sub> concentrations is reported to be 91.62%, underscoring the filter's exceptional ability to remove CO<sub>2</sub> from the air. This high percentage difference is crucial for applications where maintaining low CO<sub>2</sub> levels is essential for health and safety, such as in environments with limited ventilation or high occupancy.

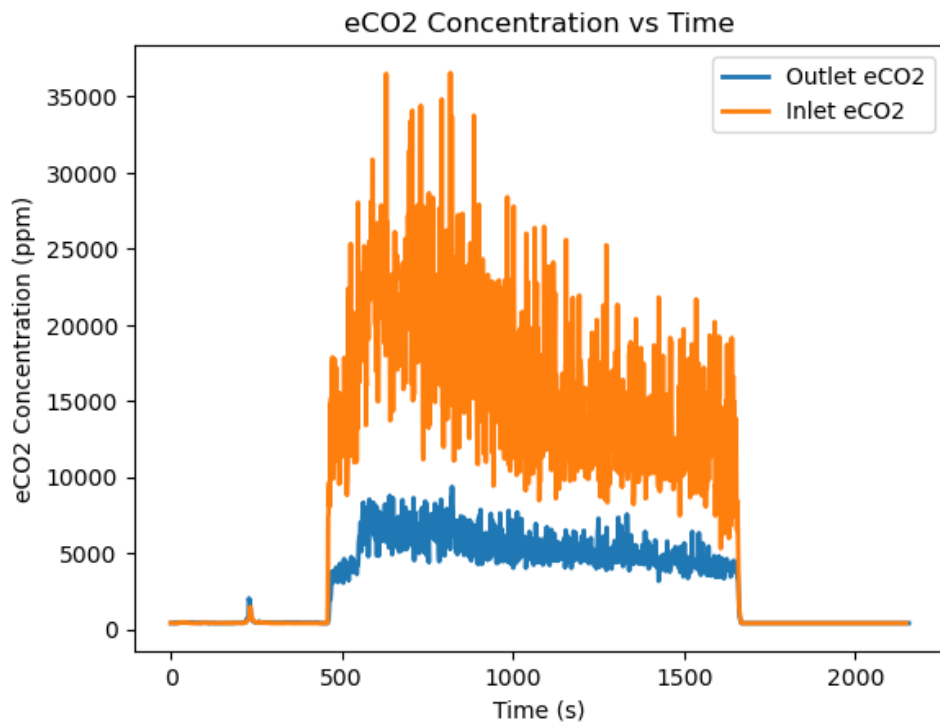


Figure 47. eCO<sub>2</sub> Concentration during filter test with a normalized portion before and after gas exposure.

In the second phase of testing, we compared the performance of the custom-designed filter with other currently used methods, including an N95 mask, a bandana, and no barrier (inlet). The test rig, configured as shown in Fig. 48, demonstrated how each material affects CO<sub>2</sub> concentration over time. Figure 49 depicts the CO<sub>2</sub> concentration decay, showing how quickly each filter returns to baseline once CO<sub>2</sub> is no longer being added to the system.

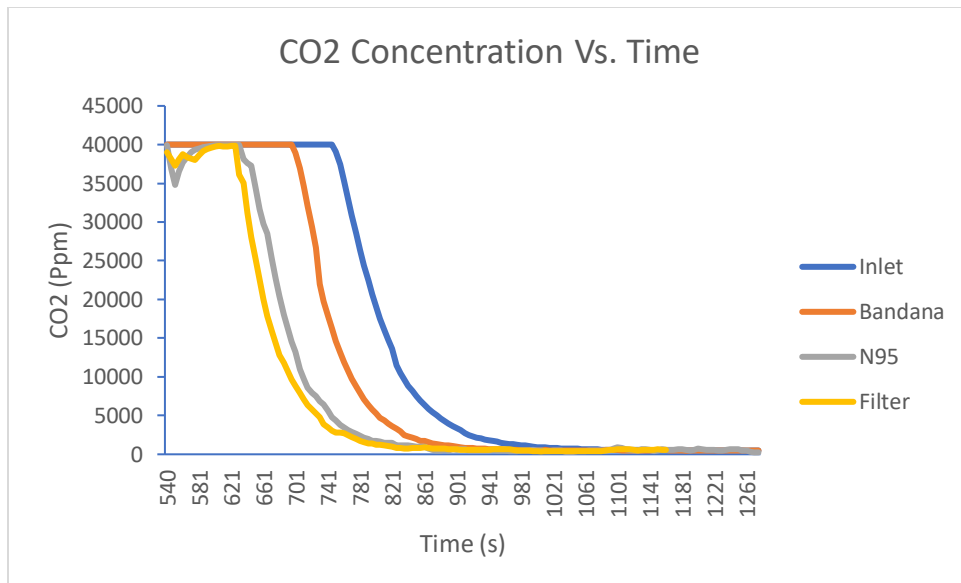


Figure 48. CO<sub>2</sub> Concentration dissipation data from SCD40 sensor

Figure 49 shows the CO<sub>2</sub> concentration accumulation until the sensor reaches its maximum value. The inlet (no barrier) accumulates CO<sub>2</sub> the fastest, followed by the bandana, which allows relatively quick accumulation. In contrast, the N95 mask and the custom filter demonstrate a slower rate of increase, indicating that these coverings are more effective at trapping CO<sub>2</sub>.

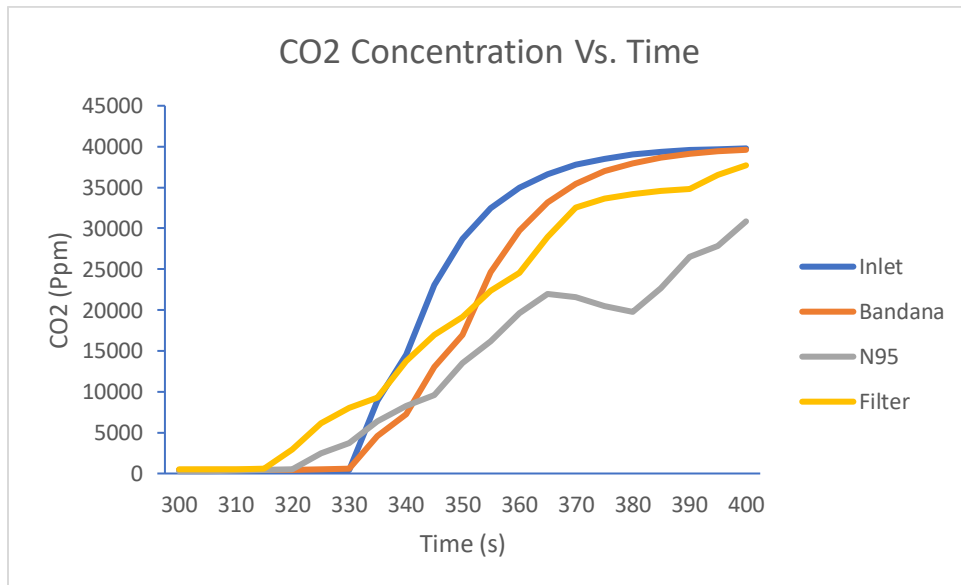


Figure 49. CO<sub>2</sub> Concentration accumulation data from SCD40 sensor

From these results, while the custom filter is beneficial, especially compared to nothing or a bandana, it does not perform similarly to the N95 mask when the N95 was fit properly to the test rig. As such when an



N95 mask is properly fitted and sealed, it is more than capable of being a good filter for firefighters. A crucial observation is that the N95 mask's remarkable performance is attributed to it being completely sealed around the test rig, an ideal condition that would not likely be replicated in the field. In real-world scenarios, achieving a perfect seal with an N95 mask can be challenging due to fit variations and movement, which could compromise its filtration efficiency. Conversely, the custom filter, designed to integrate more seamlessly with typical operational environments, is likely to perform more reliably under field conditions.

### 6.2.12 Fire Simulation Test

This test can be described as a holistic, accelerated life test, testing the air curtain effectiveness while relying on the battery, motor, hose, and face shield compatibility with a standard helmet. The test employs 3 sensors reading TVOC, eCO<sub>2</sub>, and CFM; the first two sensors, measuring air quality, are placed inside the head form's cavity, behind the mouth opening. The head form is fixed in place 1 ft above the smoke channel using a wooden test structure to ensure smoke exposure will be sufficient in quantity and to maximize use of test fuel. The smoke channel is a metal chimney resting on a raised metal fire pit, as seen in the images below. Fuel consisted of portions of paper bags (with ink), charcoal, cardboard, but mostly *Medicago polymorpha* (California burclover), a common invasive weed; makeshift wind breaks (polycarbonate, canvas) were also employed surrounding the burn pit to reduce wind effects. To capture data, air must flow through the head form's cavity, past the sensors situated in the nape; a vacuum and tape were utilized to simulate strong inhalation, covering the outlet behind the sensors and delivering a reliable 20 CFM flowrate. Tape was used to manipulate the size of the vacuum opening and the third sensor, a digital hot-wire anemometer, verified flow; at the inlet, CFM was measured at 10 CFM, which we regard as the true test flowrate. The reduction in CFM is mainly due to the smoke pad spanning over the face of the head form. Swiffer dry pads were replaced between each test to serve as visual indicators to validate analysis results, the darkness of the spots should correlate to lower TVOC and eCO<sub>2</sub> readings from sensors. Normal test procedure operated as follows: Turn on sensors, ensure baseline (clean air) measurements are saved, and begin recording timestamped TVOC data, eCO<sub>2</sub> data into nearby (and sheltered) computer. Next turn on vacuum and verify CFM, then fix vacuum into place, replace Swiffer pad, and verify inlet CFM is also expected. At this moment, the fire can be started; the smoke channel, filled halfway with a presorted mixture of fuel, is lit from underneath. The team waits until smoke in front of head form becomes sufficiently thick, and takes note of that moment in order to refer to the data. By nature, the test is difficult to standardize, smoke content and temperature varies, wind gusts can interrupt data collection, and test duration was also difficult to quantify due to occasional inconsistency in smoke exposure.

*Additional equipment:*



*Hot-wire anemometer (analog output), computer, wooden test stand, TVOC sensor, eCO<sub>2</sub> sensor, tape, Swiffer dry pads, fuel products (described above), vacuum, head form*

Before tests could be conducted, the test setup had to be designed and implemented. Once the distances between test equipment was satisfactory and power sources had been identified, the sensors and vacuum could be baselined. A handful of sample tests were performed to streamline future tests and gauge effectiveness of our fuel mixture and test rig. During some tests the power source would shut down and then ramp back up. This was likely because the fan was overwhelmed by the smoke, as it was the first time the device was being tested to filter smoke from a brushfire rather than in the test stand.



*Figure 50* Figures 50 & 51: Test Equipment: Channel, Head Form, Tape, and Test Stand

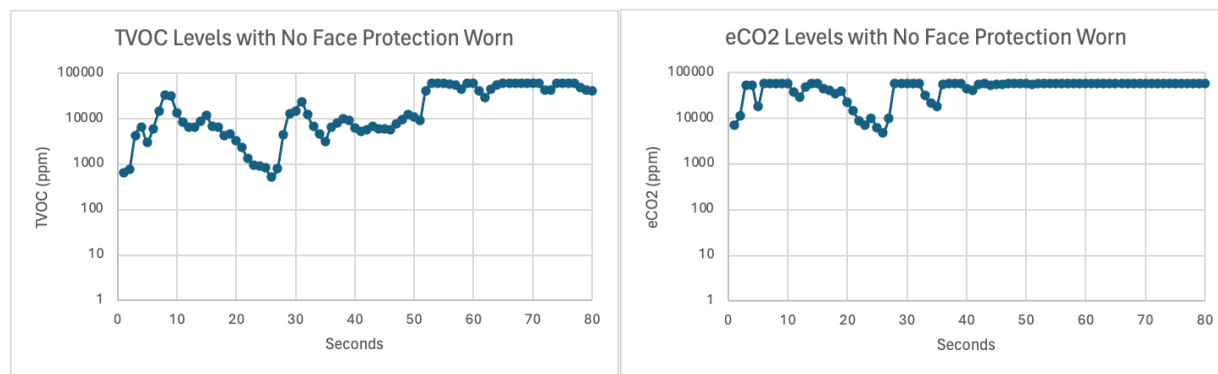
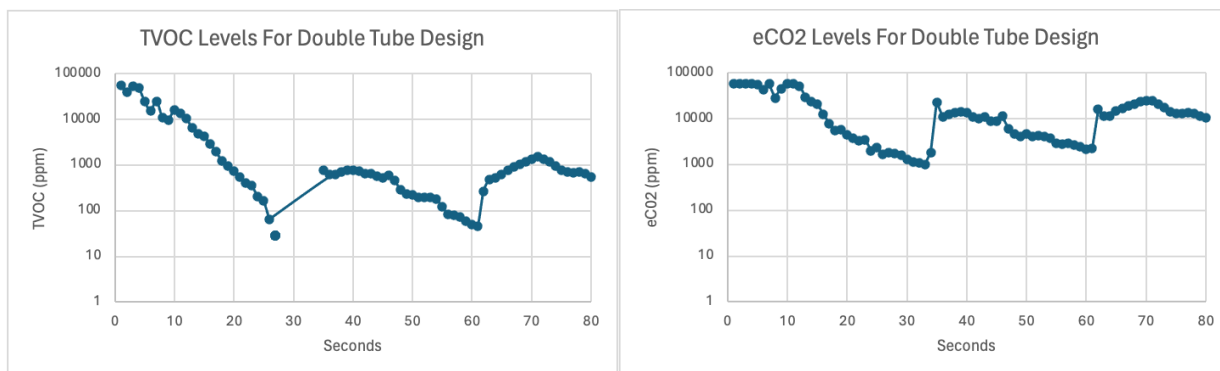


Figure 51. TVOC and eCO2 Exposure Levels with No Face Protection Worn

When comparing raw, unprotected data vs the activated air curtain numbers, the differences are certainly noticeable but require explanation. Looking first to TVOC, we can see that an unprotected face shield and helmet assembly was leaving the head form out to dry, if you will, unable to remove penetrated particulates and varying according directly to smoke exposure. When utilizing the double tube design, as seen in Figure 35, the TVOC levels, although peaking just like the no protection tests (which we will see is common), the double bar air curtain managed to actively reduce the TVOC in the breathing air around the head form. Once the assembly was full of smoke, the curtain would cyclically remove it as seen in Figure 47. The single bar tests were also encouraging, but in a different way; they were much better at keeping contaminants from entering the system, however, lacked any mechanism of clearing the air inside the assembly once penetrated by smoke. Figure 51 shows an elevated TVOC content accompanied by a flat curve, as opposed to the double bar design's parabolic cycle.

One thing to note is that during some tests, the power source was shut down and then ramped back up. This was likely because the fan was overwhelmed by the smoke, as it was the first time the device was being tested to filter smoke from a brushfire rather than in the test stand. In addition, the batteries seemed to be being drained rather quickly since the fan motor used was designed to be connected to a car battery, which was one of the hardships the team struggled to overcome as stated in Section 6.2.3.



*Figure 52.* TVOC and eCO<sub>2</sub> Levels for Double Tube Design

The double tube design is what is demonstrated in the final design of the device. This was due to the design demonstrating the lowest levels of TVOC and eCO<sub>2</sub> as seen in Figure 52 when compared to the other design choices. However, one must note that this was the only test that was powered at 100% fan speed since the other tests the fan could not handle being powered at max speed for the whole test. From Figure 52, there is a drastic decrease in TVOC ppm levels as compared to Figure 51 with no face protection at all.

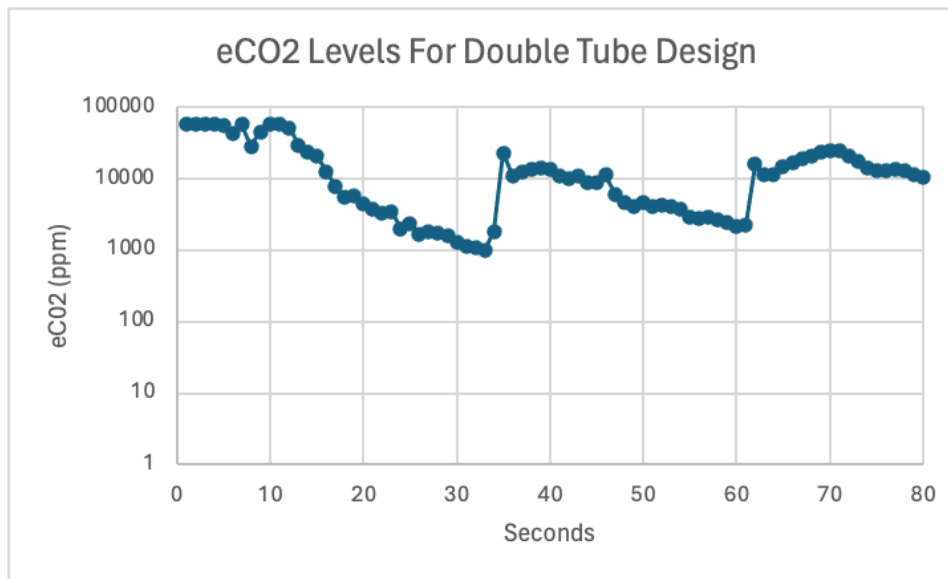


*Figure 53.* eCO<sub>2</sub> Levels  
for Double Tube Design

As stated previously, the eCO<sub>2</sub> levels shown in Figure 53 demonstrate the lowest eCO<sub>2</sub> levels from all the design choices tested. The eCO<sub>2</sub> levels in Figure 53 are drastically lower than the eCO<sub>2</sub> levels in Figure 51 with no face protection worn.

When comparing eCO<sub>2</sub> rates of exposure, the graphs are strikingly similar to those of TVOC, which helps validate the accuracy of the trends witnessed by each sensor. We observe the same recovery curve from the double bar; it allows toxins into the breathing space, but effectively removes it as the smoke increases in intensity. The story was also similar to TVOC when analyzing the results of the single bar's relationship with eCO<sub>2</sub>; the slope rarely turned downward, instead slowly (or immediately in the event of a gust) spike and remain high. Now that this phenomenon has been recorded in both important chemical groups, its important to restate the implications: the double bar proves more effective as a barrier, but the double bar offers advantages to continuous use and severity of exposure over time.

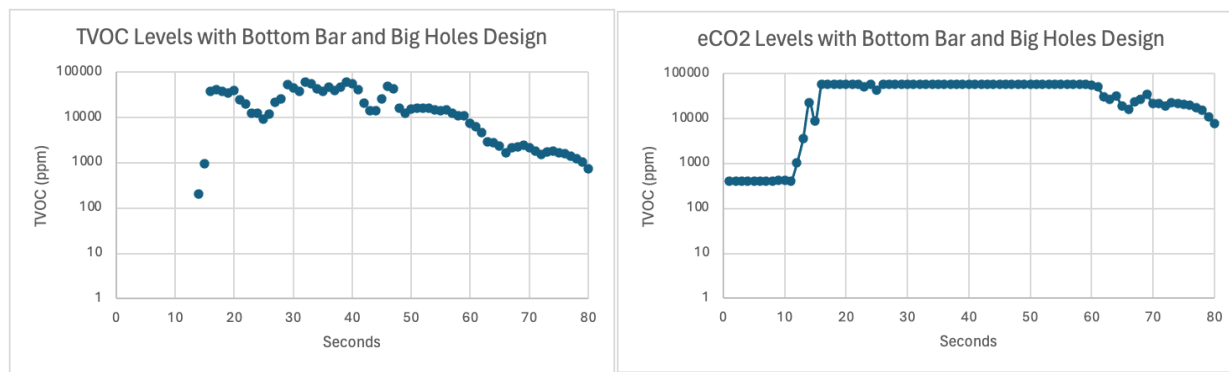


Figure 54. TVOC and eCO2 Levels for Bottom Bar Only with Big Holes Design

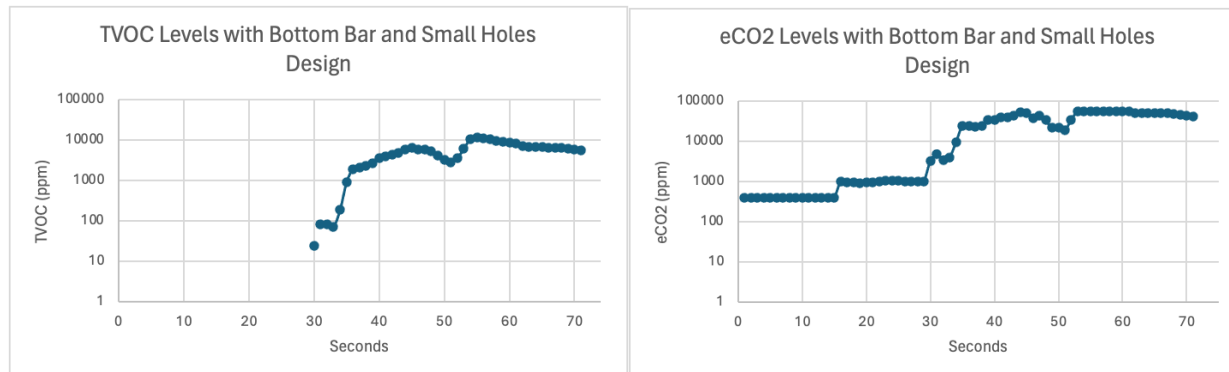


Figure 55. TVOC and eCO2 Levels for Bottom Bar Only with Small Holes Design

### 6.2.13 Gear Compatibility Test

Gear compatibility involves assessing whether the new or modified gear can seamlessly integrate with the existing equipment without causing any disruptions or malfunctions. The respirator must be designed and tested to complement the current standard setup of the firefighters. Three qualitative tests will be performed using pass or fail format; A passing result indicates prototype does not fully inhibit ability to reach any other essential equipment. Tests will be performed with operator in full gear and prototype; results will be recorded in Table 4.

*Additional equipment: Final Respirator design (Air Delivery, Battery, Fan and Filter)*

*WUI standard required equipment (donned)Standard firefighter backpack, Standard firefighter helmet*

Table 4. Test Description, Standards, and Expected Results

Requirement	Test	Measurement Procedure	Metric	Expected Result
Air Output	Air Test	Measure CFM after the filter	CFM	14 CFM
Weight	Scale Test	Measure weight three times and calculate average resultant value.	Lbs	$\leq 10$ lbs.



Duration of Use	Duration Test	Run just the fan at goal operating setting to measure battery longevity	Minutes	120 min
Heat Resistance	Heat Resistance	Heat device to 177 °C for 5 minutes, watching for any ignition, melting, dripping or separation.	Pass/Fail NFPA	Pass NFPA
Don/Doff	On/Off Test	Average time after 3 timed tests to put the device on, turn it on, then take it off.	Sec	120 Max
Adjustable Sizing	Use/Duration Test	Tighten straps of the respirator and see if the straps stay tight over duration trials (30 min, 1 hour, 2 hours). Measure the strap before and after for looseness.	Pass/Fail	Pass
Communication Interference	Noise Level Testing	Measure decibel level while speaking with and without the device equipped	dB	100 dB min
FOV	FOV Test	Place object in subject's periphery and determine angle from neutral while using the device	Degrees of vision	100° Laterally
Range of Motion	ROM Test	Have participant move at full range of motion available and measure total freedom from neutral	Degrees of movement	125 ° ↑ 75° ↔
Air Cooling	Temperature Test	Measure temperature at multiple points and take the average resultant value before and after device	ΔT (°F)	- 1-5 °F min
Filtration Quality	CO	Measure concentration before and after device	Ppm	25
	C <sub>2</sub> H <sub>4</sub>		Ppm	300
	Particulate		ppm	25
Gear Compatibility	Try On Test	Load Device into current firefighter load out and make sure everything fits and is not in the way	Pass/Fail	Pass

Table 4b. Requirements Testing Record

Requirement	Test Component or Function (units)	Test No.	Result	Pass or Fail	Req. Satisfied
Air Output	Fan Volumetric Flow Rate (cfm)	1	112	P	N



	Air Curtain Volumetric Flow Rate (cfm)	1	4.912	F			
		2	4.726	F			
		3	4.695	F			
Weight	Total Weight (lbs.)	1	4.05	P	Y		
Duration of Use	Battery Life (hours)	1	170	P	Y		
Heat Resistance	Material Resilience (visual inspection)	1	N/A	N/A	N/A		
		2	N/A	N/A			
		3	N/A	N/A			
Don and Doff	Donning Duration (seconds)	1	17.3	P	Y	Y	
		2	12.6	P			
		3	10.9	P			
	Doffing Duration (seconds)	1	5.8	P	Y	Y	
		2	5.5	P			
		3	5.3	P			
Adjustable Sizing	Operator Interface (fitment inspection)	1		P	Y		
Field of View (FOV)	FOV (degrees of vision)	1	N/A	P	Y		
		2	N/A	P			
		3	N/A	P			
Range of Motion (ROM)	Lateral ROM (degrees of movement)	1	N/A	P	Y	Y	
		2	N/A	P			
		3	N/A	P			
	Vertical ROM (degrees of movement)	1	N/A	P	Y	Y	
		2	N/A	P			
		3	N/A	P			
Air Cooling	Temperature $\Delta$ (degrees °C)	1	1	P	Y		
		2	1.3	P			
Filtration Quality	Carbon Monoxide Penetration (ppm)	1		-			
		2		-			
		3		-			
	Ethylene Penetration (ppm)	1		-			
		2		-			
		3		-			
	Particulate Penetration (ppm)	1		-			
		2		-			
		3		-			



Gear Compatibility	Existing Gear Compatibility (fitment inspection)	1	N/A	P	
				-	
Key			No Data	-	
			Pass	P	
			Fail	F	

The final design considered typical gear that firefighters wear and bring when on the job. All components are additions that work around one of the standard backpacks and helmets that they wear. The primary objective was to enhance the firefighter's capabilities without compromising the integrity or effectiveness of their standard gear. For instance, the some additions were specifically designed to fit around the contours of the standard backpack, ensuring that no critical access points or functionality were obstructed. Similarly, the helmet enhancements were engineered to avoid interference with the standard helmet's fit and protective features. The design deliberately avoided any modifications that would require altering, damaging, or removing parts of the standard equipment. Instead, it focused on add-ons that could be easily attached or detached as needed.

## 7. Conclusions and Recommendations

Over the past fifteen years, the Wildfire Conservancy has tackled significant challenges faced by wildland-urban interface (WUI) and wildland firefighters. One critical issue is the lack of adequate respiratory protection, which is essential to minimize exposure to harmful smoke and toxic materials. Studies show that firefighters have higher mortality rates from cancers and cardiovascular diseases due to their exposure to these hazardous conditions. Despite attempts by manufacturers, no respiratory protection devices for wildland firefighters meet the National Fire Protection Association (NFPA) 1984 standards, leaving them reliant on insufficient protection like N95 masks and bandanas. The WUI Fire Institute at Cal Poly and CAL FIRE, through the Wildfire Conservancy, are funding a project to develop a new respiratory device that meets NFPA standards and fulfills the practical needs of wildland firefighters. This project, First Respire, aims to create a durable, effective, and user-friendly air-respirator device.

Currently, wildland firefighters lack effective breathing protection against smoke, gas, and particle emissions during deployments. Many resort to using bandanas, which offer minimal protection against large particulates, as existing respiratory devices are heavy, provide insufficient air supply, and lack effective filtration. First Respire's air respirator aims to address these issues by improving air quality and providing



ample respiratory support, without hindering the operator's duties, communication, or field of view. The device integrates seamlessly with existing equipment and is easy to deploy and remove.

The respirator comprises two subsystems: air filter and air delivery. Initial designs considered separating these into distinct projects, but the final concept integrates them. Key considerations for the device include comfort, donning/doffing time, and duration of use, with the power source being crucial due to the firefighters' long shifts. Batteries were chosen based on feedback from local firefighters, as they already carry them for other devices.

For air filtration, the design includes a HEPA filter for particulates, a mesh filter for large debris, and an activated charcoal filter for carbon monoxide. For air delivery, a face shield with an air curtain was selected, providing clear vision and protection from debris. The fan system utilizes an axial fan, and the power source consists of AA batteries for practicality and ease of replacement. Prototyping and testing ensured the effectiveness of each subsystem and the overall integration, resulting in a viable, field-ready respirator that meets the required standards.

Over the course of this project, First Respire demonstrated that using an air curtain to provide respiratory protection for wildland firefighters is a potentially feasible alternative to the other, more restrictive, respiratory devices in development and is a concept well worth further research and development. The team also established a strong foundational base that future teams can build upon to improve the air curtain design, rather than having to start from scratch. Beyond the innovation of the air curtain design, the team implemented a novel magnetic attachment system that would allow the device to be easily retrofitted to existing wildland firefighting equipment and which enables firefighters to quickly and effortlessly put on and remove the system as needed. The team also developed a modular filter design that allows for easy replacement of used filters and a power system that would utilize AA batteries that are readily available at basecamp.

There were some challenges. By the time the air flow reached the air curtain tubes, the change in diameter to the hole sizes caused a reduction in the CFM. The CFM and back pressure are two critical factors in airflow management within a tube with holes. When the tube diameter is too small, the air velocity decreases leading to a loss in CFM due to higher air resistance losses and increased back pressure. Back pressure, exerted by the tube against the airflow, restricted the air from efficiently escaping through the holes. By increasing the number of holes, back pressure was reduced, but consequently, air velocity decreased. CFM out of the tubes depended on a balance between the back pressure and air velocity due to the small tube size.



The air flow direction went across the tube, resulting in the first few holes not having any air velocity and the last few holes having the max air velocity. The air flow was distributed all on one side of the face and caused the air curtain to have a weaker side. Uniform air curtain distribution could not be achieved with the air curtain tubes only having an inlet on one side. The final design used the cooling system, meaning that the system used the inlet on one side, resulting in an unevenly distributed air curtain.

Looking ahead, a final product based on this design is within reach with continued development and refinement. The foundation laid by this project provides a strong starting point for future efforts, allowing subsequent teams to build upon our work without needing to start from scratch. This established groundwork means that future efforts can be more focused and efficient, targeting specific areas for enhancement rather than redoing basic design steps.

Future efforts should begin with a comprehensive analysis of air curtains to determine the minimum airflow required for optimal effectiveness at target wind speeds. This foundational analysis will inform the optimization of each component in the air delivery system, working backwards from the desired airflow to ensure that each part contributes efficiently to the system's overall performance. The airflow analysis will need to consider varying environmental conditions that wildland firefighters may encounter, such as high winds and smoke density. Understanding these variables will allow for a more robust and adaptable design. The fan should be designed to maintain the required flow even at low speeds, ensuring energy efficiency and prolonged battery life. This is particularly crucial as battery longevity is a key factor in the usability of the device in the field. A power converter can help aid the power draw from the fan and help with the longevity of the battery. It would be better to design this power converter as it can be designed with a smaller switching frequency to decrease the power loss through the converter, compared to off the shelf converters that typically have a high switching frequency and use asynchronous switching (switching controlled by a transistor). What would also help would be the use of rechargeable batteries and connecting them to a battery management IC (BMIC) or a power management unit (PMU). These ICs control power being delivered from the batteries to the fan based on its need or restore charge to the batteries if they drop past a certain threshold voltage.

Additionally, optimizing the power management system to reduce energy consumption without compromising performance will be essential. For the filtration system, meeting the NFPA standard remains a priority. It is recommended to use a similar filter style to the one selected in this design, as it offers increased surface area, which helps minimize airflow resistance and maximizes filtration efficiency.

Future groups should also focus on user comfort and ease of use, incorporating feedback from firefighters who test the device in real-world conditions. Field testing across diverse environments with firefighters will be crucial to validate the device's reliability and performance under varying conditions. This hands-on



feedback will be invaluable in making necessary adjustments to improve the overall user experience. Areas such as the fit and weight distribution of the full system, and the comfort of wearing the device for extended periods need careful consideration and iterative testing.

By prioritizing these areas of development, future teams can ensure that this respiratory protection device not only meets but exceeds the evolving needs of wildland firefighters, providing them with the best possible protection in their demanding work environments.

## 8. Acknowledgements

We would like to give a heartfelt thank you to Dr. Lily Laiho, Dr. Matthew Zoerb, and Dr. iian Black for their guidance over the entirety of this year-long project. We would like to express our sincere gratitude to the Wildfire Conservancy for their unwavering support and funding of this project. Special thanks to Frank Frievalt, Matt Rahn, and Kelcey Stricker for their invaluable insights and guidance throughout the development process. We are also deeply appreciative of Captain Jason Pratt and his crew from Station 1 in San Luis Obispo for their practical input and assistance in testing. Additionally, we extend our thanks to the WUI Fire Institute at Cal Poly and CAL FIRE for their collaboration and commitment to improving firefighter safety. This project would not have been possible without the collective efforts and dedication of all involved.

## Appendix A – References

- [1] The Wildfire Conservancy, Wildland Respiratory Protection.
- [2] L. Pinkerton, S. J. Bertke, J. Yiin, M. Dahm, T. Kubale, T. Hales, M. Purdue, J. J. Beaumont and R. Daniels, "Mortality in a cohort of US firefighters from San Francisco, Chicago and Philadelphia: an update," *Occupational and Environmental Medicine*, Vols. 77, no. 2, pp. 84-93 doi: <https://doi.org/10.1136/oemed-2019-105962.>, 2020.
- [3] K. M. Navarro, M. T. Kleinman, C. E. Mackay, T. E. Reinhardt, J. R. Balmes, G. A. Broyles, R. D. Ottmar, L. P. Naher and J. W. Domitrovich, "Wildland firefighter smoke exposure and risk of lung cancer and cardiovascular disease mortality," *Environmental Research*, vol. 173, pp. 462–468, 2019, doi: <https://doi.org/10.1016/j.envres.2019.03.060.>, 2019.
- [4] California Department of Public Health, "N95 Respirator Masks FAQs," cdph.ca.gov, 29 December 2022. [Online]. Available: <https://www.cdph.ca.gov/Programs/EPO/Pages/Wildfire%20Pages/N95-Respirators-FAQs.aspx>. [Accessed 5 November 2023].
- [5] P. Garg, S. Wang, J. M. Oakes, C. Bellini and M. J. Gollner, "The effectiveness of filter material for respiratory protection worn by wildland firefighters," *Fire Safety Journal*, vol. 139, no. Science Direct, 2023.
- [6] J. Johnson, "Firefighters test respirators to protect health," *San Francisco Chronicle*, p. A001, 14 October 2023.
- [7] National Fire Protection Association, "NFPA 1984," *NFPA 1984: Standard on Respirators for Wildland Fire-Fighting Operations and Wildland Urban Interface Operations*, 2022.
- [8] R.H. Spector, "Visual Fields," Nih.gov, 2015. [Online]. Available: <https://www.ncbi.nlm.nih.gov/books/NBK220/>.
- [9] V. F. Ferrario, C. Sforza, G. Serrao, G. Grassi and E. Mossi, "Active range of motion of the head and cervical spine: a three-dimensional investigation in healthy young adults," *Journal of Orthopaedic Research*, vol. 20, no. 1, pp. 122-129 doi: [https://doi.org/10.1016/s0736-0266\(01\)00079-1](https://doi.org/10.1016/s0736-0266(01)00079-1), 2002.
- [10] "MAC-X 2-6 ft Expandable Ultra Flex Helmet Air Pumper System Hose," sxsaddicts.com, [Online]. Available: <https://sxsaddicts.com/products/mac-x-expandable-pumper-hose-with-cuffs>. [Accessed 7 November 2023].

- [11] Cal Fire/San Diego County Fire, "How many pounds does a firefighter carry during a wildland fire?," 7 July 2019. [Online]. Available: <https://www.facebook.com/CALFIRESANDIEGO/photos/a.706566349392199/2286156474766504/?type=3>. [Accessed 7 November 2023].
- [12] B. on H. S. Policy and I. of Medicine, "Defining PAPRs and Current Standards," [www.ncbi.nlm.nih.gov](http://www.ncbi.nlm.nih.gov), 7 May 2015. [Online]. Available: [www.ncbi.nlm.nih.gov/books/NBK294223/](http://www.ncbi.nlm.nih.gov/books/NBK294223/).
- [13] O. O. a. Ц. Борисович, "Method of respiratory and eye protection against aerosols and protection device for implementation thereof". Russia Patent RU2407567C1, 27 December 2010.
- [14] 龚露露 and Sanhe Jiubao Technology Co, "Smoke-proof helmet for fire fighting". China Patent CN209915110U, 10 January 2020.
- [15] CALFIRE, *Redding Respirator Survey Data*, 2023.
- [16] A Fresher Home, *How To Tell Tell Which Way A Fan Blows*, 2018.
- [17] Frico, *Technical Handbook - Air Curtains*, [https://www.frico.net/fileadmin/user\\_upload/frico/Pdf/technical\\_handbook\\_frico\\_air\\_curtains\\_en\\_2021.pdf](https://www.frico.net/fileadmin/user_upload/frico/Pdf/technical_handbook_frico_air_curtains_en_2021.pdf) [Accessed Feb. 25, 2024].
- [18] Adafruit Industries, *Adafruit SCD-40 - True CO<sub>2</sub>, Temperature and Humidity Sensor*.
- [19] Adafruit Industries, *Adafruit SPG30 Air Quality Sensor Breakout - VOC and eCO<sub>2</sub>*.
- [20] L-Com, an INFINITE brand, *Carbon Monoxide Gas Sensor Module, 10-10000 ppm, Analog and TTL level Output, MQ7 Sensing Element*.
- [21] C.P.S.U.L Obispo, "Academic Programs and Planning," 2024. [Online]. Available: [https://academicprograms.calpoly.edu/content/academicpolicies/sustainability\\_lo](https://academicprograms.calpoly.edu/content/academicpolicies/sustainability_lo) .
- [22] American National Standard Institute, *ANSI - 2020*, 2020.
- [23] Acoustical Society of America, "S3.2," in *Section 3.2: Method for Measuring the Intelligibility of Speech over Communication Systems*, 2020.
- [24] First Respire, *Team Contract*, 2023.

[25] Code of Federal Regulations, "42 CFR 84," in *Title 42 Chapter 84: Approval of Respiratory Protective Devices*, 2009.

[26] Code of Federal Regulations, "29 CFR 1910.134," in *Title 29 Chapter 1910: Occupational Safety and Health Standards*, 2009.

## Appendix B – Contact Information

### First Respire Team

Jack Adema – Manufacturing Engineering  
Phone: 805-458-1670  
Email: [jadema@calpoly.edu](mailto:jadema@calpoly.edu)

Payton Mayer – Electrical Engineering  
Phone: 360-609-1336  
Email: [pjmayer@calpoly.edu](mailto:pjmayer@calpoly.edu)

Tommy Ozawa – General Engineering  
Phone: 650-931-7193  
Email: [toozawa@calpoly.edu](mailto:toozawa@calpoly.edu)

Oliver Pilon – Biomedical Engineering  
Phone: 505-241-9362  
Email: [opilon@calpoly.edu](mailto:opilon@calpoly.edu)

Xaviera Pons – Electrical Engineering  
Phone: 714-715-1209  
Email: [xpons@calpoly.edu](mailto:xpons@calpoly.edu)

Calder Wood – Mechanical Engineering  
Phone: 734-353-0617  
Email: [cwood22@calpoly.edu](mailto:cwood22@calpoly.edu)

### Project Advisors/Sponsors/Resources

Dr. iian Black – Project Advisor  
Phone: 805-756-0691  
Email: [iiblack@calpoly.edu](mailto:iiblack@calpoly.edu)  
Office Location: 092M-B102

Dr. Lily Laiho – Project Sponsor  
Phone: 805-756-2172  
Email: [llaiho@calpoly.edu](mailto:llaiho@calpoly.edu)  
Office Location: 013-260A

Dr. Matthew Zoerb – Project Sponsor  
Phone: 805-756-2578  
Email: [mzoerb@calpoly.edu](mailto:mzoerb@calpoly.edu)  
Office Location: 180-304A

Frank Frievalt – Director of WUI Fire Institute  
Phone: 805-736-3000  
Email: [ffrieval@calpoly.edu](mailto:ffrieval@calpoly.edu)  
Office Location: 010-253

Matt Rahn – Executive Director of Wildfire Conservancy  
Phone: 619-846-1916  
Email: [mattrahn@wildfireconservancy.org](mailto:mattrahn@wildfireconservancy.org)

Kelcey Stricker – Health and Safety Director, Wildfire Conservancy  
Phone: 619-952-7706  
Email: [kelceystricker@wildfireconservancy.org](mailto:kelceystricker@wildfireconservancy.org)



## Appendix C - QFD: House of Quality

		Engineering Requirements (Hows)											Benchmarks				
Customer Requirements (Step #1) Requirements (Whats)		Weighting (1 to 5)	Weight	Respiratory Resistance	Duration of Use	Heat Resistance	Donning/Doffing Time	Comfortable/Adjustable Sizing	Communication Interference	Field of View	Motion Inhibition	Air Cooling	Filtration Quality	Gear Compatibility	Unit Cost	Bandana	Nsg
Customer Requirements (Step #2)	Lightweight	4	9					7					5	9	9		
	Cannot Interfere W/ Communication	4		6			3		9					8	7		
	Cannot Inhibit Motion	4	4	4				2		9			6	8	8		
	Cannot Inhibit Field of View	3								9			5	8	7		
	Comfortable	2	6	7	4			8			7			7	5		
	Low Maintenance/Easily Servicable	3			7	4					6	6	6	9	9	3	
	Compatible W/ Other Equipment	4					3			6	6		9	9	9		
	Easy to Take Off/Put On	3	5				9	2					6	8	8		
	Long Battery Life	5	8		7									3	N/a	N/a	
	Improve Air Quality	3		8					3			9	5	0	8		
	Fire/Heat Resistant	4				9								4	6	4	
	Filter Must Last at Least 1 Shift	4		4	7							8		N/a	2		
	Cannot Interfere W/ Respiration	5	9	2					5			7		0	6		
	Affordable	1	2		7							8		9	8	8	
Units		kg	mmH2O	Hours	°C	Seconds	mm	% Max Db	°	°	°C	ppm	Yes/No	\$			
Targets		2.28	25	8	177		120	140x200	80	100	125	5	25	Yes	400		
Benchmark #1		0.055	0	12	210		6	100 x 100	100	100	125	0	0	Yes	20		
Benchmark #2		0.255	150	0.5	171		3	140x200	90	100	125	0	95%	Yes	1.2		
Importance Scoring		121	139	94	63		51	58	70	51	60	14	120	128	40		
Importance Rating (%)		87	100	68	45		37	42	50	37	43	10	86	92	29		

## Appendix D - Pugh Matrices

Pugh matrices are requirement-based matrices that directly compare various designs with the same set of criteria. This method is efficient at estimating feasibility and usefulness with respect to a datum (generally a popular or common design that you're attempting to out-perform). The group included four Pugh matrices are included which were used to select several elements of the groups conceptual prototype during the design process.

- Mask Design:

- Active Filter Design:

		Alternative Concepts:		Depth Filtration		Surface Filtration				
Concept Selection Legend		Importance Rating	PAPR STD FILTER	Granular	Block	Bag	Woven	Ceramic		
Better	+			+	+	+	S	+		
Same	S			+	+	+	+	+		
Worse	-			-	+	+	-	-		
Key Criteria				S	-	-	+	+		
Duration of Use	7			S	S	S	S	S		
Heat Resistance	5			-	+	S	+	+		
Min Particle Size	6			S	S	+	-	+		
Air Flow Resistance	7			+	S	S	S	S		
Motion Impediment	8			+	-	-	+	+		
Gear Compatibility	9			-	+	S	+	+		
Unit Cost	3			S	S	+	-	+		
Size	6			+	S	S	S	S		
Recyclability/Reusability	4			+	-	-	+	+		
Aesthetic?	1			S	+	S	+	+		
Sum of Positives				4	4	4	5	7		
Sum of Negatives				2	2	2	1	1		
Sum of Sames				4	4	4	3	2		
Weighted Sum of Positives				22	21	21	26	36		
Weighted Sum of Negatives				15	11	11	6	6		
TOTALS				7	10	10	20	30		



- Power Design:

Concept Selection Legend		Importance Rating	9V Batteries	Portable Charger Power Bank	Portable Power Station	Power Bank Solar Charger	18 Volt Lithium Battery USB Charger Adapter	3M PAPR Battery	A/A/AA/AAA Batteries
Better	+								
Same	S								
Worse	-								
Key Criteria									
Rechargeable	5	0	+	+	+	+	S	S	
Voltage	10	0	-	+	-	+	S	-	
Max Weight	6	0	+	-	S	S	S	+	
Duration of Use	10	0	+	+	-	+	-	-	
Heat Resistance	10	0	S	-	+	+	+	S	
Motion Impediment	7	0	S	-	+	S	S	S	
Gear Compatibility	6	0	S	-	S	S	+	S	
Unit Cost	8	0	+	-	-	-	-	-	
Size	8	0	S	-	S	S	S	+	
Sum of Positives			4	3	3	4	2	2	
Sum of Negatives			1	6	3	1	2	3	
Sum of Sames			4	0	3	4	5	4	
Weighted Sum of Positives			29	25	22	35	16	14	
Weighted Sum of Negatives			10	45	28	8	18	28	
Totals			19	-20	-6	27	-2	-14	

- Passive Filter Design:

Concept Selection Legend		Importance Rating	N-95	Alternative 1	Alternative 2	Alternative 3	Alternative 4	Alternative 5	Alternative 6
Better	+								
Same	S								
Worse	-								
Key Criteria									
Duration of Use	7			S	+	+	+	+	+
Heat Resistance	5			+	S	S	+	S	+
Min Particle Size	6			+	S	S	S	S	S
Air Flow Resistance Filter	7			S	S	+	+	+	-
Motion Impediment	8			-	+	+	-	+	S
Gear Compatibility	9			S	S	S	-	S	S
Unit Cost	3			-	-	-	-	-	S
Size	6			-	+	S	-	S	+
Recyclability/Reusability	4			S	S	S	S	S	S
Sum of Positives				2	3	3	3	3	3
Sum of Negatives				3	1	1	4	1	1
Sum of Sames				4	5	5	2	5	5
Weighted Sum of Positives				22	63	66	57	66	54
Weighted Sum of Negatives				51	3	3	104	3	7
Totals				-29	60	63	-47	63	47



- Fan Design:

	Importance Rating	Alternative Concepts		
		Mixed Flow Fan	Centrifugal Fan	Axial Flow
<b>Key Criteria</b>		Datum		
Air Flow Pressure	10		+	-
Air Flow Volume	9		-	+
Communication Impediment (Noisiness)	2		-	+
Battery Life	4		-	+
Cost	1		S	S
Durability	6		+	-
Efficiency	3		-	+
Heat Resistance	5		S	S
Size	7		+	-
Weight	8		+	-
Sum of Positives		4	4	
Sum of Negatives		4	4	
Sum of Sames		2	2	
Weighted Sum of Positives		31	18	
Weighted Sum of Negatives		18	31	
TOTALS		13	-13	



## Appendix E - Customer Requirements

### Wildfire Respiratory Protection Device Engineering Requirements

Spec. #	Parameter Description	Requirement or Target (units)	Tolerance	Risk	Compliance
1*	Respiratory Resistance	*	Maximum	H	A, T, S
2	Weight	10 (lbs.)	Maximum	H	T, I
3*	Duration of Use	2 (Hours)*	Minimum	H	A, T
4	Heat Resistance	177 (°C)	+10( °C), -0 (°C)	H	T, S
5	Donning/Doffing Time	120 (Seconds)	Maximum	M	T, I
6	Adjustable Sizing	140 x 200 (mm)	±50 mm	M	I
7	Communication Interference	80% (intelligibility)	Minimum	H	A, T
8	Field of View	100° laterally	Minimum	H	T, S
9	Motion Inhibition (RoM)	125° and 75°	±5°	M	T, S
10	Air Cooling	5 (°F)	Minimum	L	T, S
11	Filtration Quality (CO)	25 (ppm)	Goal	M	A, T
12	Gear Compatibility	Compatible with current equipment	Go/No	H	I
13	Unit Cost	\$400	± \$100	L	I
Spec. #	Parameter Description	Adjustment Justification	Previous Specification		
1*	Respiratory Resistance	Previous specification intended for SCBA, NFPA configurations. Following sponsor discussions, requirements were shifted to Add Calcs (We can probe for low pressure zones with an analog sensor)	Exhalation: 80 (mmH <sub>2</sub> O) Inhalation: 25 (mmH <sub>2</sub> O)		
3*	Duration of Use	Following the PDR, Duration of Use was reduced to 2 hours (minimum) operating time. This adjustment is constrained by the design's power supply redesign, specifically module battery packs.	10 Hours		

### Key

Risk Factors	H - High	M - Medium	L - Low
--------------	----------	------------	---------

Compliance Methods	A - Analysis	T - Test	S - Similarity to Existing Designs	I - Inspection
--------------------	--------------	----------	------------------------------------	----------------

## Appendix F - Technical Specifications

Included below are the NFPA design and performance requirements that apply to the customer requirements, as well as descriptions of the appropriate test methods.

Wildfire Respiratory Protection Device Design/Performance Requirements (As Applicable)

NFPA 1984 Design Requirements (Sec. 6):

**1: Pass Design Inspection**

**NFPA 1984 6.1.1**

Certified organization inspects and evaluates following design requirements detailed in Section 6 .

**2: Respirator Effectiveness A**

**NFPA 1984 6.2.1**

Certified organization inspects and evaluates following design requirements specified by 42 CFR 84 .

**3: Respirator Effectiveness B**

**NFPA 1984 6.3.1**

Perform standard filtration testing 29 CFR 1910 and certify minimum protection factor of 10 on step 134. Record procedure and results for traceability and verification.

**4: Accommodating Eyewear**

**NFPA 1984 6.4.1** (Fulfill either NFPA 1984 6.4.1 or 6.4.2)

Section 6.4.1.1 corresponds to a full-face covering design & Section 6.4.1.2 corresponds to a partial face covering design .

**4.1.1: Accommodating Eyewear (Full-Face)**

**NFPA 1984 6.4.1.1**

Ensure NIOSH certified eyewear is incorporated into design. Record procedure and results for traceability and verification.

**4.1.2: Accommodating Eyewear (Partial Face)**

**NFPA 1984 6.4.1.2**

Ensure NIOSH certified eyewear is compatible with or incorporated into design. Record procedure and results for traceability and verification.

**5: Material/Part Safety**

**NFPA 1984 6.6.1**

All non-fabric components included in final design must be safe to handle, i.e., no burrs, sharp edges, rough spots, etc.. Record procedure and results for traceability and verification. **NFPA 1984 Performance Requirements (Sec. 7.1):**

**1: Heat Resilience**

**NFPA 1984 7.1.1**

Perform thermal test detailed in Section 8.1, record procedure and results for traceability and verification.

**2: External Ignition Resistance**



## **NFPA 1984 7.1.2**

Perform thermal test detailed in Section 8.2 to exterior parts and materials and ensure test piece does not ignite following conclusion of test. Record procedure and results for traceability and verification.

## **3: Donning and Doffing**

### **NFPA 1984 7.1.5**

Perform donning test detailed in Section 8.6 to full assembly. Step 8.6.6.1 cannot exceed 2 minutes. Record procedure and results for traceability and verification.

## **4: Communication Effectiveness**

### **NFPA 1984 7.1.6**

Perform communication hindrance test detailed in Section 8.7. Must perform 80% or higher. Record procedure and results for traceability and verification.

## **5: Breathing Resistance**

### **NFPA 1984 7.1.8**

Perform respiration test detailed in Section 8.9. To pass, specimen tested under 150 lpm (liters/min) must experience a maximum of 25mm w.c. (water column) inhalation resistance and 80mm w.c. in exhalation resistance.

## **6: Carbon Monoxide Protection**

### **NFPA 1984 7.2.3**

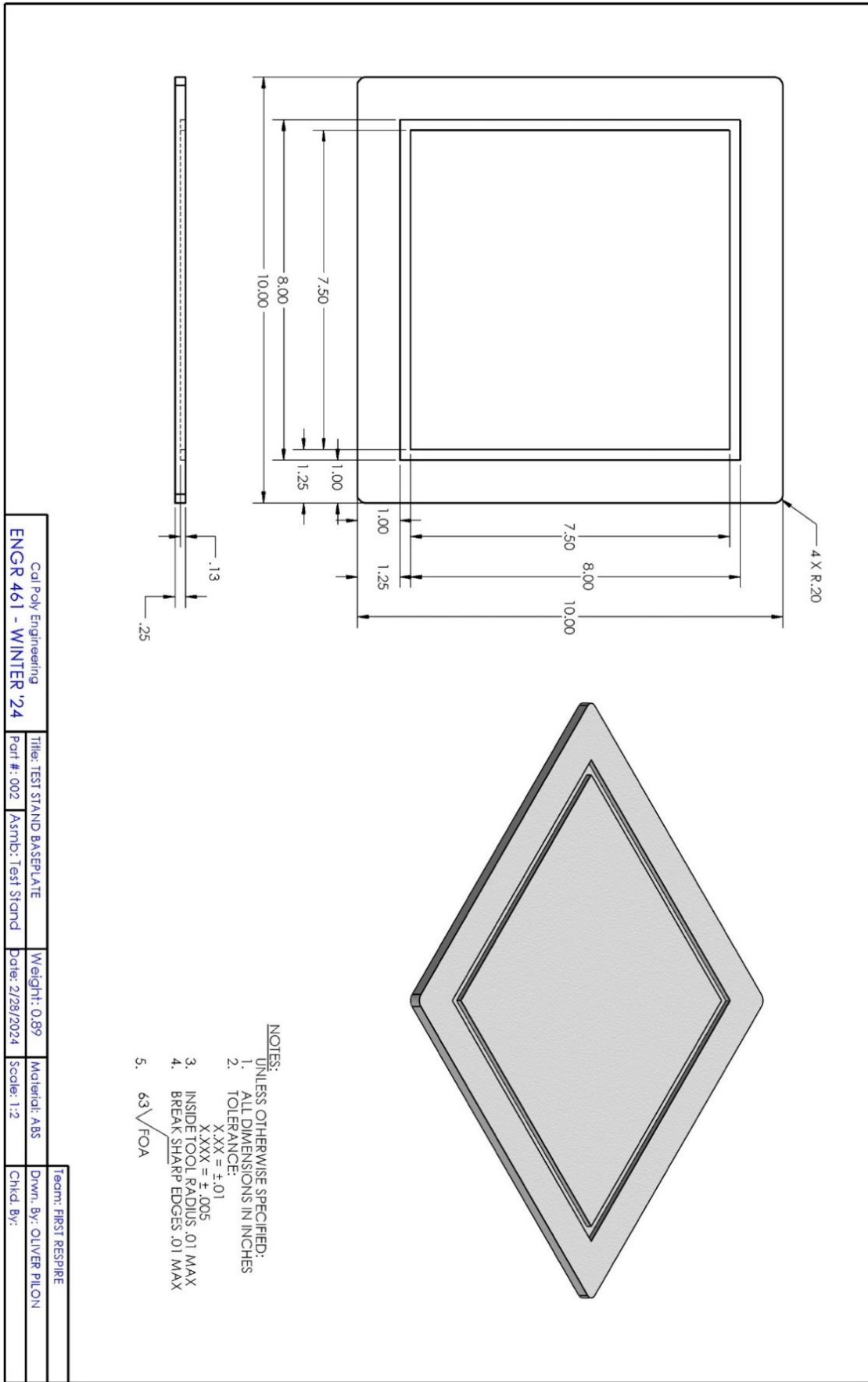
Perform respiration test detailed in either Section 8.9 or 8.10 . To pass, applicable components must not exceed appropriate values specified in Table 8.10.4(a) or 8.11.4 (NFPA 1984).

## Appendix G – Final Drawings

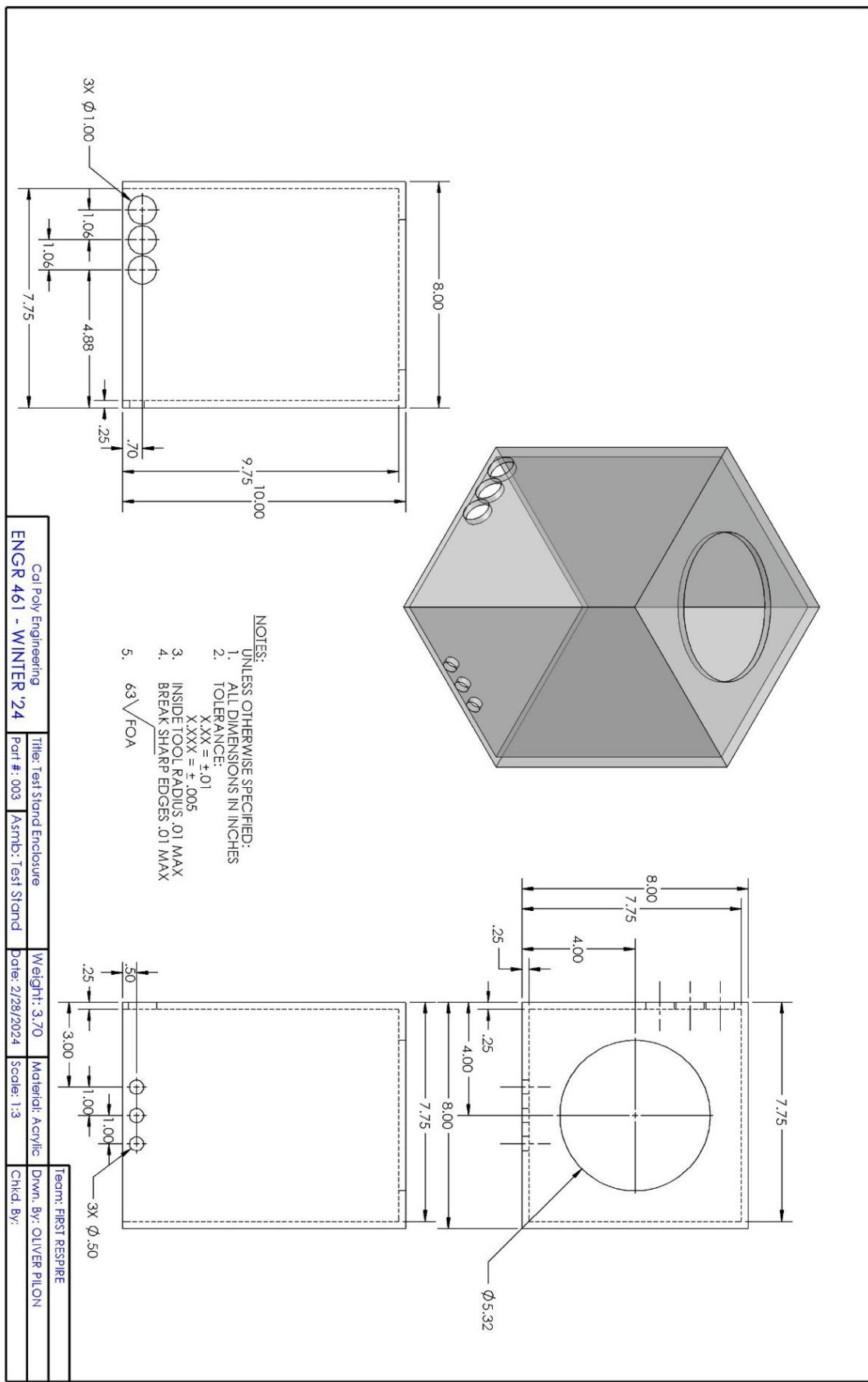
For ease of reference within the report, a letter designation has been assigned to each drawing as follows:

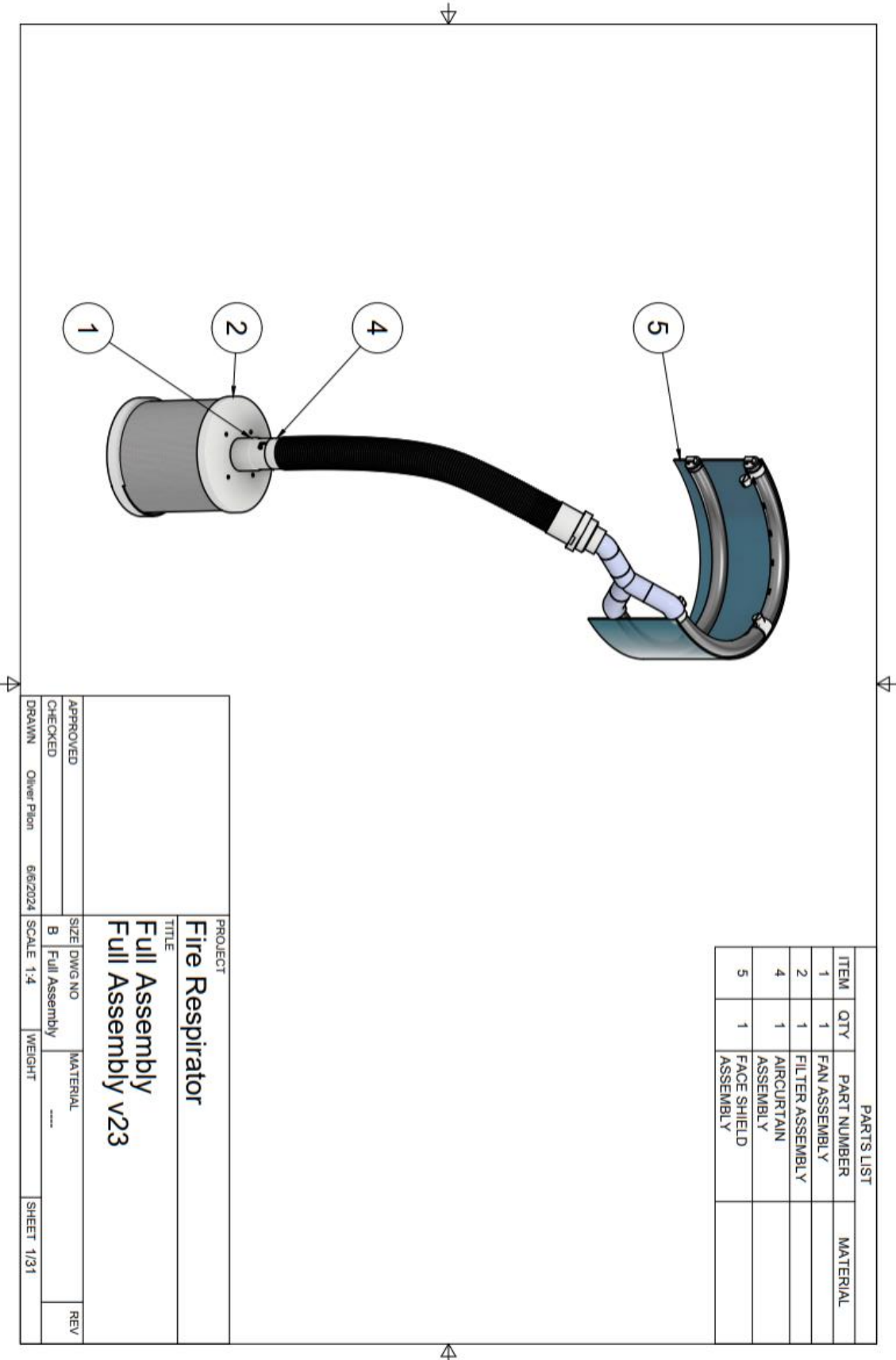
- A. TEST STAND BASEPLATE
- B. Test Stand Enclosure
- C. Full Assembly Full Assembly v23
- D. Full Assembly FAN ASSEMBLY
- E. Full Assembly Fan Mount v2
- F. Full Assembly Fan2Hose v3
- G. Full Assembly Component3 v5
- H. Full Assembly FILTER ASSEMBLY
- I. Full Assembly FilterCapV5 v6
- J. Full Assembly FilterFanCap v6
- K. Full Assembly Curtain testing 7 v2
- L. Full Assembly V11 Assembly Double v3
- M. Full Assembly Cooling curtain V3 v2
- N. Full Assembly Curtain End Cap 1 v3
- O. Full Assembly Shoulder Junction v3
- P. Full Assembly Magnetic Attachment – Curtain Right Side v3
  - \* This component goes on the left side because the curtain was modeled upside down.
- Q. Full Assembly Magnetic Attachment – Curtain Left Side v3
  - \* This component goes on the right side because the curtain was modeled upside down.
- R. Full Assembly Magnetic Attachment – Curtain Front v3
- S. Full Assembly Magnetic Attachment – Helmet Front
- T. Full Assembly Magnetic Attachment – Helmet Front Cap
- U. Full Assembly Magnetic Attachment – Helmet Side
- V. Full Assembly Magnetic Attachment – Helmet Side Cap
- W. Good Filter Test Rig Good Filter Test Rig v15
- X. Good Filter Test Rig ARDUINO FILTER CAP
- Y. Senor Outlet Holder Senor Outlet Holder v3
- Z. Good Filter Test Rig Sensor Holder + Arduino Cover
- AA. Good Filter Test Rig TESTRIG MOUNT
- BB. Good Filter Test Rig FILTER STANDIN
- CC. Good Filter Test Rig Arduino Holder





Cal Poly Engineering	Title: TEST STAND BASEPLATE	Weight: 0.89	Material: ABS	Team: FIRST RESP <small>RE</small> E
ENG R 461 - WINTER '24	Part #: 002	Asmb: Test Stand	Date: 2/28/2024	Drawn By: OLIVER PILON Chkd By:

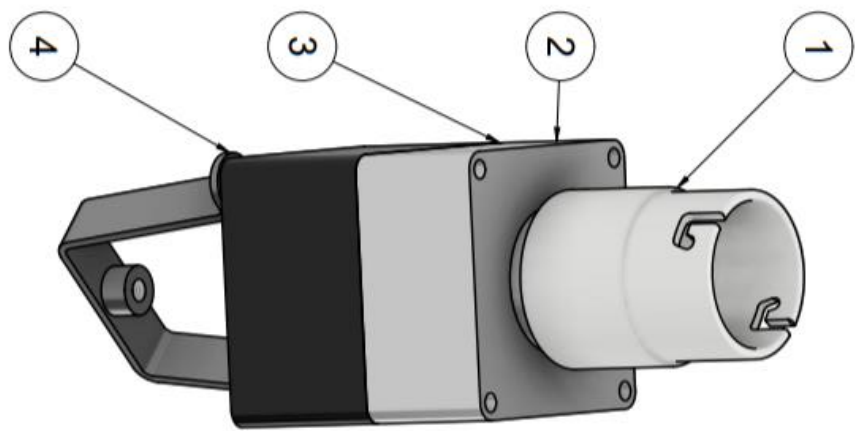






CAL POLY

▽



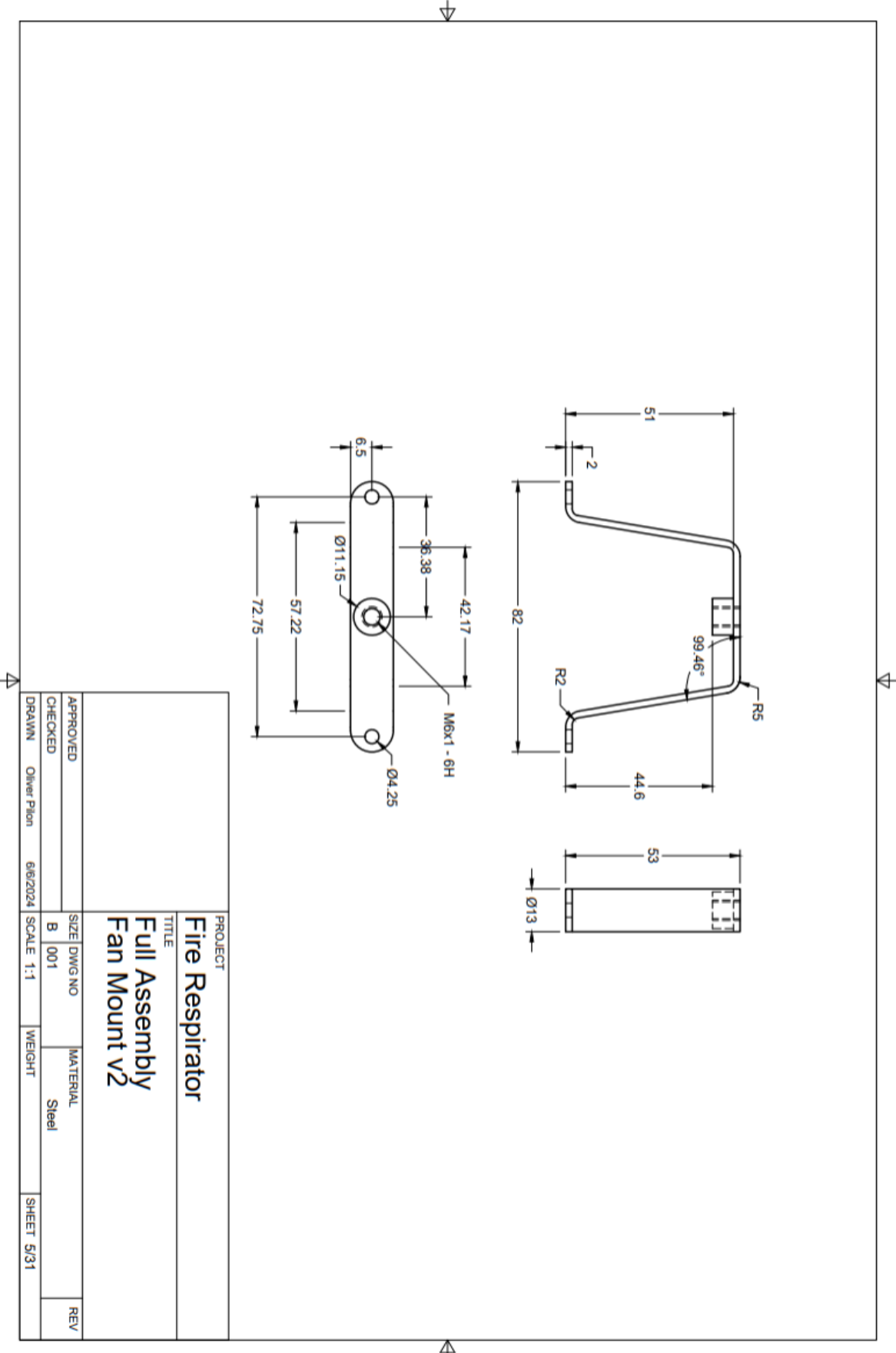
▽

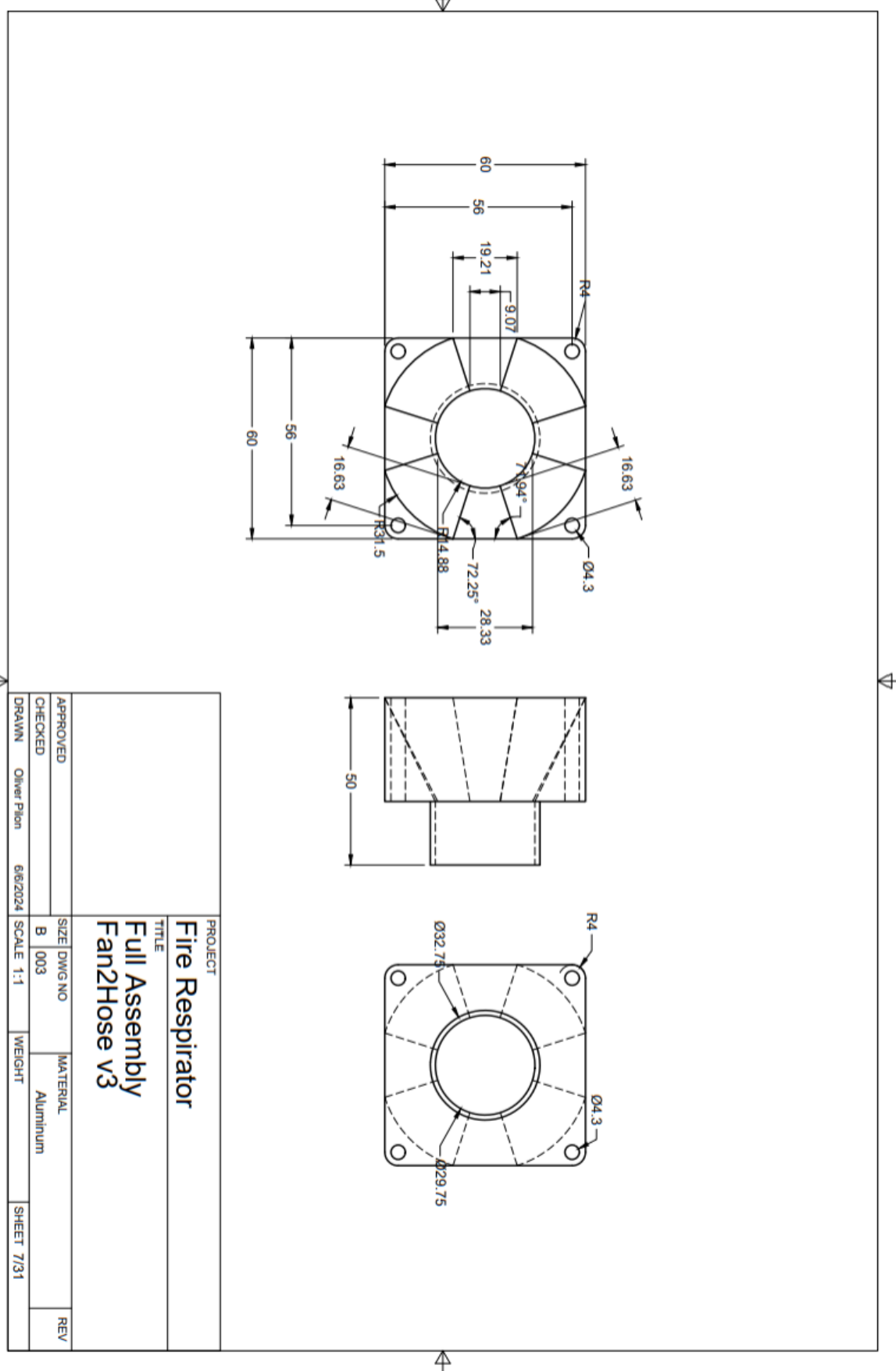
PROJECT	
Fire Respirator	
TITLE	Full Assembly
FAN ASSEMBLY	
APPROVED	SIZE DWG NO
CHECKED	B FAN ASSEMBLY MATERIAL
DRAWN	SCALE 1:1 WEIGHT
	REV
	SHEET 3/31

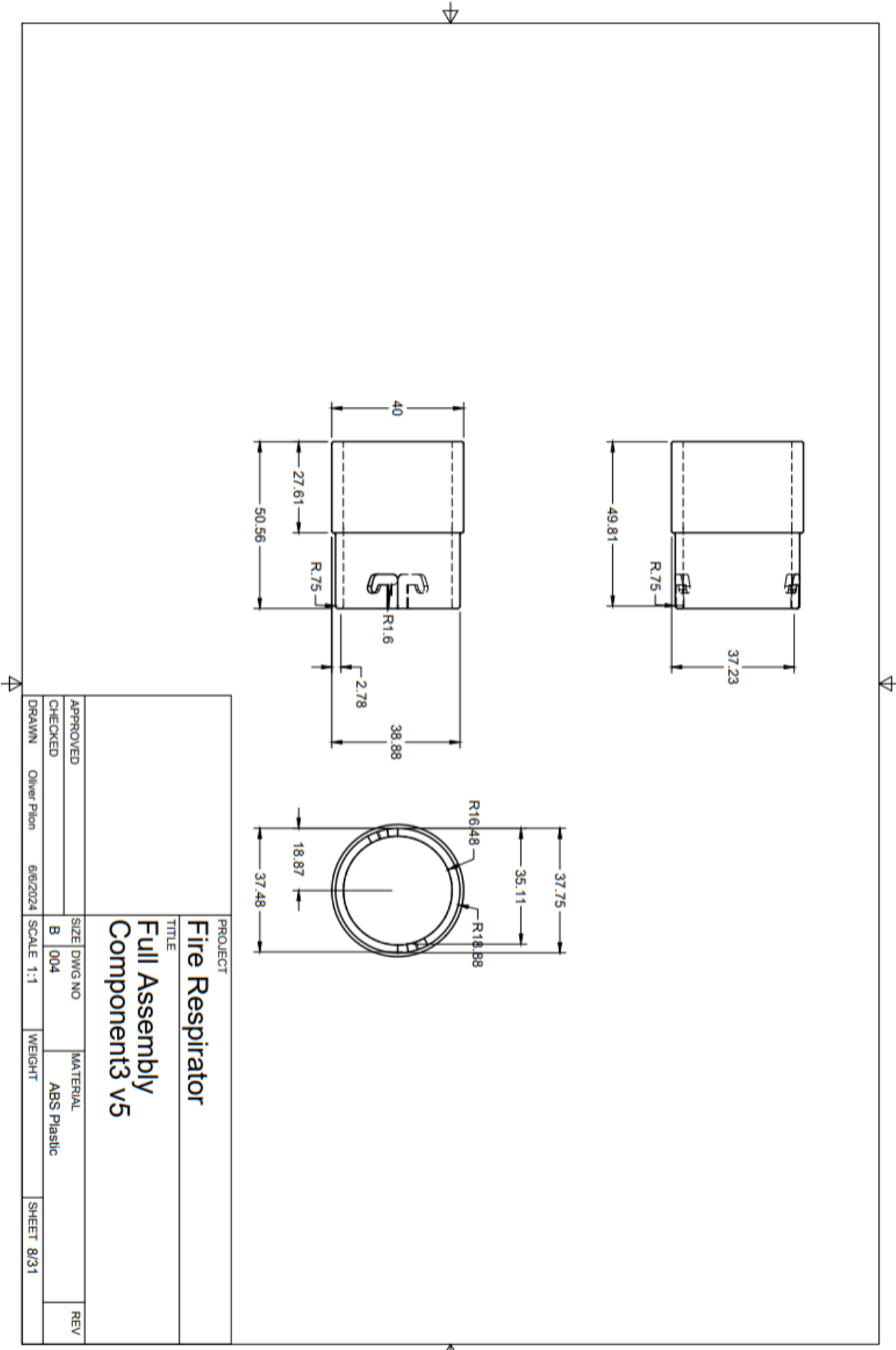
PARTS LIST			
ITEM	QTY	PART NUMBER	MATERIAL
1	1	004	ABS PLASTIC
2	1	003	ALUMINUM
3	1	002	ACETAL RESIN, BLACK
4	1	001	STEEL

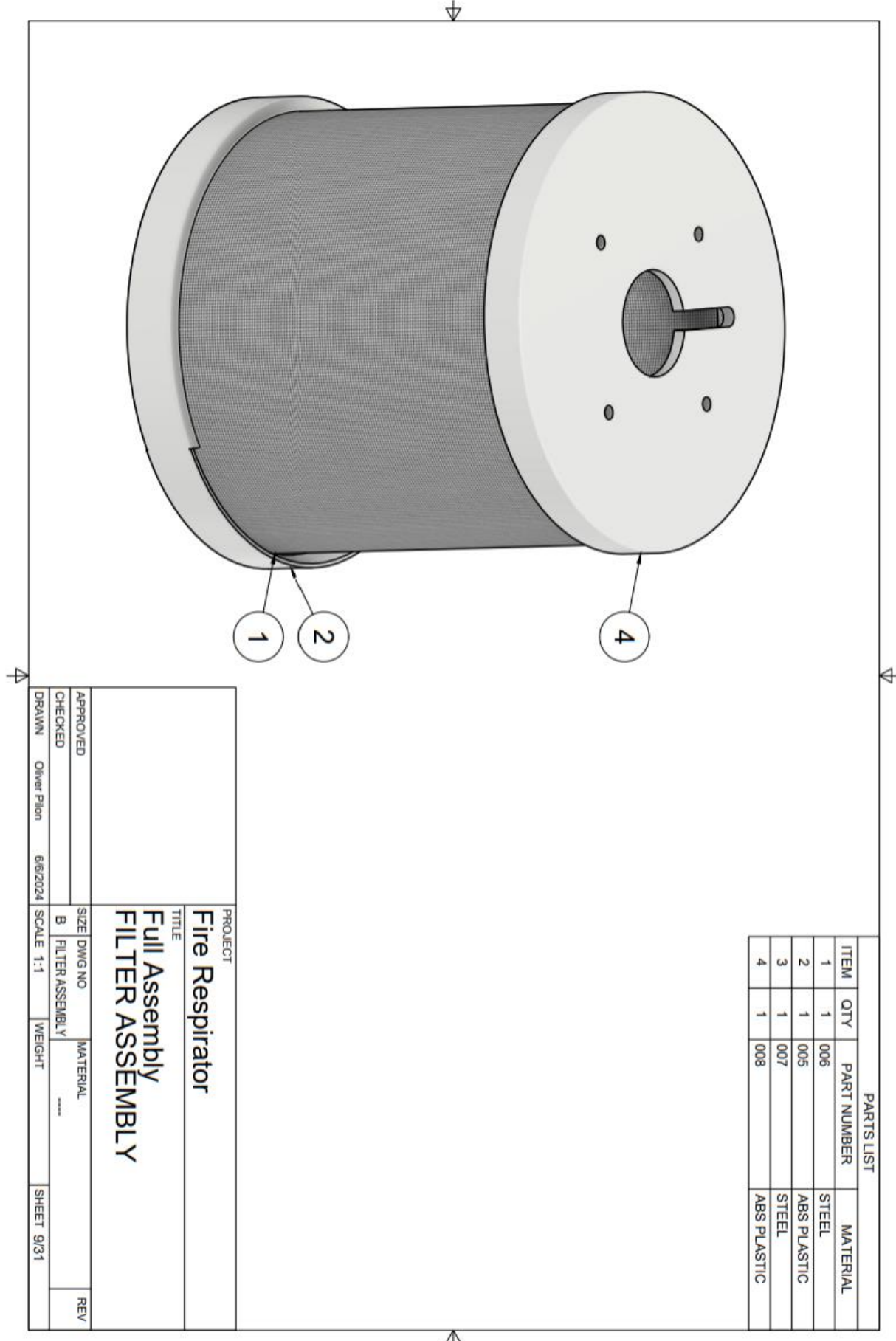
7

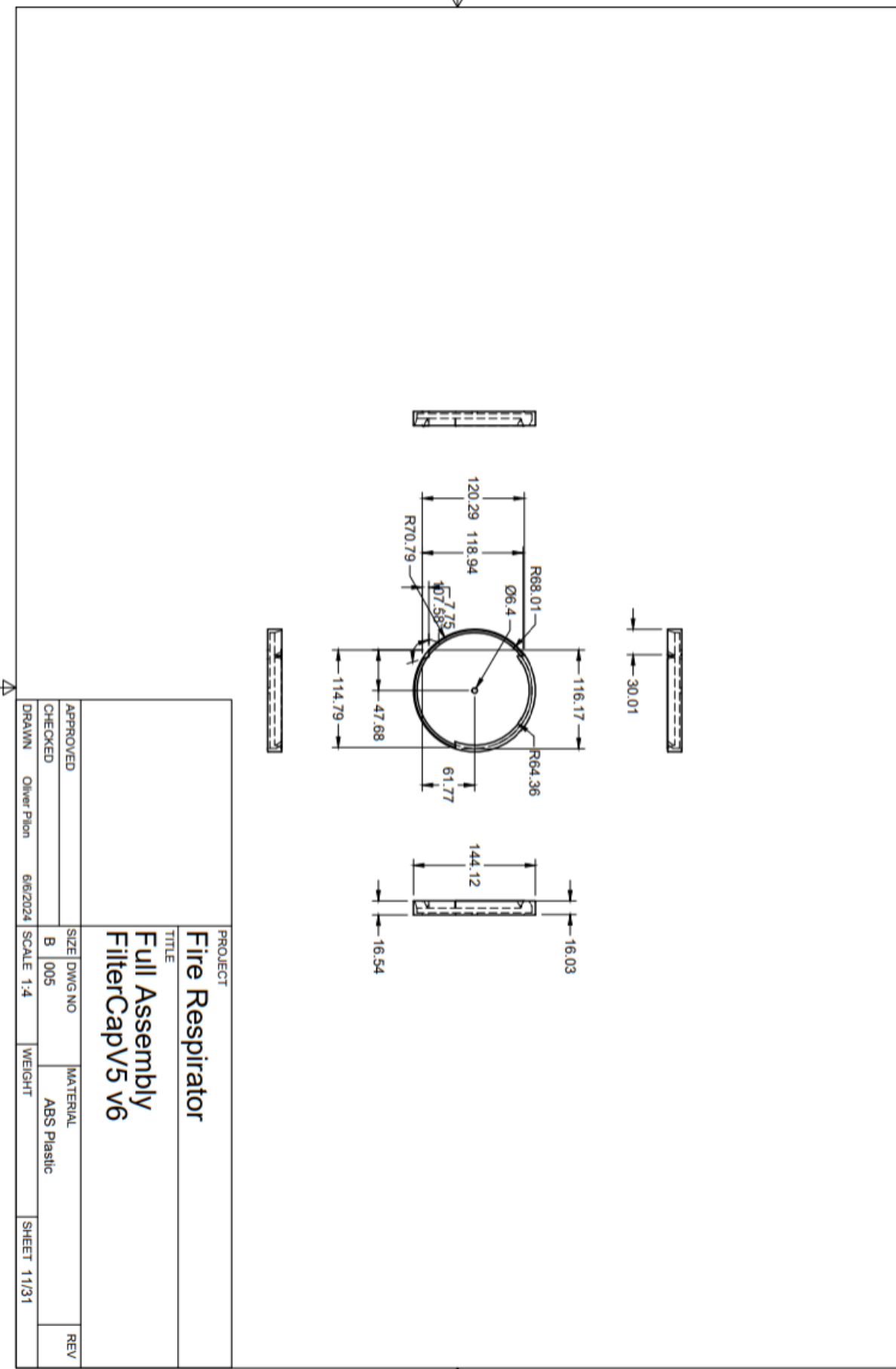
▽

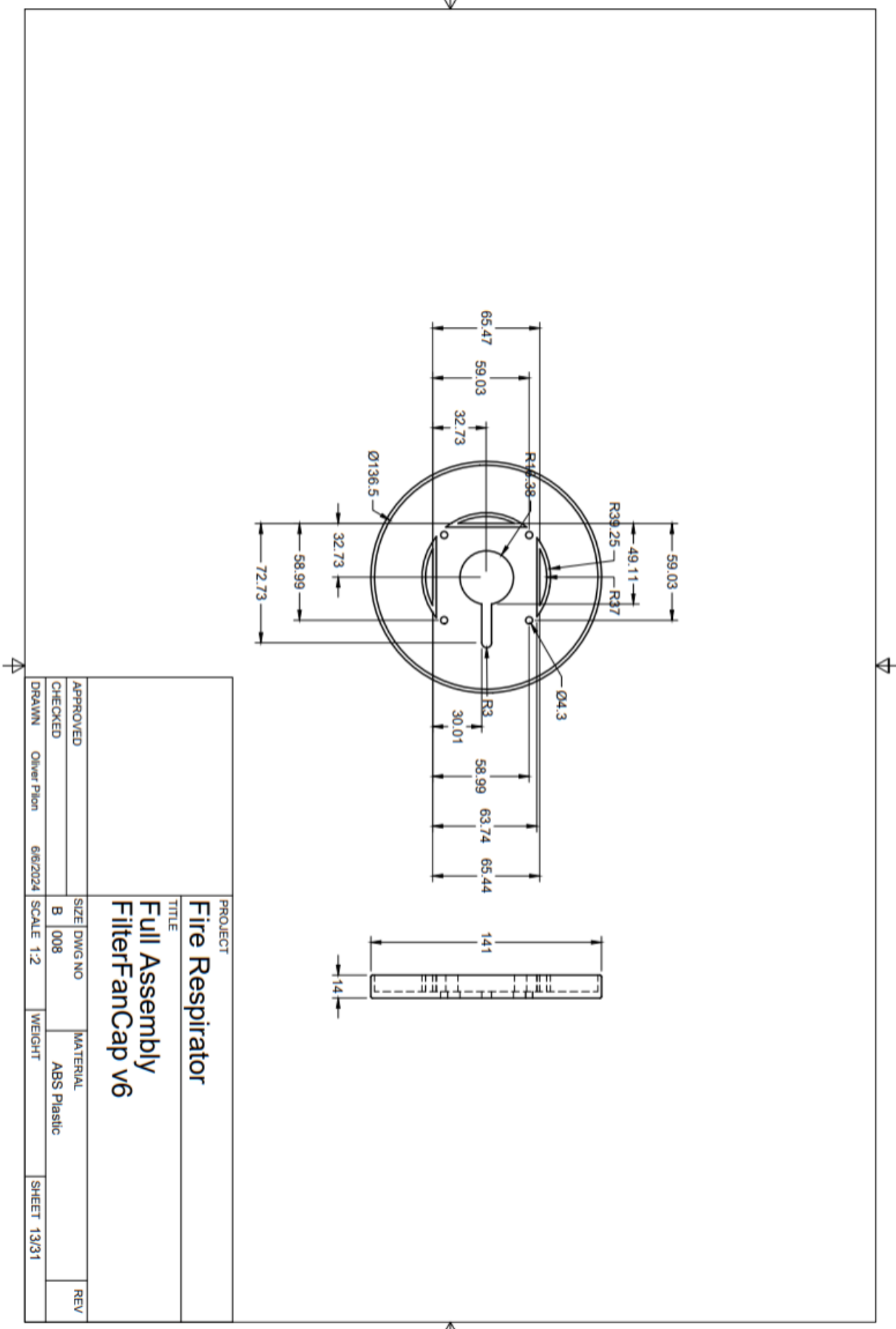


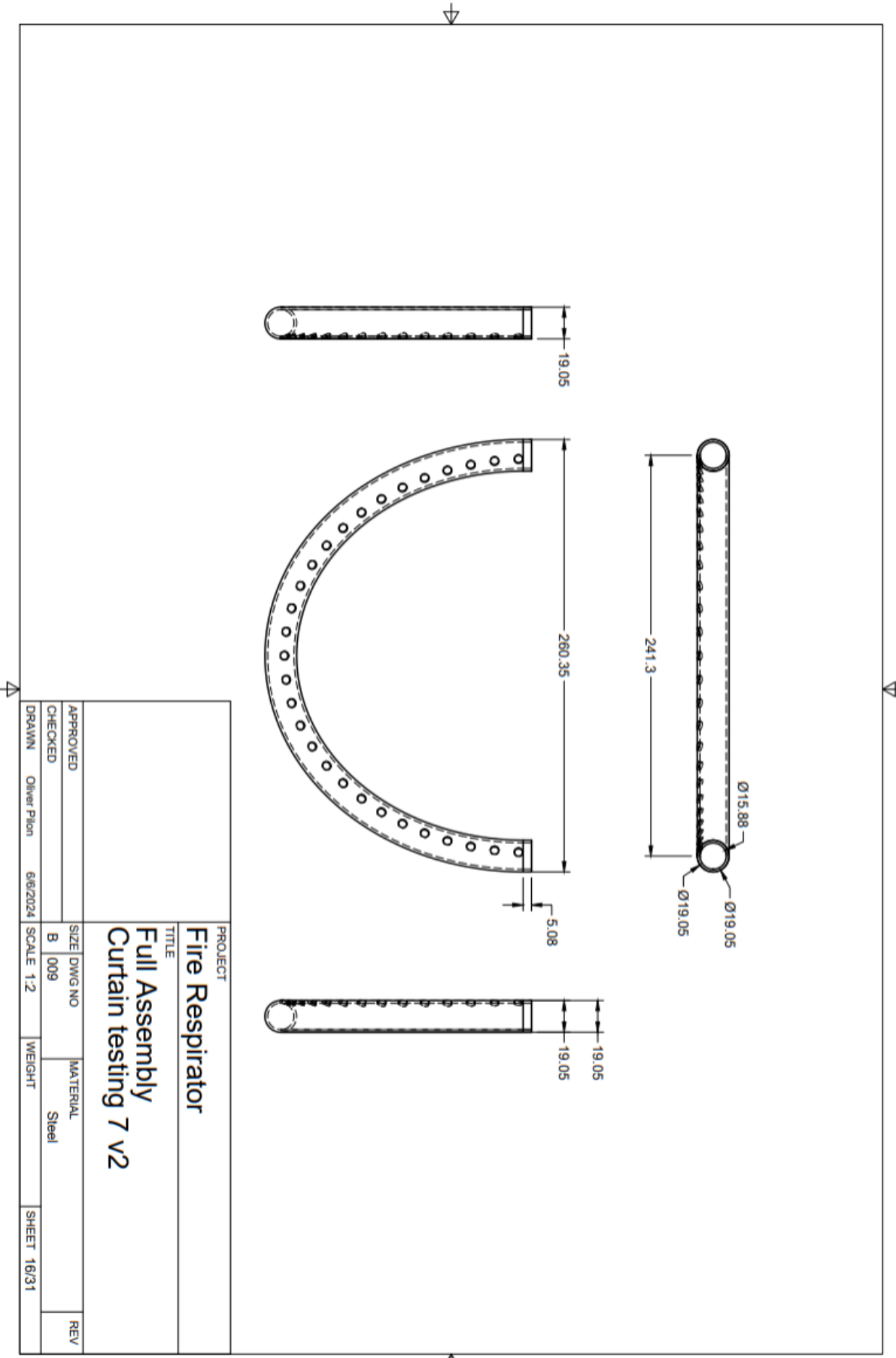








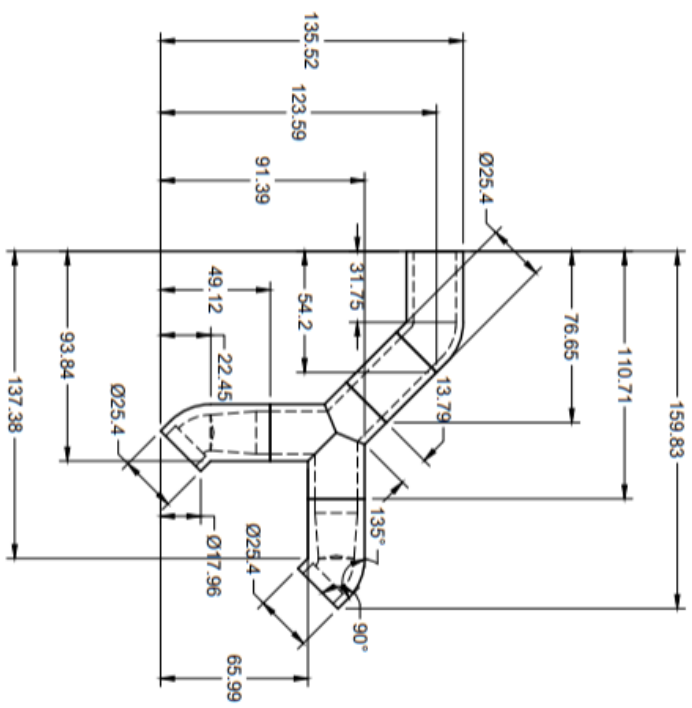






↑

PROJECT	
Fire Respirator	
TITLE	
APPROVED	SIZE DWG NO
CHECKED	B 010 MATERIAL
DRAWN	Oliver Pilan 6/6/2024 SCALE 1:2 WEIGHT
SHEET 17/31	

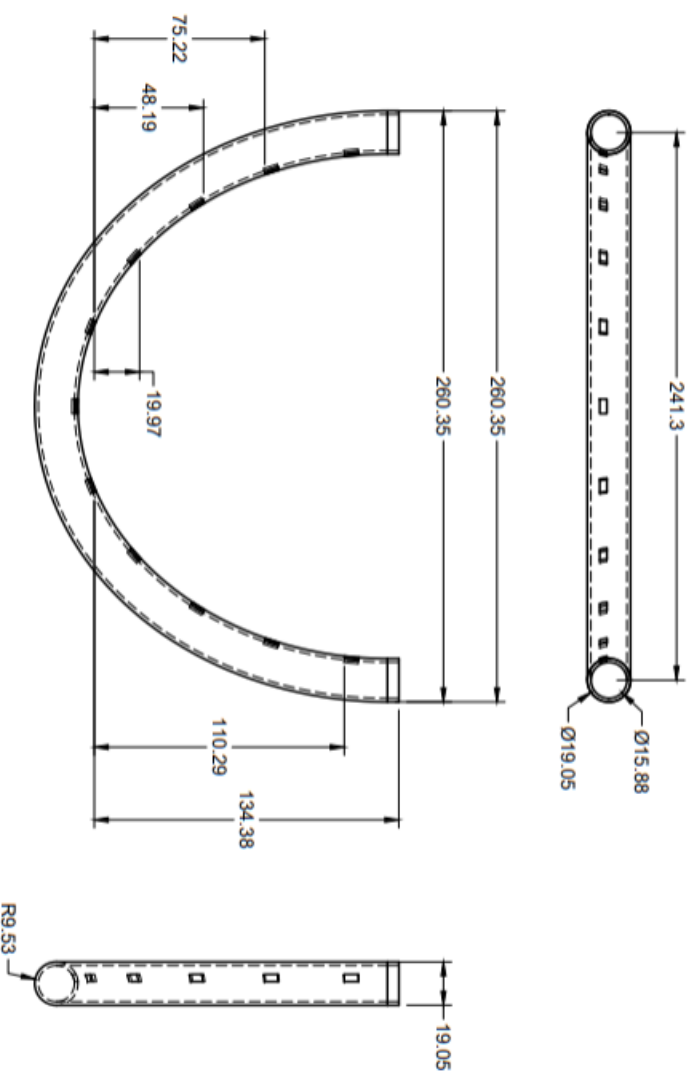


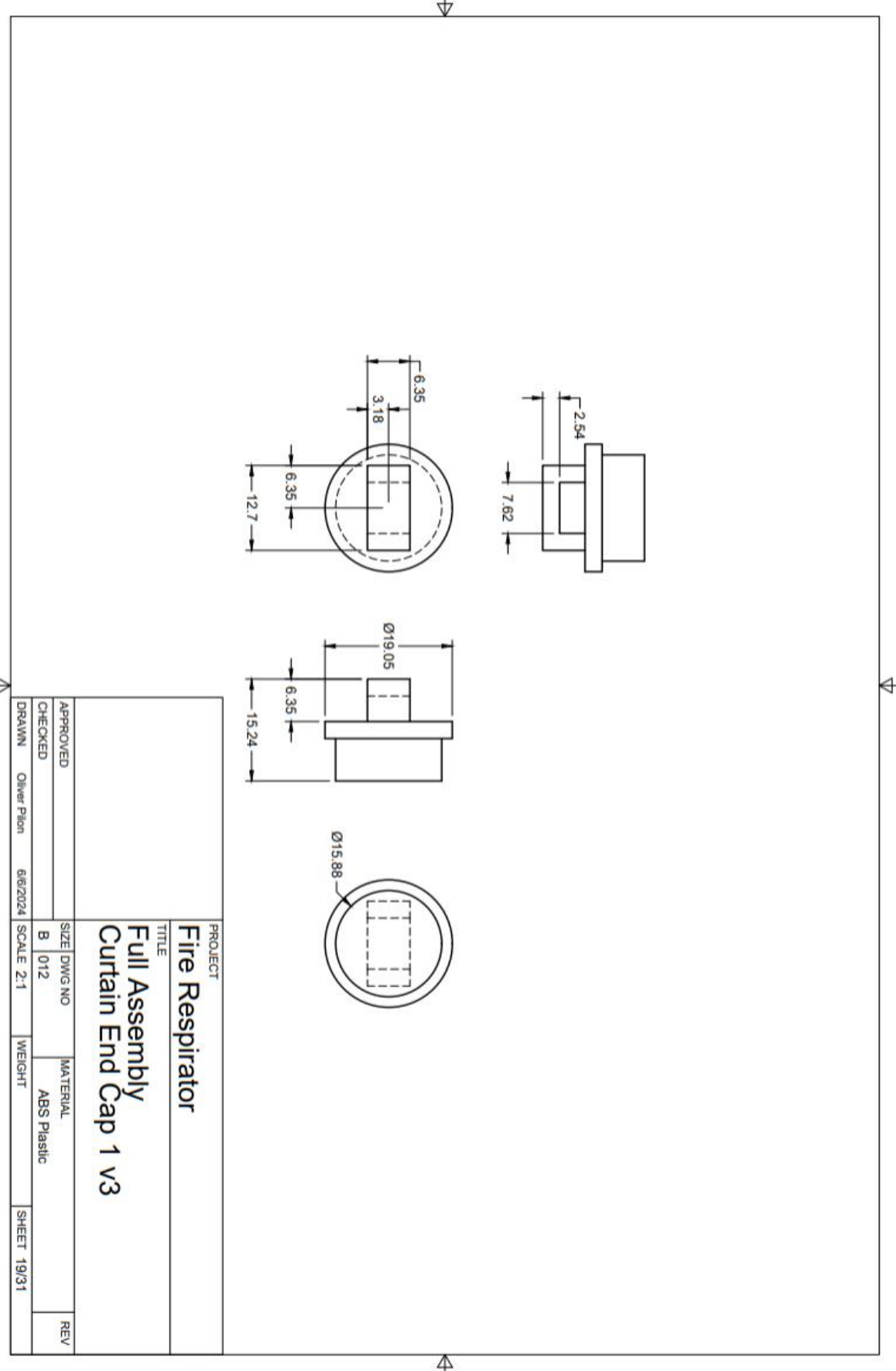
↓

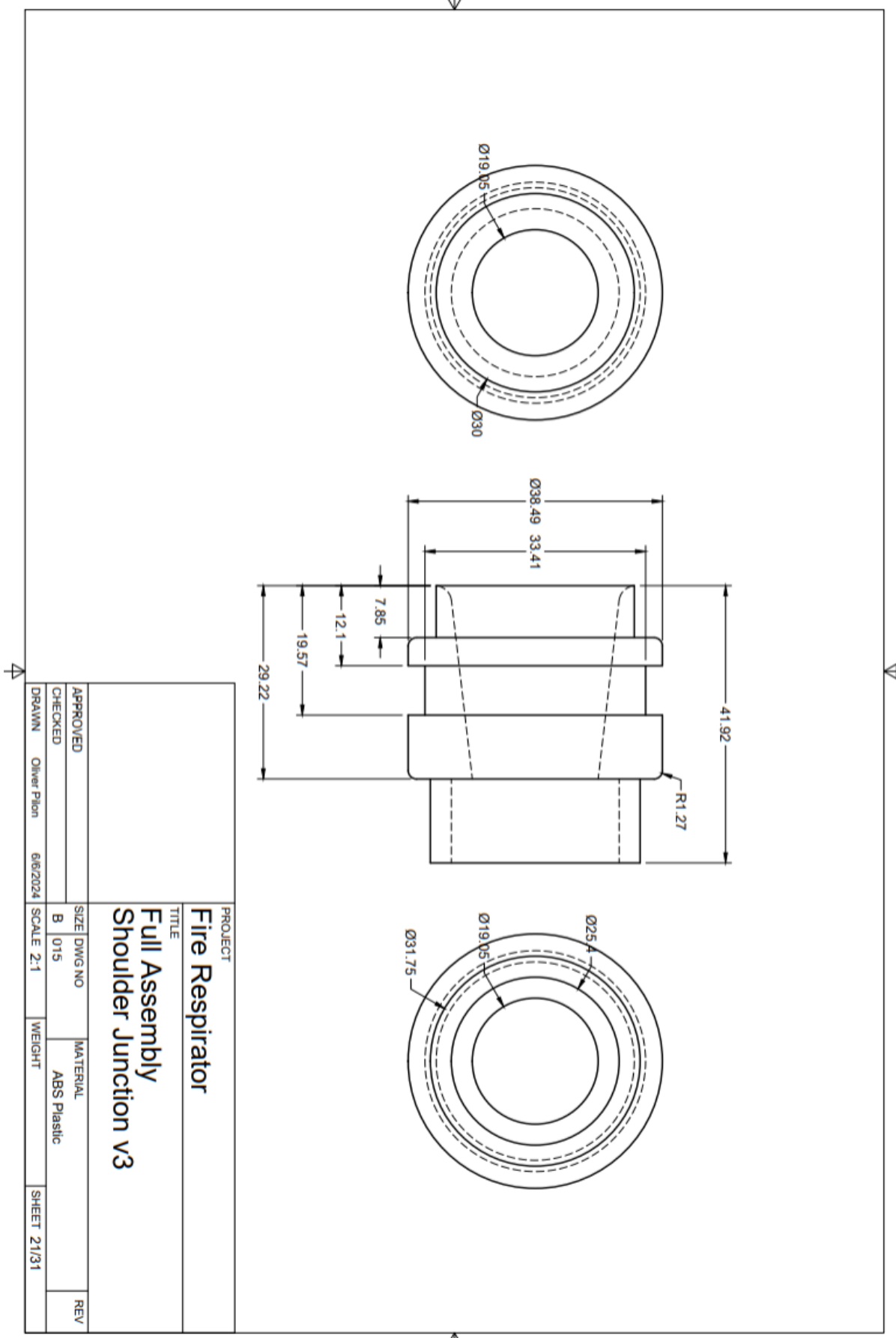
↓



PROJECT	
Fire Respirator	
TITLE	
APPROVED	SIZE DWG NO
CHECKED	B 011 MATERIAL
DRAWN	Oliver Pilon 6/6/2024 SCALE 1:2
	WEIGHT REV
	SHEET 18/31







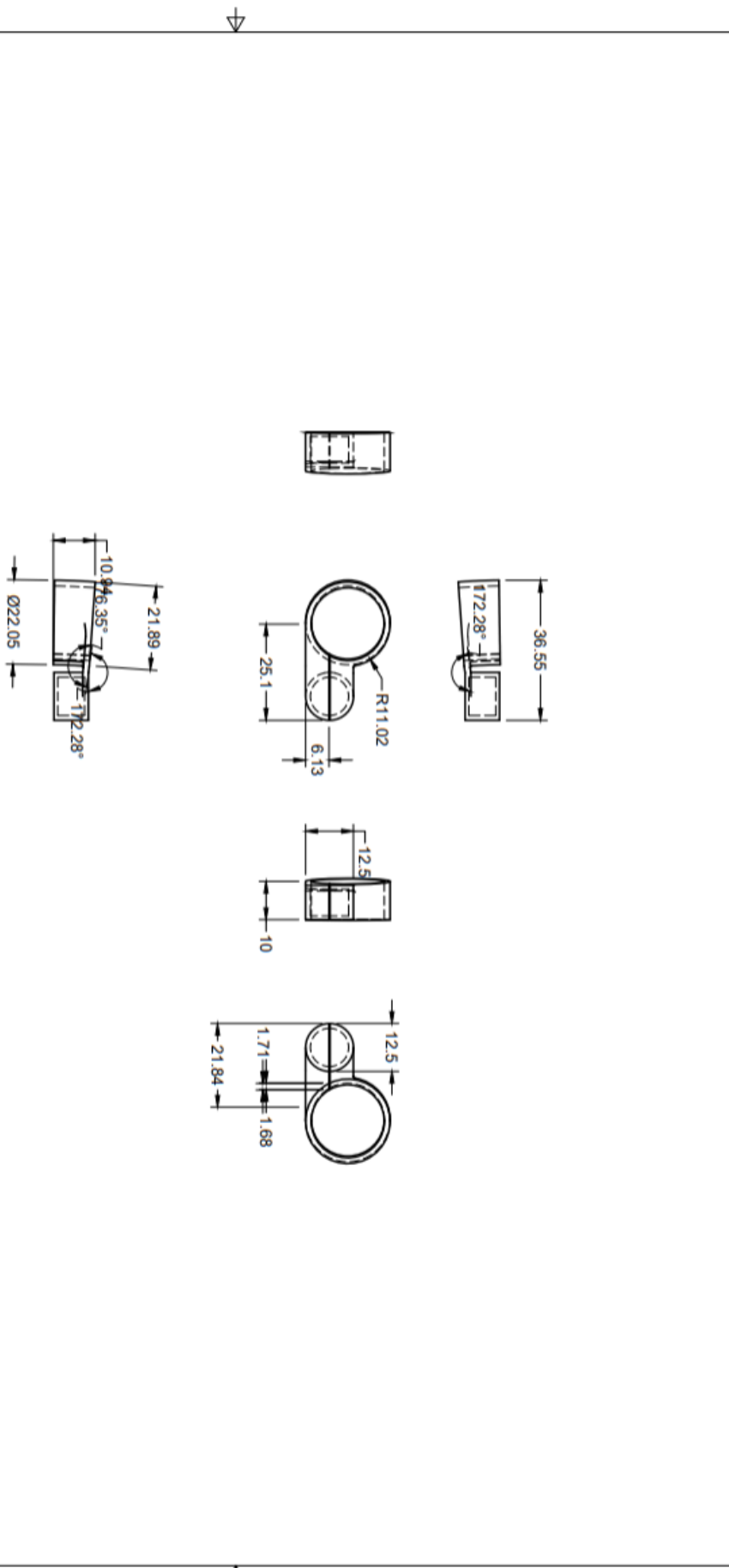


CAL POLY

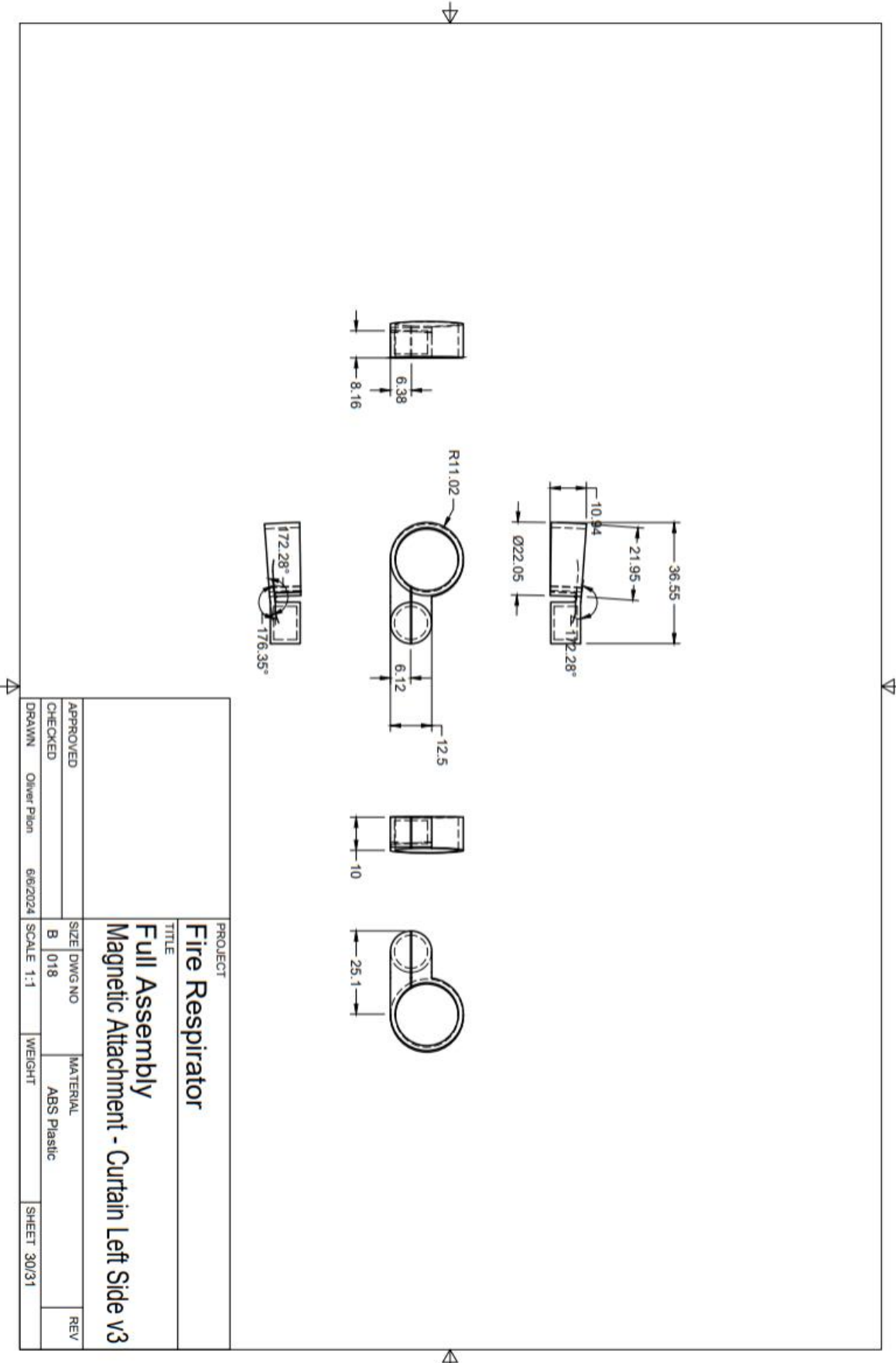
▽

9

APPROVED		SIZE	DWG NO	MATERIAL	REV
CHECKED		B	17	ABS Plastic	
DRAWN	Oliver Pilion	6/6/2024	SCALE 1:1	WEIGHT	SHEET 29/31



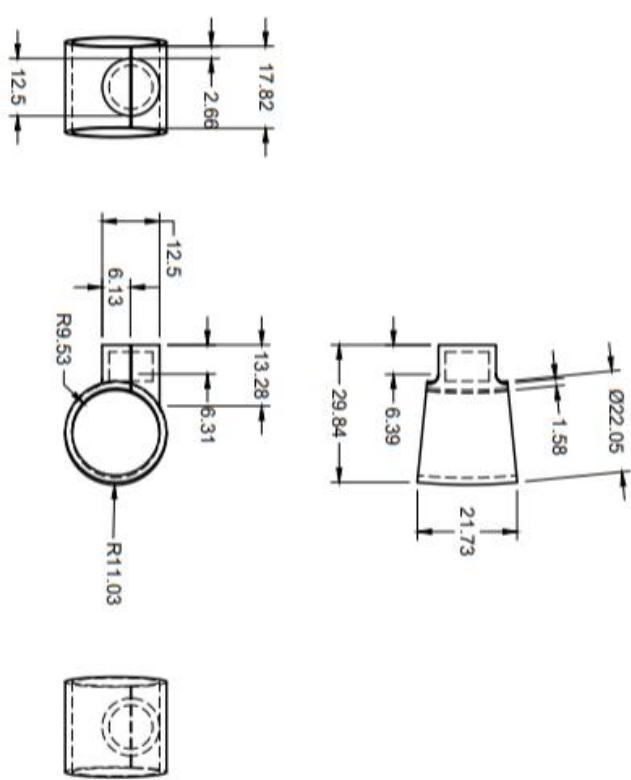
4





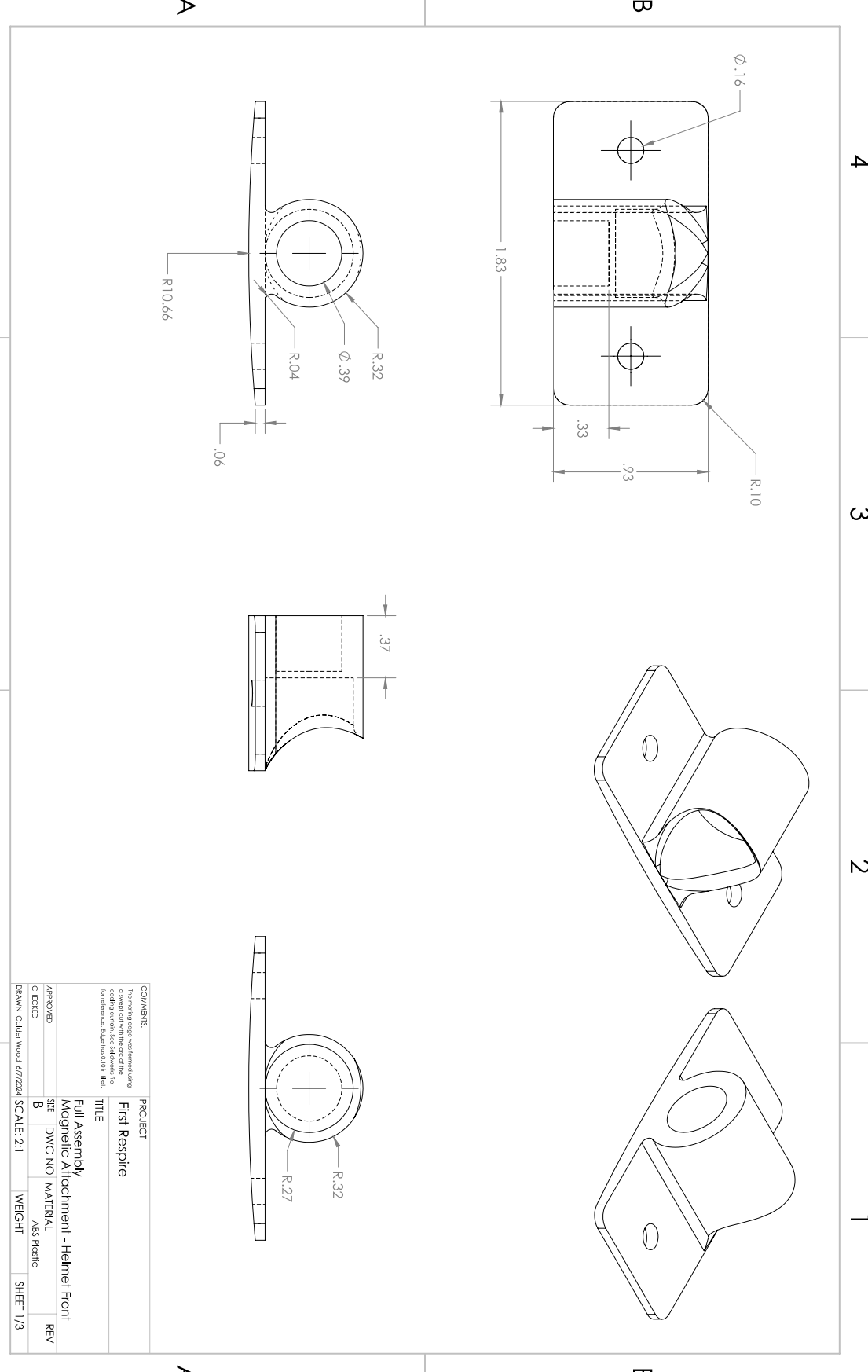
CAL POLY

PROJECT			
Fire Respirator			
TITLE			
Full Assembly			
APPROVED	SIZE B	DWG NO 019	MATERIAL ABS Plastic
CHECKED			REV
DRAWN	Oliver Pilon	SCALE 1:1	WEIGHT
	6/6/2024		SHEET 31/31





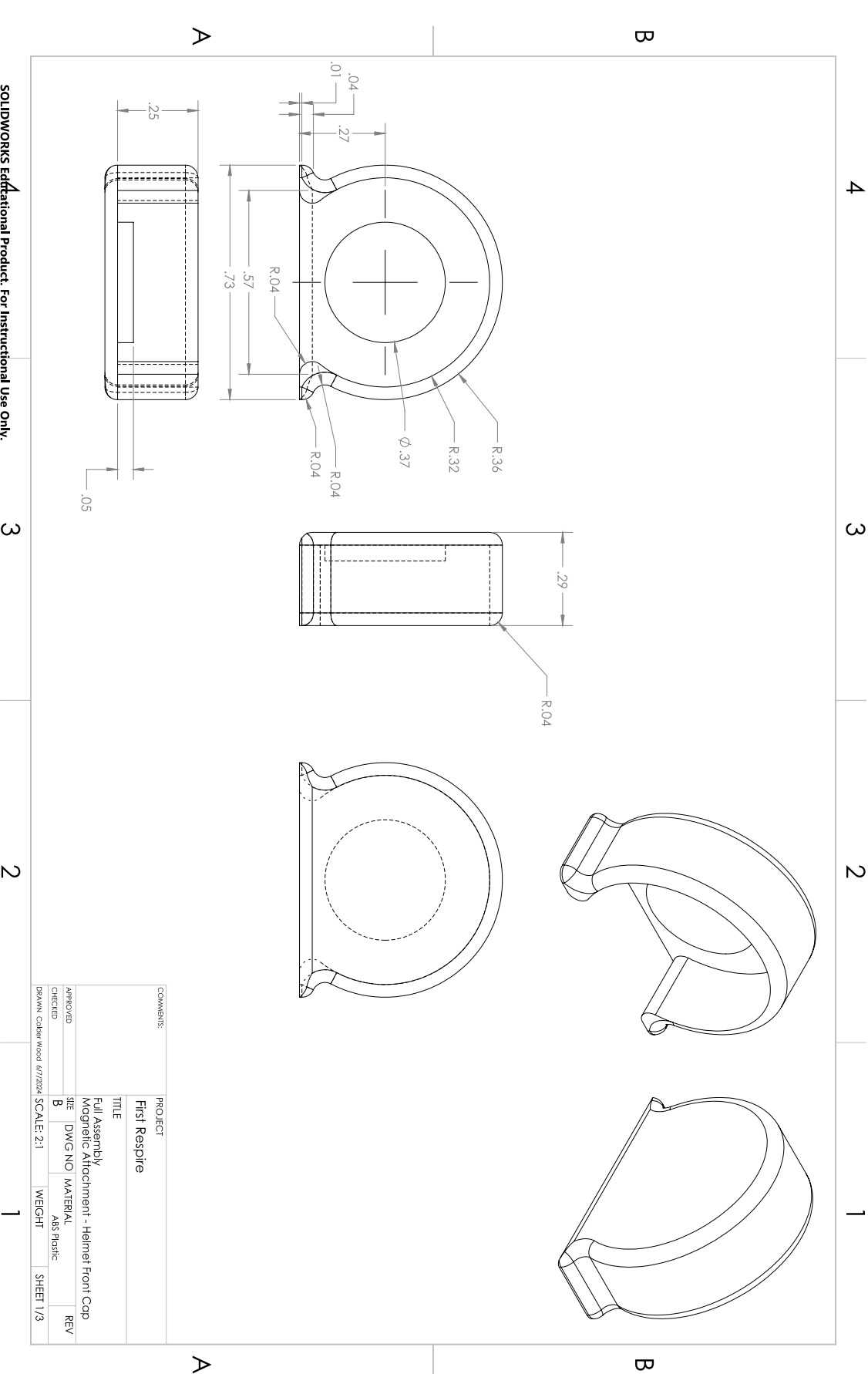
SOLIDWORKS Educational Product. For Instructional Use Only.





CAL POLY

SOLIDWORKS Educational Product. For Instructional Use Only.





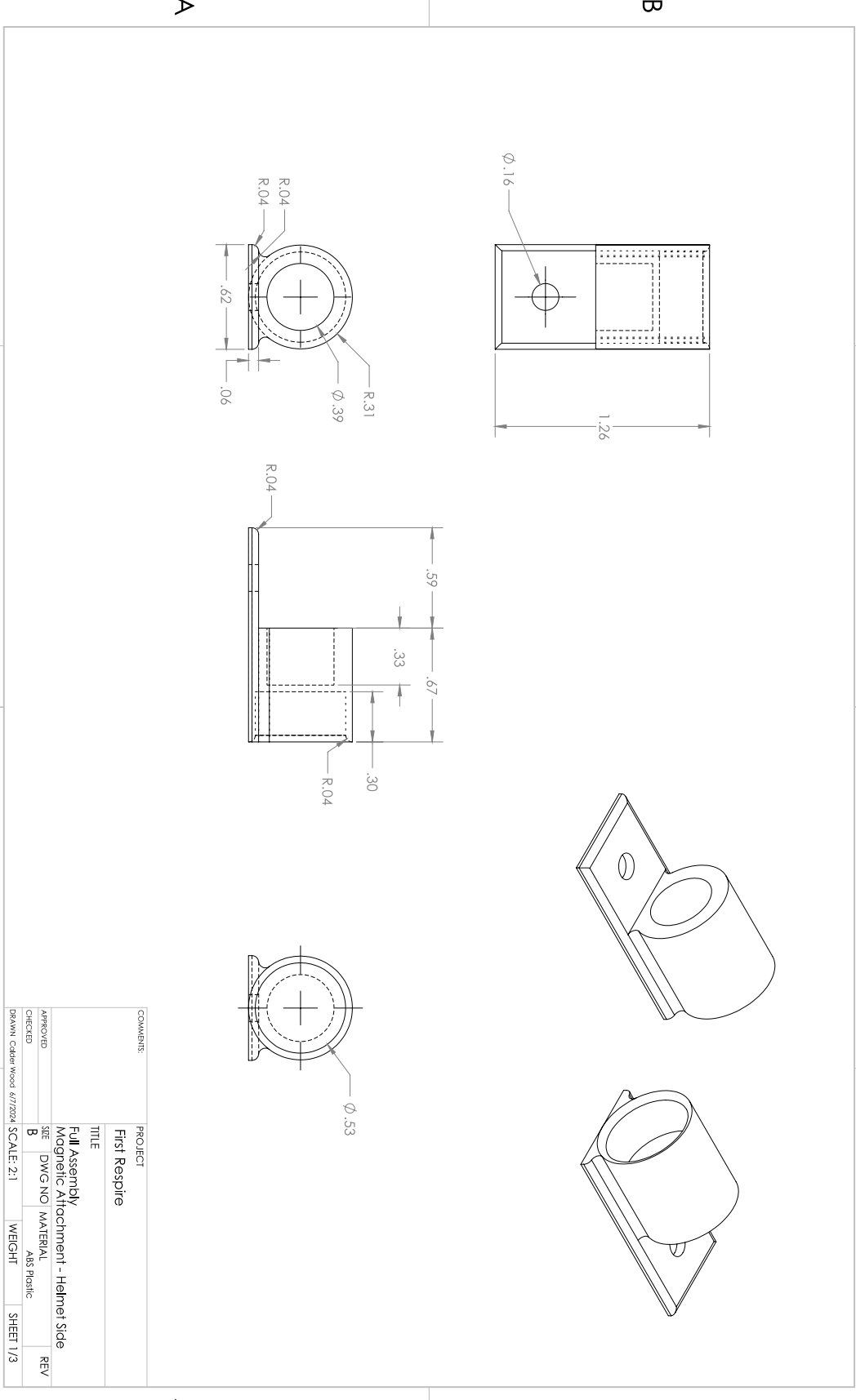
SOLIDWORKS Educational Product. For Instructional Use Only.

1

2

3

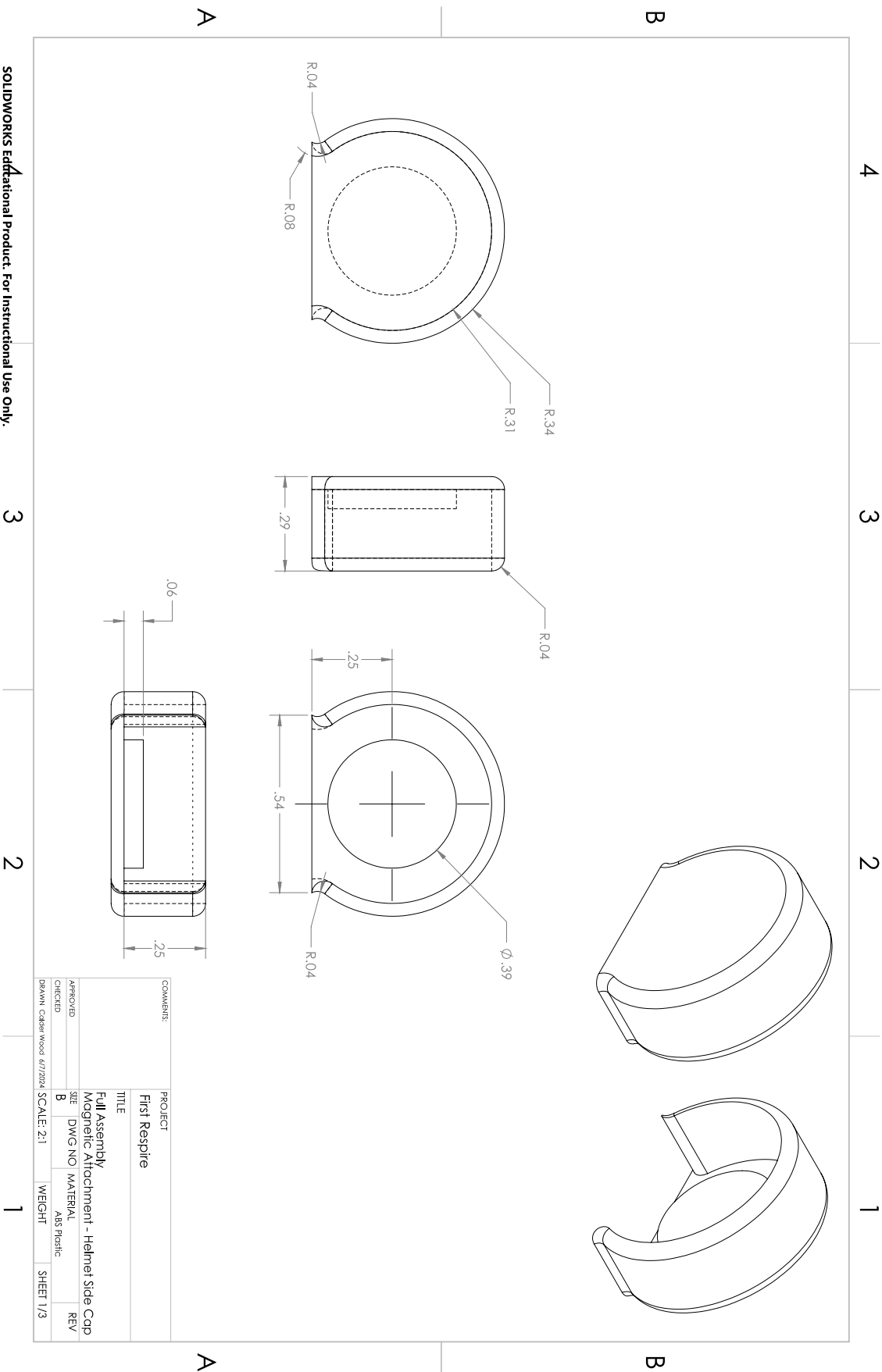
4

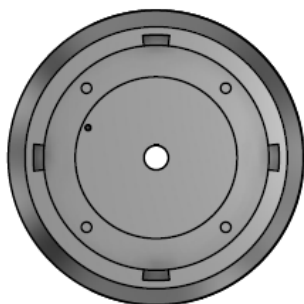
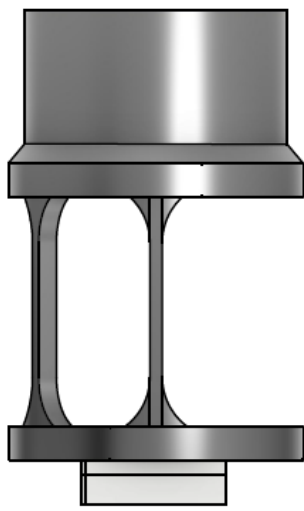




CAL POLY

SOLIDWORKS Educational Product. For Instructional Use Only.



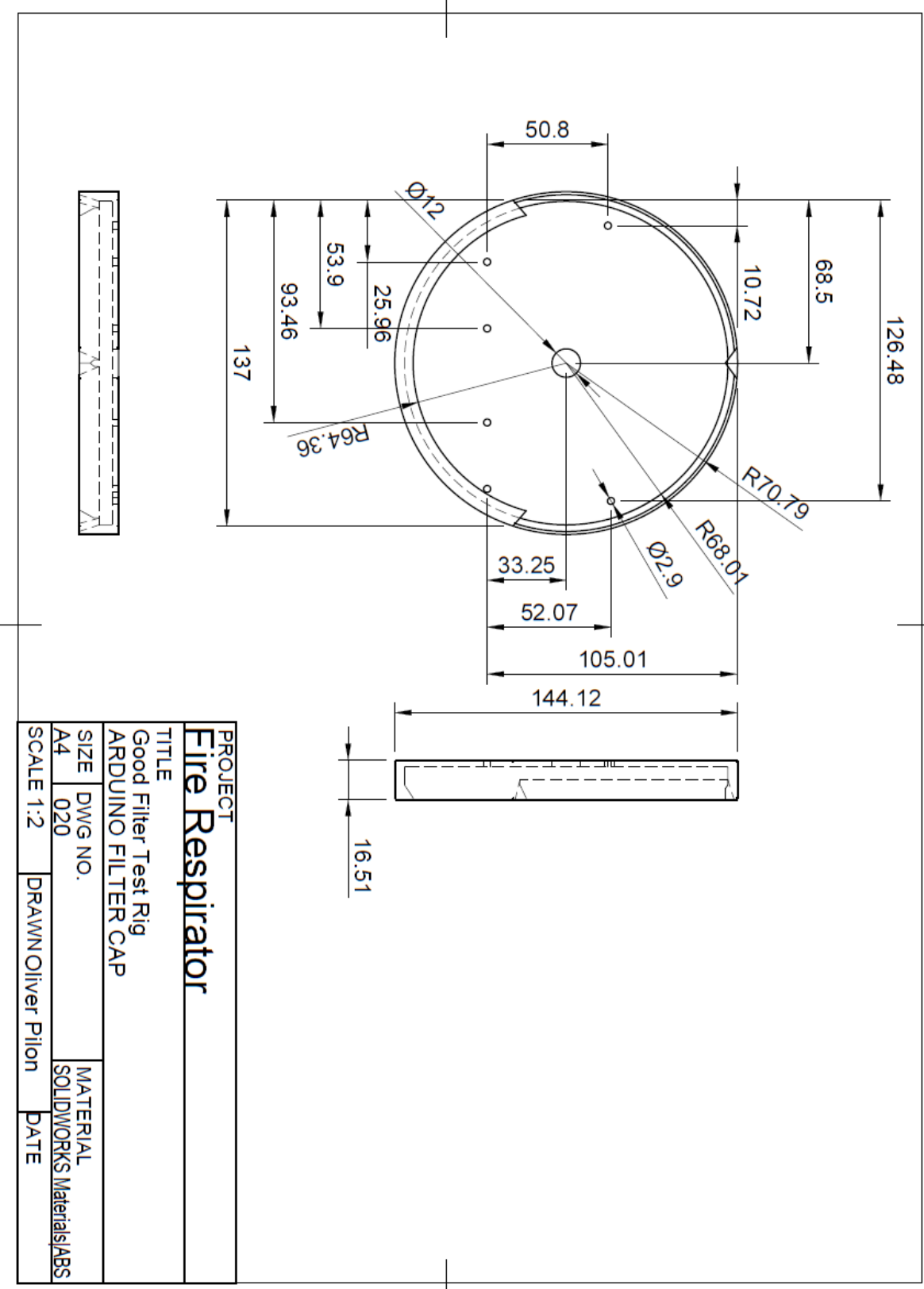


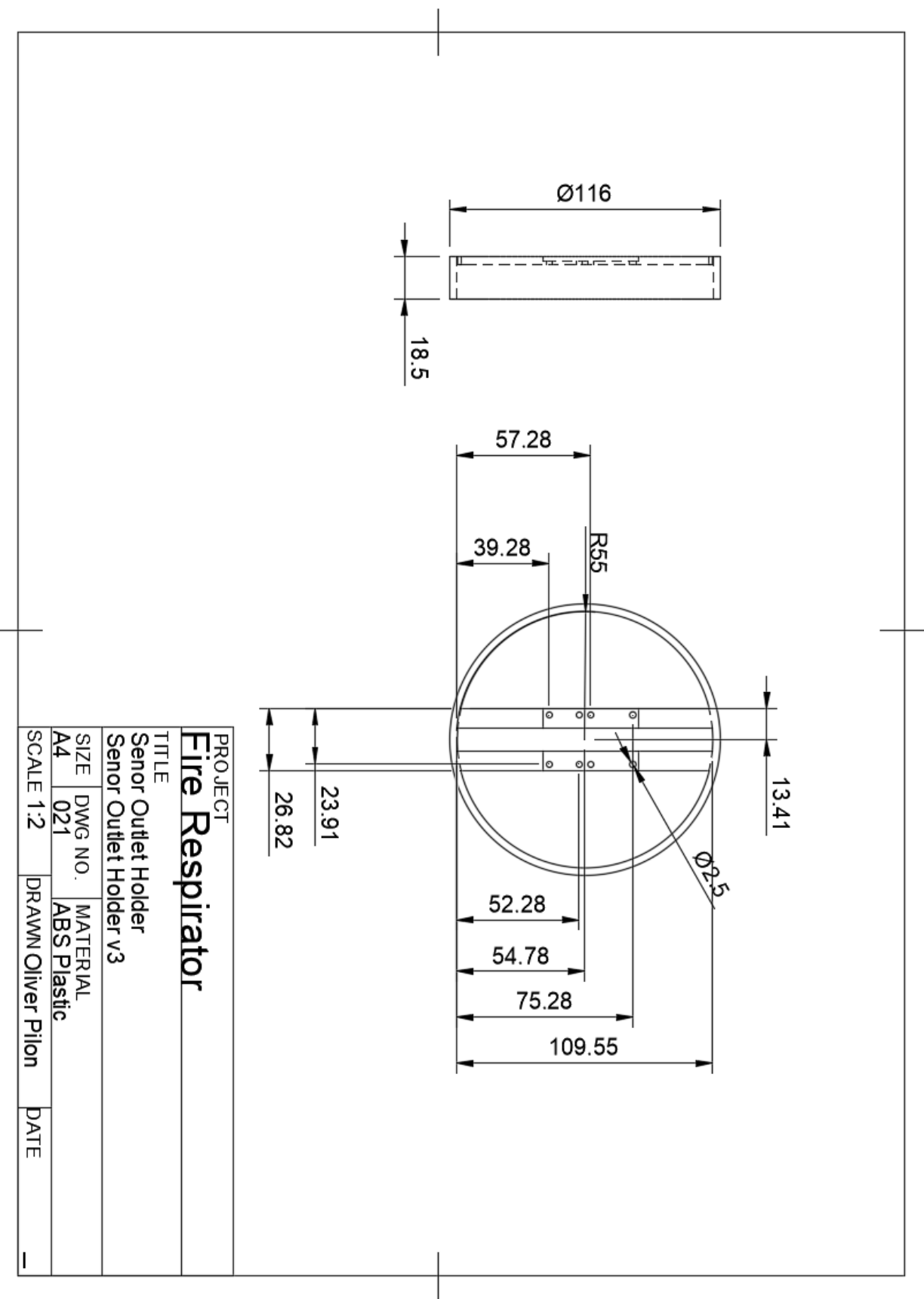
**PROJECT**  
**Fire Respirator**

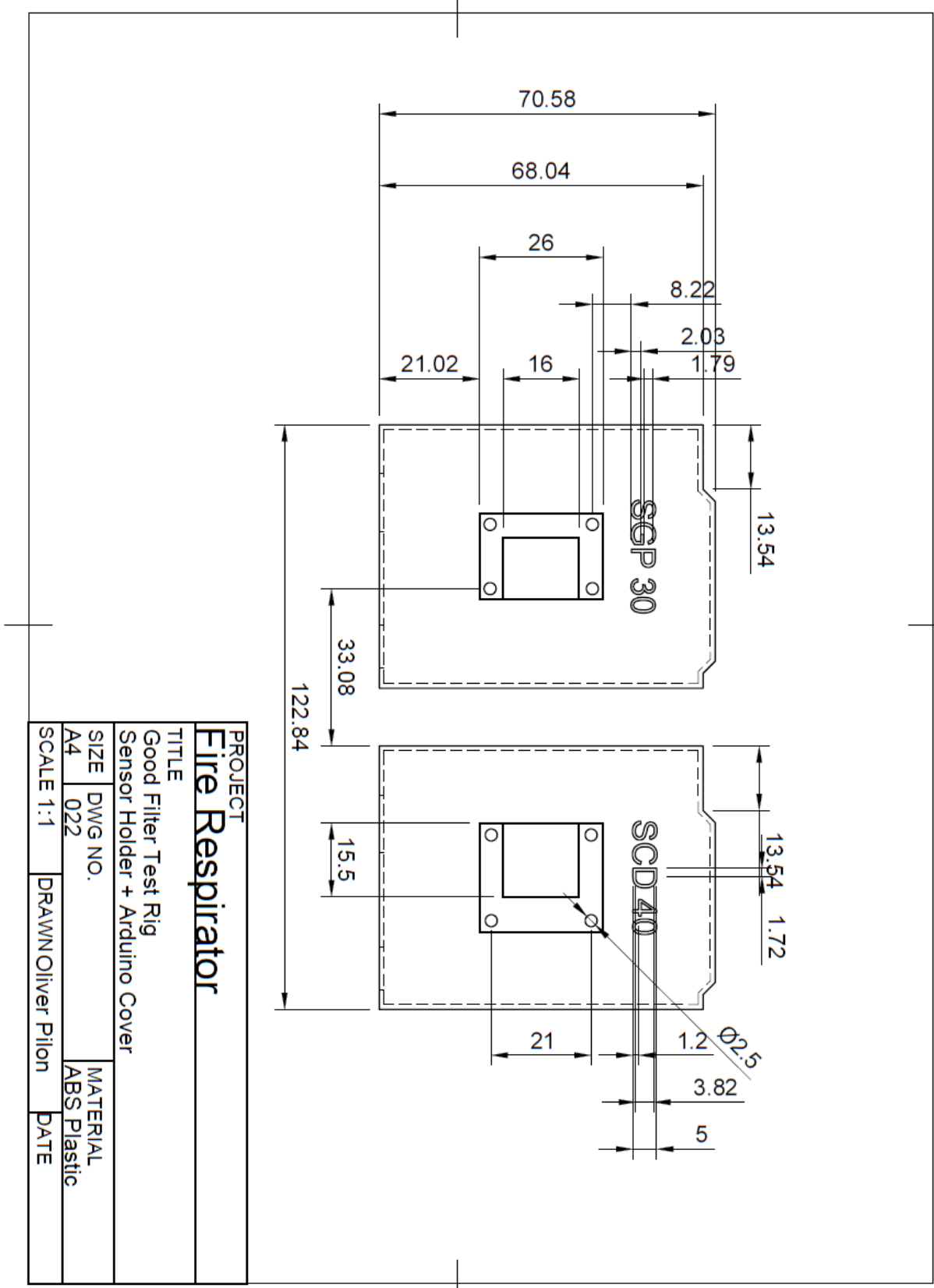
**TITLE**

Good Filter Test Rig  
Good Filter Test Rig v15

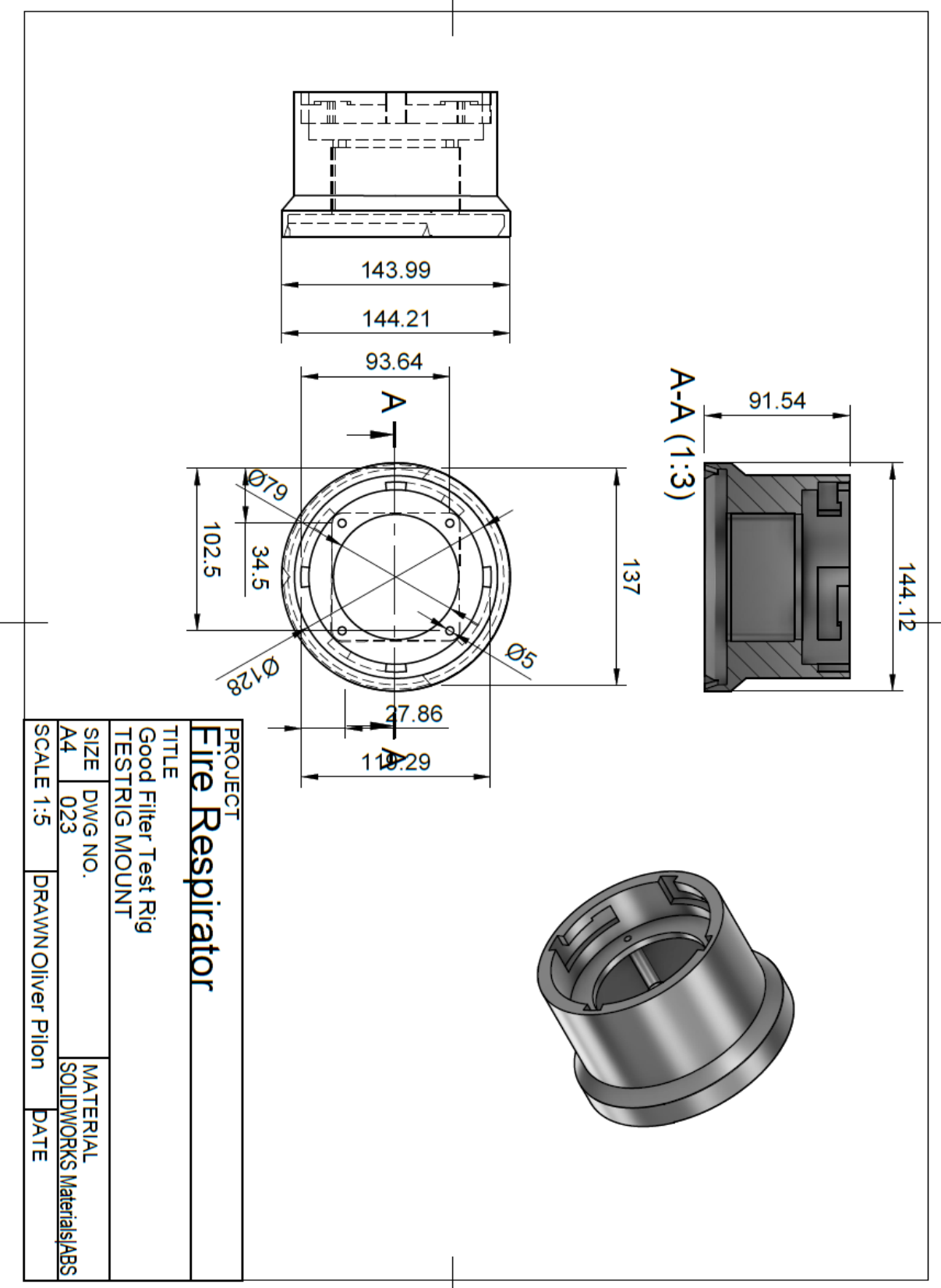
SIZE	DWG NO.	MATERIAL
A4	Good Filter Test Rig	----
SCALE 1:3	DRAWN Oliver Pilon	DATE

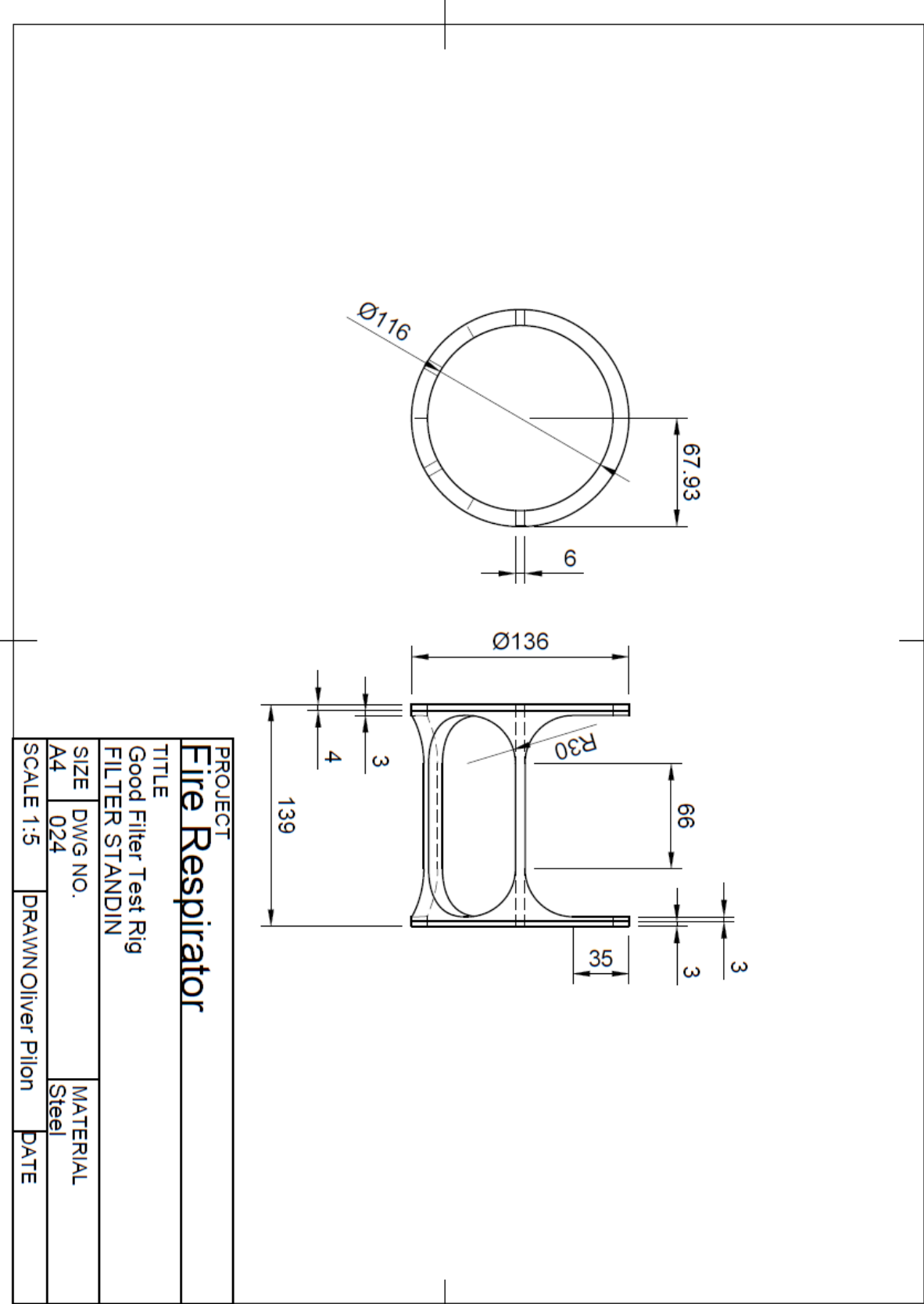


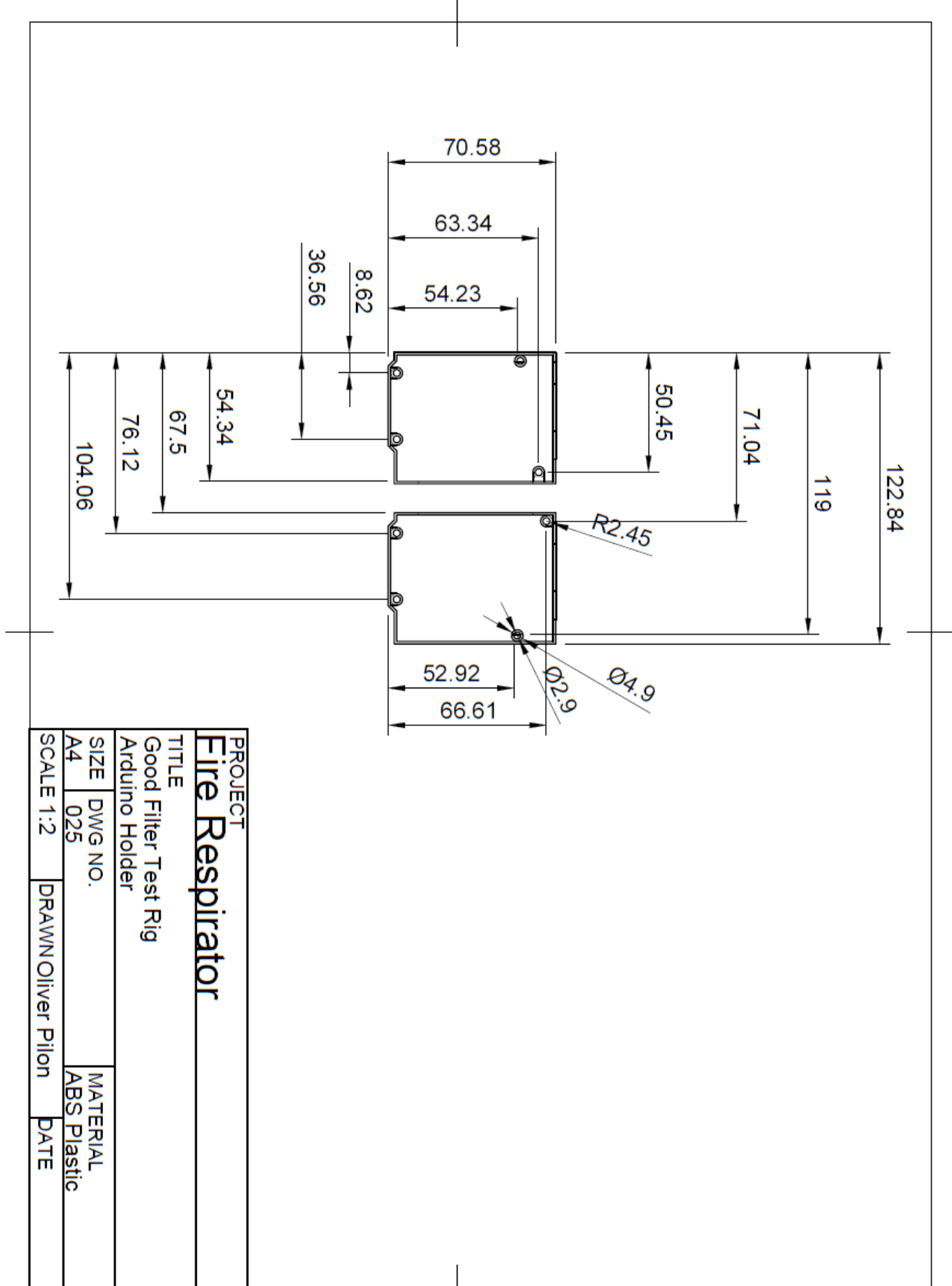




PROJECT	
TITLE	Fire Respirator
Sensor Holder + Arduino Cover	
SIZE	DWG NO.
A4	022
SCALE 1:1	DRAWN BY Oliver Pilon
	DATE









## Appendix H – Vendor Supplied Specifications and Datasheets

- MT3608 Boost Converter:

### ELECTRICAL CHARACTERISTICS

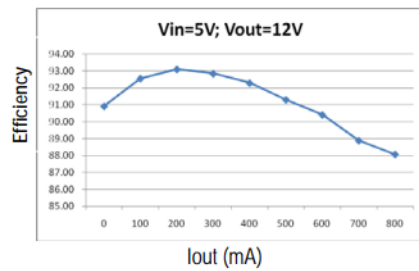
( $V_{IN}=V_{EN}=5V$ ,  $T_A = 25^\circ C$ , unless otherwise noted.)

Parameter	Conditions	MIN	TYP	MAX	unit
Operating Input Voltage		2		24	V
Under Voltage Lockout				1.98	V
Under Voltage Lockout Hysteresis			100		mV
Current (Shutdown)	$V_{EN}=0V$		0.1	1	$\mu A$
Quiescent Current (PFM)	$V_{FB}=0.7V$ , No switch		100	200	$\mu A$
Quiescent Current (PWM)	$V_{FB}=0.5V$ , switch		1.6	2.2	mA
Switching Frequency			1.2		MHz
Maximum Duty Cycle	$V_{FB} = 0V$	90			%
EN Input High Voltage		1.5			V
EN Input Low Voltage				0.4	V
FB Voltage		0.588	0.6	0.612	V
FB Input Bias Current	$V_{FB} = 0.6V$	-50	-10		nA
SW On Resistance (1)			80	150	$m\Omega$
SW Current Limit (1)	$V_{IN}= 5V$ , Duty cycle=50%		4		A
SW Leakage	$V_{SW} = 20V$			1	$\mu A$
Thermal Shutdown			155		$^\circ C$

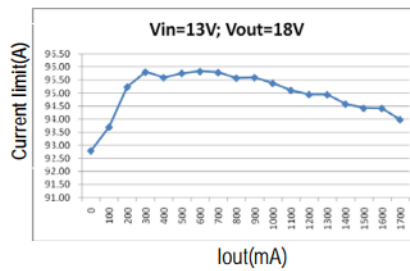


## TYPICAL OPERATING CHARACTERISTICS

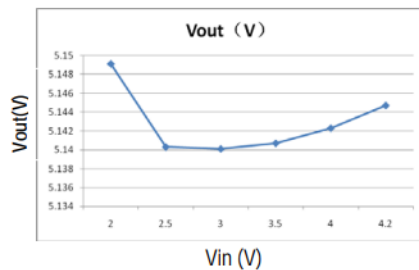
Efficiency Curve



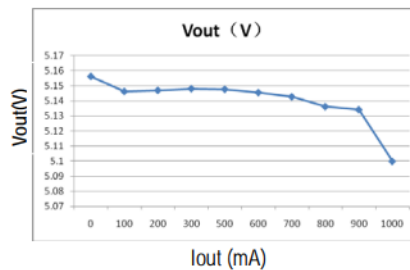
Efficiency Curve



line Regulation



Load regulation



- Neodymium N40SH Disc Magnets:

DESCRIPTION	REVIEW(0)
Neodymium Magnets High Temperature N40SH 0.375 inch x 0.25 inch Thick Neodymium Iron Boron NdFeB disc Magnet	
N40SH grade is for high temperature applications. Operating temperature: 300 degree F (150 degree C) Much stronger and cheaper than other types of high temp magnets such as SmCo, Alnico and ceramic magnets.	
Neodymium magnets are the world's strongest magnets. All magnets are not created equal! Applied Magnets offers the highest quality magnets with consistent performance at lowest price. Our strong magnets are designed & manufactured to meet stringent quality standards using the latest technology.	
Neodymium magnet (also known as Neo, NdFeB, NIB or super magnet), a type of rare earth magnet, is a permanent magnet made from neodymium, iron, boron and other minor elements.	
Nickel-Copper-Nickel 3 layer coated for maximum durability and protection against corrosion	
ISO Certified, top notch quality and superior performance guaranteed	
Super Powerful N40SH Neodymium Magnets, Stronger than N38, N38SH, N35SH and N35	
Approximate Pull Force: 8 lbs	
BrMax: 12900 gauss	
Magnetized through the Thickness, poles are on the long surfaces	
Contact us for high temp neodymium magnets wholesale discount	

## Appendix I – Air Curtain Calculations Excel

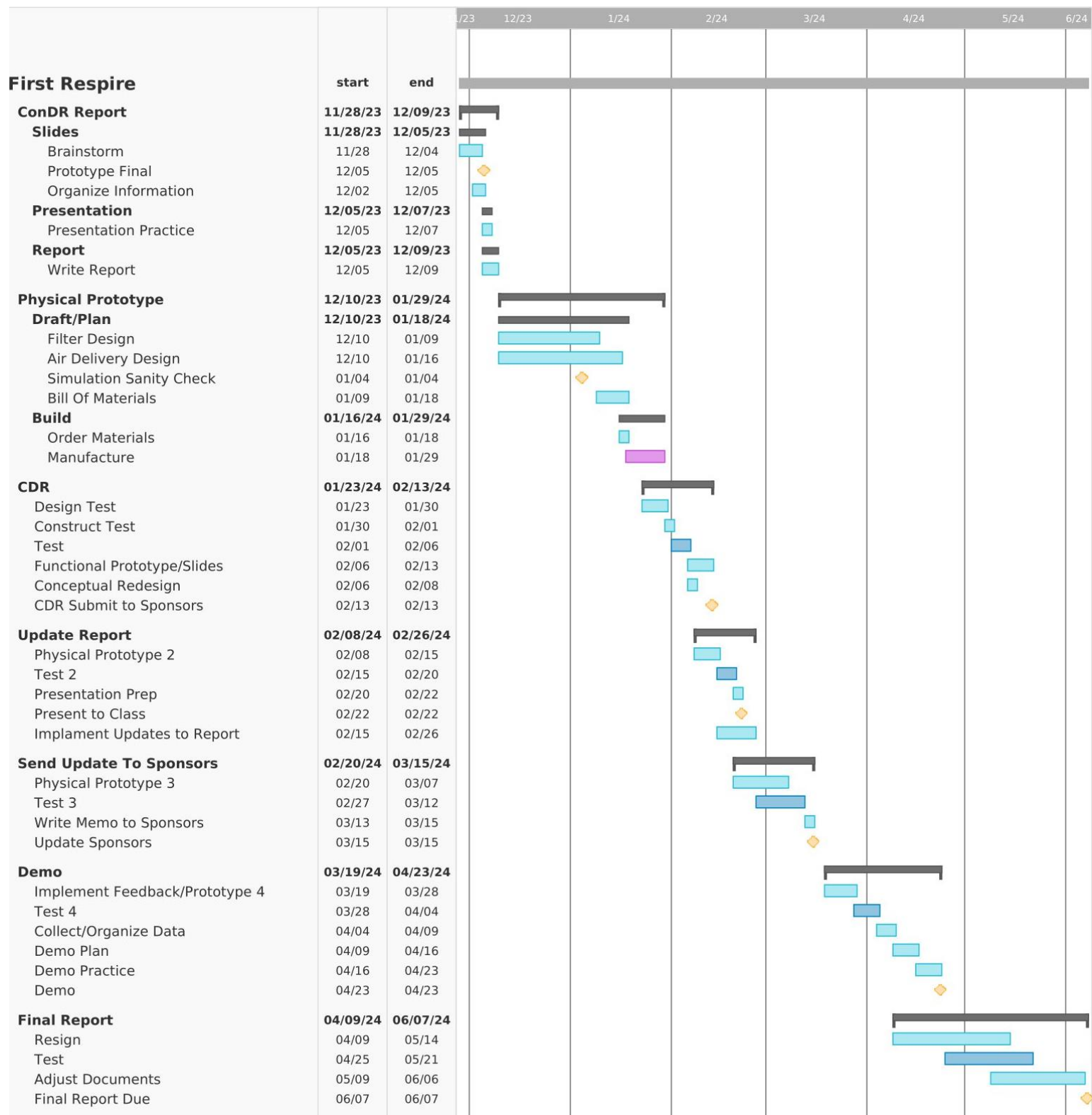
<b>Known/Assumed</b>			
Ambient air pressure, $P_a$ [kPa]	101.325	Atmospheric pressure	
Temperature of ambient air, $T_a$ [ $^{\circ}$ C]	32.600		
Density of ambient air, $\rho_a$ [kg/m <sup>3</sup> ]	1.155		
Air curtain air pressure, $P_c$ [kPa]	101.325	Atmospheric pressure	
Temperature of air curtain air, $T_c$ [ $^{\circ}$ C]	29.800	Corresponds to approx. 5°F of cooling	
Density of air curtain air, $\rho_c$ [kg/m <sup>3</sup> ]	1.165		
Windspeed, $V_a$ [km/h]	40.000		
Height of air curtain, $H$ [m]	0.300		
Width of air curtain, $W$ [m]	0.400		
$g$ [m <sup>2</sup> /s]	9.810	Typical range 0.6-0.9 w/ higher values for gases and vapors	
Discharge coefficient, $C_d$	0.750	Wind load perpendicular to the air curtain	
Wind direction coefficient, $C_v$	0.600		
$\Delta x$	2.032	cm	
$\Delta y$	8.700	cm	
<b>Calculations/Analysis</b>			
Airflow due to temperature differential, $Q_T$ [m <sup>3</sup> /s]	0.004778		
Airflow due to wind stress, $Q_v$ [m <sup>3</sup> /s]	0.8		
Total airflow, $Q_{Tot}$ [m <sup>3</sup> /s]	0.805	Measured value	
		Measured value	
Max. allowable horizontal air curtain deflection, $\Delta x$ [cm]	2.032	Measured from vertical	
Min. vertical distance covered for $\Delta x$ , $\Delta y$ [cm]	8.7		
Max. allowable air curtain angle, $\theta$	13.14651		
Number of outlet holes	20		
Diameter of outlet holes, $d$ [cm]	1		
Total area of outlets, $A$ [m <sup>2</sup> ]	0.001571		
Air curtain velocity, $V_c$ [m/s]	120.7679		
Air curtain flow rate, $Q_c$ [m <sup>3</sup> /min]	11.38211		
Air curtain flow rate, $Q_c$ [CFM]	401.9554		



		V <sub>a</sub> [mph]								
		0	5	10	15	20	25	30		
Total area of outlets, A [cm <sup>2</sup> ]		Q <sub>c</sub> [CFM]		Mac Air Max						
0.1		0.190427179	6.6038582	13.017289	19.43072	25.844151	32.257582	38.671013		139
0.2		0.2693047	9.3392658	18.409227	27.479188	36.549149	45.61911	54.689072		139
0.3		0.32982955	11.438218	22.546606	33.654995	44.763383	55.871772	66.98016		139
0.4		0.380854359	13.207716	26.034578	38.861441	51.688303	64.515165	77.342027		139
0.5		0.425808118	14.766676	29.107544	43.448411	57.789279	72.130147	86.471015		139
0.6		0.466449422	16.176083	31.885716	47.59535	63.304983	79.014617	94.724251		139
0.7		0.503822959	17.472167	34.44051	51.408854	68.377197	85.345541	102.31388		139
0.8		0.538609399	18.678532	36.818454	54.958376	73.098299	91.238221	109.37814		139
0.9		0.571281538	19.811575	39.051868	58.292161	77.532454	96.772747	116.01304		139
1		0.602183615	20.883233	41.164283	61.445333	81.726382	102.00743	122.28848		139
2		0.851616235	29.533352	58.215087	86.896823	115.57856	144.26029	172.94203		139
3		1.043012617	36.170821	71.29863	106.42644	141.55425	176.68205	211.80986		139
4		1.20436723	41.766467	82.328566	122.89067	163.45276	204.01486	244.57696		139
5		1.346523498	46.696329	92.046135	137.39594	182.74575	228.09555	273.44536		139
6		1.475042588	51.153266	100.83149	150.50971	200.18794	249.86616	299.54438		139
7		1.593228089	55.251842	108.91046	162.56907	216.22768	269.8863	323.54491		139
8		1.703232471	59.066703	116.43017	173.79365	231.15712	288.52059	345.88406		139
9		1.806550845	62.6497	123.49285	184.336	245.17915	306.0223	366.86544		139
10		1.904271793	66.038582	130.17289	194.3072	258.44151	322.57582	386.71013		139
11		1.997217106	69.261849	136.52648	203.79111	271.05575	338.32038	405.58501		139
12		2.086025233	72.341642	142.59726	212.85288	283.10849	353.36411	423.61973		139
13		2.171203901	75.295568	148.41993	221.5443	294.66866	367.79303	440.91739		139
14		2.253164771	78.137904	154.02264	229.90738	305.79212	381.67686	457.5616		139
15		2.332247112	80.880415	159.42858	237.97675	316.52492	395.07309	473.62125		139
16		2.40873446	83.532933	164.65713	245.78133	326.90553	408.02973	489.15393		139
17		2.48286665	86.103777	169.72469	253.3456	336.96651	420.58742	504.20833		139
18		2.554848706	88.600055	174.64526	260.69047	346.73567	432.78088	518.82609		139
19		2.624857523	91.027903	179.43095	267.834	356.23704	444.64009	533.04313		139
20		2.693046996	93.392658	184.09227	274.79188	365.49149	456.1911	546.89072		139
21		2.759551998	95.698997	188.63844	281.57789	374.51733	467.45678	560.39622		139
22		2.824491518	97.951046	193.0776	288.20416	383.33071	478.45727	573.58382		139
23		2.887971163	100.15247	197.41697	294.68146	391.94596	489.21046	586.47495		139
24		2.950085176	102.30653	201.66298	301.01942	400.37587	499.73232	599.08876		139
25		3.010918075	104.41617	205.82141	307.22666	408.63191	510.03716	611.44241		139
26		3.070546003	106.48401	209.89748	313.31095	416.72442	520.13789	623.55135		139
27		3.12903785	108.51246	213.89589	319.27931	424.66274	530.04616	635.42959		139
28		3.186456178	110.50368	217.82091	325.13814	432.45537	539.77259	647.08982		139
29		3.242858011	112.45965	221.67645	330.89324	440.11004	549.32683	658.54363		139
30		3.298295497	114.38218	225.46606	336.54995	447.63383	558.71772	669.8016		139
31		3.352816471	116.27292	229.19303	342.11313	455.03324	567.95334	680.87345		139
32		3.406464941	118.13341	232.86035	347.58729	462.31423	577.04117	691.76812		139
33		3.459281501	119.96504	236.4708	352.97656	469.48232	585.98808	702.49384		139
34		3.511303691	121.76913	240.02695	358.28478	476.5426	594.80043	713.05825		139
35		3.56256631	123.54687	243.53118	363.51549	483.4998	603.48411	723.46841		139
36		3.61310169	125.2994	246.9857	368.672	490.35829	612.04459	733.73089		139
37		3.662939929	127.02775	250.39256	373.75737	497.12218	620.48698	743.85179		139
38		3.712109108	128.7329	253.75368	378.77447	503.79526	628.81604	753.83683		139
39		3.76063547	130.41575	257.07086	383.72598	510.38109	637.03621	763.69132		139
40		3.808543586	132.07716	260.34578	388.61441	516.88303	645.15165	773.42027		139



## Appendix J – Gantt Chart



## Appendix K – Safety Checklist

ENGR 460 Interdisciplinary Senior Design Project II

### SENIOR PROJECT CRITICAL DESIGN REVIEW HAZARD IDENTIFICATION CHECKLIST

Y    N

- Do all hazardous actions in the design have adequate guarding to prevent exposure?
- Are accelerations and decelerations in the design adequately mitigated or protected from user exposure?
- Are all electrical systems in the design properly grounded?
- Are there any large capacity batteries or electrical voltages above 40 V (AC or DC) in the system?
- Is there any stored energy in the system (e.g., batteries, flywheels, hanging weights, pressurized fluids) when the system is either on or off?
- Are there any explosive or flammable liquids, gases, dust, or fuel integrated into the system?
- Are materials known to be hazardous to humans involved in either the design or manufacturing of the design?
- Have all rotating components, including pinch points and shear points, been adequately guarded to prevent accidents?
- Are there any exposed hot surfaces or components that could pose a burn risk to users?
- Is there proper ventilation or control measures in place for potential exposure to harmful fumes or gases?
- Have all potential sources of noise in the design been assessed, and measures implemented to mitigate excessive noise levels?
- Are there any sharp edges, protruding objects, or potential cutting hazards in the design that need to be addressed?
- Is the design free from any tripping hazards or obstacles that could pose a risk to users?
- Are all lifting and carrying tasks within the design evaluated for ergonomic safety and compliance?
- Have potential ergonomic issues, such as awkward postures or repetitive motions, been considered and addressed in the design?
- Are there any confined spaces within the system, and if so, are proper safety measures in place?
- Have all potential chemical exposures, including cleaning agents or process chemicals, been identified, and controlled?
- Is the design in compliance with all relevant safety standards and regulations?
- Have emergency shutdown procedures and safety protocols been established and communicated for the system?
- Is there a comprehensive safety training program in place for users and maintenance personnel involved with the design?

### Appendix K – SGP30 Sensor Code for Fire Simulation Test



```
#include <Wire.h>
#include "Adafruit_SGP30.h"
#include <EEPROM.h>

Adafruit_SGP30 sgp;

/* return absolute humidity [mg/m^3] with approximation formula
 * @param temperature [°C]
 * @param humidity [%RH]
 */
uint32_t getAbsoluteHumidity(float temperature, float humidity) {
    const float absoluteHumidity = 216.7f * ((humidity / 100.0f) * 6.112f *
exp((17.62f * temperature) / (243.12f + temperature)) / (273.15f +
temperature)); // [g/m^3]
    const uint32_t absoluteHumidityScaled = static_cast<uint32_t>(1000.0f *
absoluteHumidity); // [mg/m^3]
    return absoluteHumidityScaled;
}

// Variables to store the baseline values
uint16_t eCO2_base, TVOC_base;

// Variables to keep track of time
unsigned long previousMillis = 0;
const unsigned long interval = 90 * 60 * 1000; // 90 minutes in milliseconds

void setup() {
    Serial.begin(115200);
    while (!Serial) { delay(10); } // Wait for serial console to open!

    Serial.println("SGP30 test");

    if (!sgp.begin()){
        Serial.println("Sensor not found :(");
        while (1);
    }
    Serial.print("Found SGP30 serial #");
    Serial.print(sgp.serialnumber[0], HEX);
    Serial.print(sgp.serialnumber[1], HEX);
    Serial.println(sgp.serialnumber[2], HEX);

    // Check if we have saved baseline values and set them
    if (loadBaselineFromEEPROM()) {
        sgp.setIAQBaseline(eCO2_base, TVOC_base);
        Serial.println("Loaded baseline from EEPROM");
    } else {
        Serial.println("No baseline found, using default initialization");
    }
}
```



```
// PLX-DAQ specific initialization message
Serial.println("CLEARDATA"); // Clear any existing data
Serial.println("LABEL,TVOC,eCO2,Raw H2,Raw Ethanol"); // Define column
headers
}

void loop() {
    unsigned long currentMillis = millis();

    if (!sgp.IAQmeasure()) {
        Serial.println("Measurement failed");
        return;
    }

    if (!sgp.IAQmeasureRaw()) {
        Serial.println("Raw Measurement failed");
        return;
    }

    // Send data in a format compatible with PLX-DAQ
    Serial.print(sgp.TVOC); Serial.print(",");
    Serial.print(sgp.eCO2); Serial.print(",");
    Serial.print(sgp.rawH2); Serial.print(",");
    Serial.println(sgp.rawEthanol);

    delay(1000);

    // Check if 90 minutes have passed
    if (currentMillis - previousMillis >= interval) {
        previousMillis = currentMillis;
        if (sgp.getIAQBaseline(&eCO2_base, &TVOC_base)) {
            saveBaselineToEEPROM(eCO2_base, TVOC_base);
            Serial.print("Saved baseline: eCO2: 0x"); Serial.print(eCO2_base, HEX);
            Serial.print(" & TVOC: 0x"); Serial.println(TVOC_base, HEX);
        } else {
            Serial.println("Failed to get baseline readings");
        }
    }
}

// Function to save baseline values to EEPROM
void saveBaselineToEEPROM(uint16_t eCO2_base, uint16_t TVOC_base) {
    EEPROM.put(0, eCO2_base);
    EEPROM.put(2, TVOC_base);
}

// Function to load baseline values from EEPROM
```



```
bool loadBaselineFromEEPROM() {
    EEPROM.get(0, eCO2_base);
    EEPROM.get(2, TVOC_base);
    if (eCO2_base != 0xFFFF && TVOC_base != 0xFFFF) {
        return true;
    }
    return false;
}
```

## Appendix L – SCD-40 Sensor Code for Fire Simulation Test

```
/*
 * Copyright (c) 2021, Sensirion AG
 * All rights reserved.
 *
 * Redistribution and use in source and binary forms, with or without
 * modification, are permitted provided that the following conditions are
 * met:
 *
 * * Redistributions of source code must retain the above copyright notice,
 * this
 *   * list of conditions and the following disclaimer.
 *
 * * Redistributions in binary form must reproduce the above copyright
 * notice,
 *   * this list of conditions and the following disclaimer in the
 * documentation
 *   * and/or other materials provided with the distribution.
 *
 * * Neither the name of Sensirion AG nor the names of its
 * contributors may be used to endorse or promote products derived from
 * this software without specific prior written permission.
 *
 * THIS SOFTWARE IS PROVIDED BY THE COPYRIGHT HOLDERS AND CONTRIBUTORS "AS
 * IS"
 *   * AND ANY EXPRESS OR IMPLIED WARRANTIES, INCLUDING, BUT NOT LIMITED TO,
```

THE

\* IMPLIED WARRANTIES OF MERCHANTABILITY AND FITNESS FOR A PARTICULAR  
PURPOSE  
  
\* ARE DISCLAIMED. IN NO EVENT SHALL THE COPYRIGHT HOLDER OR CONTRIBUTORS  
BE  
  
\* LIABLE FOR ANY DIRECT, INDIRECT, INCIDENTAL, SPECIAL, EXEMPLARY, OR  
\* CONSEQUENTIAL DAMAGES (INCLUDING, BUT NOT LIMITED TO, PROCUREMENT OF  
\* SUBSTITUTE GOODS OR SERVICES; LOSS OF USE, DATA, OR PROFITS; OR BUSINESS  
\* INTERRUPTION) HOWEVER CAUSED AND ON ANY THEORY OF LIABILITY, WHETHER IN  
\* CONTRACT, STRICT LIABILITY, OR TORT (INCLUDING NEGLIGENCE OR OTHERWISE)  
\* ARISING IN ANY WAY OUT OF THE USE OF THIS SOFTWARE, EVEN IF ADVISED OF  
THE  
  
\* POSSIBILITY OF SUCH DAMAGE.  
\*/

```
#include <Arduino.h>
#include <SensirionI2CScd4x.h>
#include <Wire.h>

SensirionI2CScd4x scd4x;

void printUInt16Hex(uint16_t value) {
    Serial.print(value < 4096 ? "0" : "");
    Serial.print(value < 256 ? "0" : "");
    Serial.print(value < 16 ? "0" : "");
    Serial.print(value, HEX);
}

void printSerialNumber(uint16_t serial0, uint16_t serial1, uint16_t
serial2) {
    Serial.print("Serial: 0x");
    printUInt16Hex(serial0);
    printUInt16Hex(serial1);
```

```
    printUInt16Hex(serial2);
    Serial.println();
}

void setup() {

    Serial.begin(9600);
    while (!Serial) {
        delay(100);
    }

    Wire.begin();

    uint16_t error;
    char errorMessage[256];

    scd4x.begin(Wire);

    // stop potentially previously started measurement
    error = scd4x.stopPeriodicMeasurement();
    if (error) {
        Serial.print("Error trying to execute stopPeriodicMeasurement():
");
        errorToString(error, errorMessage, 256);
        Serial.println(errorMessage);
    }

    uint16_t serial0;
    uint16_t serial1;
    uint16_t serial2;
    error = scd4x.getSerialNumber(serial0, serial1, serial2);
    if (error) {
        Serial.print("Error trying to execute getSerialNumber(): ");
    }
}
```

```
        errorToString(error, errorMessage, 256);
        Serial.println(errorMessage);
    } else {
        printSerialNumber(serial0, serial1, serial2);
    }

    // Start Measurement
    error = scd4x.startPeriodicMeasurement();
    if (error) {
        Serial.print("Error trying to execute startPeriodicMeasurement():
");
        errorToString(error, errorMessage, 256);
        Serial.println(errorMessage);
    }

    Serial.println("Waiting for first measurement... (5 sec)");
    Serial.print("CO2");
    Serial.print("\t");
    Serial.print("Temperature");
    Serial.print("\t");
    Serial.print("Humidity");
    Serial.print("\n");
}

void loop() {
    uint16_t error;
    char errorMessage[256];

    delay(5000);

    // Read Measurement
    uint16_t co2;
    float temperature;
```



```
float humidity;

error = scd4x.readMeasurement(co2, temperature, humidity);
if (error) {
    Serial.print("Error trying to execute readMeasurement(): ");
    errorToString(error, errorMessage, 256);
    Serial.println(errorMessage);
} else if (co2 == 0) {
    Serial.println("Invalid sample detected, skipping.");
} else {
    //Serial.print("Co2:");
    Serial.print(co2);
    Serial.print("\t");
    //Serial.print("Temperature:");
    Serial.print(temperature);
    Serial.print("\t");
    //Serial.print("Humidity:");
    Serial.println(humidity);
}
}
```



Python Data Processing Code 2:

```
import pandas as pd
import numpy as np
import matplotlib.pyplot as plt

def import_data(file_path):
    sgp30 = pd.read_excel(file_path, sheet_name='SGP30_Outlet')
    scd40 = pd.read_excel(file_path, sheet_name='SCD40_Outlet')
    isgp30 = pd.read_excel(file_path, sheet_name='SGP30_Inlet')
    iscd40 = pd.read_excel(file_path, sheet_name='SCD40_Inlet')
    return sgp30, scd40, isgp30, iscd40

def process_time_data(sgp30, scd40, isgp30, iscd40):
    t_start = max(sgp30.iloc[0, 0], scd40.iloc[0, 0], isgp30.iloc[0, 0], iscd40.iloc[0, 0])
    sgp30['Difference'] = (sgp30.iloc[:, 0] - t_start) * 86400
    scd40['Difference'] = (scd40.iloc[:, 0] - t_start) * 86400
    isgp30['Difference'] = (isgp30.iloc[:, 0] - t_start) * 86400
    iscd40['Difference'] = (iscd40.iloc[:, 0] - t_start) * 86400

    sgp30 = sgp30[sgp30['Difference'] >= 0]
    scd40 = scd40[scd40['Difference'] >= 0]
    isgp30 = isgp30[isgp30['Difference'] >= 0]
    iscd40 = iscd40[iscd40['Difference'] >= 0]

    return sgp30, scd40, isgp30, iscd40

def calculate_concentrations(data, value_col, time_col):
    min_conc = np.min(data.iloc[:, value_col])
    max_conc = np.max(data.iloc[:, value_col])
    avg_conc = np.mean(data.iloc[:, value_col])
    trend = np.poly1d(np.polyfit(data.iloc[:, time_col], data.iloc[:, value_col], 1))

    if value_col in [3, 4]:
        data.iloc[:, value_col] = max_conc - data.iloc[:, value_col]
        min_conc, max_conc = max_conc - min_conc, max_conc - max_conc
    return min_conc, max_conc, avg_conc, trend

def process_inlet_data(isgp30, iscd40):
    inconcin, finconcin, aveconcin, trendsin = [], [], [], []

    for i in range(1, 5):
        min_conc, max_conc, avg, trend = calculate_concentrations(isgp30, i, 5)
        inconcin.append(min_conc)
        finconcin.append(max_conc)
        aveconcin.append(avg)
        trendsin.append(trend)

    min_conc, max_conc, avg, trend = calculate_concentrations(iscd40, 1, 4)
    inconcin.append(min_conc)
    finconcin.append(max_conc)
    aveconcin.append(avg)
    trendsin.append(trend)
```



```
    return inconcin, finconcin, aveconcin, trendsin

def process_outlet_data(sgp30, scd40):
    inconc, finconc, aveconc, trends = [], [], [], []

    for i in range(1, 5):
        min_conc, max_conc, avg, trend = calculate_concentrations(sgp30, i, 5)
        inconc.append(min_conc)
        finconc.append(max_conc)
        aveconc.append(avg)
        trends.append(trend)

    min_conc, max_conc, avg, trend = calculate_concentrations(scd40, 1, 4)
    inconc.append(min_conc)
    finconc.append(max_conc)
    aveconc.append(avg)
    trends.append(trend)

    return inconc, finconc, aveconc, trends

def create_data_tables(inconcin, finconcin, aveconcin, inconc, finconc, aveconc):
    chem_list = ['TVOC', 'eCO2', 'CO2', 'H2', 'Ethonal']
    dict_inlet = {'Min Concentration': inconcin, 'Max Concentration': finconcin, 'Average Concentration': aveconcin}
    dict_outlet = {'Min Concentration': inconc, 'Max Concentration': finconc, 'Average Concentration': aveconc}

    inlet = pd.DataFrame(dict_inlet)
    inlet.index = chem_list
    inlet = inlet.round(2)

    outlet = pd.DataFrame(dict_outlet)
    outlet.index = chem_list
    outlet = outlet.round(2)

    return inlet, outlet

def synchronize_data(isgp30, sgp30, value_col, offset=10):
    iN = isgp30.iloc[:, value_col]
    first_output_value_inlet = iN[iN >= 0.9 * iN.mean()].iloc[0]
    iN = iN[iN >= 0.9 * first_output_value_inlet]
    inlet_min_index = iN.index[0]
    inlet_max_index = iN.index[-1]

    outlet_start_index = sgp30.index[sgp30.index >= inlet_min_index][0]
    outlet_end_index = sgp30.index[sgp30.index >= inlet_max_index][offset]

    oN = sgp30.iloc[:, value_col]
    oN = oN.loc[outlet_start_index:outlet_end_index]

    if len(oN) > len(iN) + offset:
        oN = oN.iloc[:len(iN) + offset]

    return iN, oN
```



```
def calculate_avg_percent_diff(iN, oN):
    min_length = min(len(oN), len(iN))
    return np.mean(np.abs((oN[:min_length].values - iN[:min_length].values) / iN[:min_length].values)) * 100

def plot_subplots(axes, iN, oN, inlet_data, outlet_data, xlabel, ylabel, title, labels):
    axes[0].plot(oN.reset_index(drop=True), label=f'Outlet {labels[0]}', linewidth=2)
    axes[0].plot(iN.reset_index(drop=True), label=f'Inlet {labels[0]}', linewidth=2)
    axes[0].set_xlabel(xlabel)
    axes[0].set_ylabel(ylabel)
    axes[0].set_title(title)
    axes[0].legend()

    axes[1].plot(outlet_data['Difference'], outlet_data.iloc[:, 1], linewidth=2, label=f'Outlet {labels[1]}')
    axes[1].plot(inlet_data['Difference'], inlet_data.iloc[:, 1], linewidth=2, label=f'Inlet {labels[1]}')
    axes[1].set_xlabel(xlabel)
    axes[1].set_ylabel(ylabel)
    axes[1].set_title(f'{labels[1]} Concentration vs Time')
    axes[1].legend()

def plot_data(sgp30, isgp30, scd40, iscd40, iNtvoc, oNtvoc, iNeco2, oNeco2, iNco2, oNco2, iNh2, oNh2, iNeth, oNeth):
    fig, axes = plt.subplots(1, 2, figsize=(25, 10))
    plot_subplots(axes, iNtvoc, oNtvoc, isgp30, sgp30, 'Time (s)', 'TVOC', 'Normalized TVOC over Time', ['TVOC', 'TVOC'])
    plt.tight_layout()
    plt.show()

    fig, axes = plt.subplots(3, 1, figsize=(25, 10))
    axes[0].plot(sgp30['Difference'], sgp30.iloc[:, 2], linewidth=2, label='Outlet eCO2 (sgp30)')
    axes[0].plot(scd40['Difference'], scd40.iloc[:, 1], linewidth=2, label='Outlet CO2 (scd40)')
    axes[0].plot(isgp30['Difference'], isgp30.iloc[:, 2], linestyle='--', linewidth=2, label='Inlet eCO2 (sgp30)')
    axes[0].plot(iscd40['Difference'], iscd40.iloc[:, 1], linestyle='--', linewidth=2, label='Inlet CO2 (scd40)')
    axes[0].set_xlabel('Time (s)')
    axes[0].set_ylabel('Concentration')
    axes[0].set_title('eCO2 and CO2 Concentration vs Time')
    axes[0].legend()

    axes[1].plot(oNeco2.reset_index(drop=True), label='Outlet eCO2', linewidth=2)
    axes[1].plot(iNeco2.reset_index(drop=True), label='Inlet eCO2', linewidth=2)
    axes[1].set_xlabel('Time (s)')
    axes[1].set_ylabel('Concentration')
    axes[1].set_title('Normalized eCO2 Concentration vs Time')
    axes[1].legend()

    axes[2].plot(oNco2.reset_index(drop=True), label='Outlet CO2', linewidth=2)
    axes[2].plot(iNco2.reset_index(drop=True), label='Inlet CO2', linewidth=2)
    axes[2].set_xlabel('Time (s)')
    axes[2].set_ylabel('Concentration')
    axes[2].set_title('Normalized CO2 Concentration vs Time')
```



```
axs[2].legend()
plt.tight_layout()
plt.show()

fig, axs = plt.subplots(1, 2, figsize=(25, 10))
plot_subplots(axs, iNh2, oNh2, isgp30, sgp30, 'Time (s)', 'H2', 'Normalized H2 over Time', ['H2', 'H2'])
plt.tight_layout()
plt.show()

fig, axs = plt.subplots(1, 2, figsize=(25, 10))
plot_subplots(axs, iNeth, oNeth, isgp30, sgp30, 'Time (s)', 'Ethanol', 'Normalized Ethanol over Time', ['Ethanol', 'Ethanol'])
plt.tight_layout()
plt.show()

def main(file_path):
    sgp30, scd40, isgp30, iscd40 = import_data(file_path)
    sgp30, scd40, isgp30, iscd40 = process_time_data(sgp30, scd40, isgp30, iscd40)

    inconcin, finconcin, aveconcin, trendsin = process_inlet_data(isgp30, iscd40)
    inconc, finconc, aveconc, trends = process_outlet_data(sgp30, scd40)

    inlet, outlet = create_data_tables(inconcin, finconcin, aveconcin, inconc, finconc, aveconc)
    print("Inlet Data:")
    print(inlet)
    print("\nOutlet Data:")
    print(outlet)

    iNtvoc, oNtvoc = synchronize_data(isgp30, sgp30, 1, offset=10)
    iNeco2, oNeco2 = synchronize_data(isgp30, sgp30, 2, offset=10)
    iNco2, oNco2 = synchronize_data(iscd40, scd40, 1, offset=10)
    iNh2, oNh2 = synchronize_data(isgp30, sgp30, 3, offset=10)
    iNeth, oNeth = synchronize_data(isgp30, sgp30, 4, offset=10)

    avg_percent_diff_tvoc = calculate_avg_percent_diff(iNtvoc, oNtvoc)
    avg_percent_diff_eco2 = calculate_avg_percent_diff(iNeco2, oNeco2)
    avg_percent_diff_co2 = calculate_avg_percent_diff(iNco2, oNco2)
    avg_percent_diff_h2 = calculate_avg_percent_diff(iNh2, oNh2)
    avg_percent_diff_eth = calculate_avg_percent_diff(iNeth, oNeth)

    plot_data(sgp30, isgp30, scd40, iscd40, iNtvoc, oNtvoc, iNeco2, oNeco2, iNco2, oNco2, iNh2, oNh2, iNeth, oNeth)
    print(f"Average percent difference between outlet and inlet TVOC: {avg_percent_diff_tvoc:.2f}%")
    print(f"Average percent difference between outlet and inlet eCO2: {avg_percent_diff_eco2:.2f}%")
    print(f"Average percent difference between outlet and inlet CO2: {avg_percent_diff_co2:.2f}%")
    print(f"Average percent difference between outlet and inlet H2: {avg_percent_diff_h2:.2f}%")
    print(f"Average percent difference between outlet and inlet Ethanol: {avg_percent_diff_eth:.2f}%")
```



CAL POLY

```
file_path = 'Data\FilterTest_5_26_2024.xlsx'  
main(file_path)
```



Python Data Processing Code 2:

```
import pandas as pd
import numpy as np
import matplotlib.pyplot as plt

# Import Data
def import_data(file_path):
    sgp30 = pd.read_excel(file_path, sheet_name='SGP30_Outlet')
    scd40 = pd.read_excel(file_path, sheet_name='SCD40_Outlet')
    isgp30 = pd.read_excel(file_path, sheet_name='SGP30_Inlet')
    iscd40 = pd.read_excel(file_path, sheet_name='SCD40_Inlet')
    return sgp30, scd40, isgp30, iscd40

# Time Processing with Rolling Average
def process_time_data(sgp30, scd40, isgp30, iscd40, window_size=5):
    t_start = max(sgp30.iloc[0, 0], scd40.iloc[0, 0], isgp30.iloc[0, 0], iscd40.iloc[0, 0])
    sgp30['Difference'] = (sgp30.iloc[:, 0] - t_start) * 86400
    scd40['Difference'] = (scd40.iloc[:, 0] - t_start) * 86400
    isgp30['Difference'] = (isgp30.iloc[:, 0] - t_start) * 86400
    iscd40['Difference'] = (iscd40.iloc[:, 0] - t_start) * 86400

    sgp30 = sgp30[sgp30['Difference'] >= 0].copy()
    scd40 = scd40[scd40['Difference'] >= 0].copy()
    isgp30 = isgp30[isgp30['Difference'] >= 0].copy()
    iscd40 = iscd40[iscd40['Difference'] >= 0].copy()

    # Calculate rolling averages
    sgp30['TVOC_Rolling'] = sgp30.iloc[:, 1].rolling(window=window_size).mean()
    sgp30['eCO2_Rolling'] = sgp30.iloc[:, 2].rolling(window=window_size).mean()
    sgp30['H2_Rolling'] = sgp30.iloc[:, 3].rolling(window=window_size).mean() if 'H2' in sgp30.columns else None
    sgp30['Ethanol_Rolling'] = sgp30.iloc[:, 4].rolling(window=window_size).mean() if 'Ethanol' in sgp30.columns else None

    scd40['CO2_Rolling'] = scd40.iloc[:, 1].rolling(window=window_size).mean()

    isgp30['TVOC_Rolling'] = isgp30.iloc[:, 1].rolling(window=window_size).mean()
    isgp30['eCO2_Rolling'] = isgp30.iloc[:, 2].rolling(window=window_size).mean()
    isgp30['H2_Rolling'] = isgp30.iloc[:, 3].rolling(window=window_size).mean() if 'H2' in isgp30.columns else None
    isgp30['Ethanol_Rolling'] = isgp30.iloc[:, 4].rolling(window=window_size).mean() if 'Ethanol' in isgp30.columns else None

    iscd40['CO2_Rolling'] = iscd40.iloc[:, 1].rolling(window=window_size).mean()

    return sgp30, scd40, isgp30, iscd40

# Calculate Concentrations and Trends
def calculate_concentrations(data, value_col, time_col):
    min_conc = np.min(data.iloc[:, value_col])
    max_conc = np.max(data.iloc[:, value_col])
    avg_conc = np.mean(data.iloc[:, value_col])
    trend = np.poly1d(np.polyfit(data.iloc[:, time_col], data.iloc[:, value_col], 1))
```



```
return min_conc, max_conc, avg_conc, trend

# Process Inlet Data
def process_inlet_data(isgp30, iscd40):
    inconcin, finconcin, aveconcin, trendsin = [], [], [], []

    for i in range(1, 5):
        min_conc, max_conc, avg, trend = calculate_concentrations(isgp30, i, 5)
        inconcin.append(min_conc)
        finconcin.append(max_conc)
        aveconcin.append(avg)
        trendsin.append(trend)

    min_conc, max_conc, avg, trend = calculate_concentrations(iscd40, 1, 4)
    inconcin.append(min_conc)
    finconcin.append(max_conc)
    aveconcin.append(avg)
    trendsin.append(trend)

    return inconcin, finconcin, aveconcin, trendsin

# Process Outlet Data
def process_outlet_data(sgp30, scd40):
    inconc, finconc, aveconc, trends = [], [], [], []

    for i in range(1, 5):
        min_conc, max_conc, avg, trend = calculate_concentrations(sgp30, i, 5)
        inconc.append(min_conc)
        finconc.append(max_conc)
        aveconc.append(avg)
        trends.append(trend)

    min_conc, max_conc, avg, trend = calculate_concentrations(scd40, 1, 4)
    inconc.append(min_conc)
    finconc.append(max_conc)
    aveconc.append(avg)
    trends.append(trend)

    return inconc, finconc, aveconc, trends

# Create Data Tables
def create_data_tables(inconcin, finconcin, aveconcin, inconc, finconc, aveconc):
    chem_list = ['TVOC', 'eCO2', 'CO2', 'H2', 'Ethanol']
    dict_inlet = {'Min Concentration': inconcin, 'Max Concentration': finconcin, 'Average Concentration': aveconcin}
    dict_outlet = {'Min Concentration': inconc, 'Max Concentration': finconc, 'Average Concentration': aveconc}

    inlet = pd.DataFrame(dict_inlet)
    inlet.index = chem_list
    inlet = inlet.round(2)

    outlet = pd.DataFrame(dict_outlet)
    outlet.index = chem_list
    outlet = outlet.round(2)
```



```
return inlet, outlet

# Main function to execute the process
def main(file_path):
    sgp30, scd40, isgp30, iscd40 = import_data(file_path)
    sgp30, scd40, isgp30, iscd40 = process_time_data(sgp30, scd40, isgp30, iscd40)

    inconcin, finconcin, aveconcin, trendsin = process_inlet_data(isgp30, iscd40)
    inconc, finconc, aveconc, trends = process_outlet_data(sgp30, scd40)

    inlet, outlet = create_data_tables(inconcin, finconcin, aveconcin, inconc, finconc,
                                         aveconc)
    print("Inlet Data:")
    print(inlet)
    print("\nOutlet Data:")
    print(outlet)

    return sgp30 # Return sgp30 for further processing

# Execute the main function with the file path
file_path = 'Data/FilterTest_5_26_2024.xlsx'
sgp30 = main(file_path)
# Ensure these variables are defined from your previous function outputs
sgp30, scd40, isgp30, iscd40 = import_data(file_path)
sgp30, scd40, isgp30, iscd40 = process_time_data(sgp30, scd40, isgp30, iscd40)

# Process inlet and outlet data to get trends
inconcin, finconcin, aveconcin, trendsin = process_inlet_data(isgp30, iscd40)
inconc, finconc, aveconc, trends = process_outlet_data(sgp30, scd40)

# TVOC Concentration vs Time for sgp30 and isgp30
plt.figure()
plt.plot(sgp30.iloc[:, 5], sgp30.iloc[:, 1], linewidth=2, label='Outlet TVOC')
# plt.plot(sgp30.iloc[:, 5], trends[0](sgp30.iloc[:, 5]), label='Outlet Trend Line')
plt.plot(isgp30.iloc[:, 5], isgp30.iloc[:, 1], linewidth=2, label='Inlet TVOC')
# plt.plot(isgp30.iloc[:, 5], trendsin[0](isgp30.iloc[:, 5]), linestyle='--', label='Inlet Trend Line')
plt.xlabel('Time (s)')
plt.ylabel('TVOC Concentration (ppb)')
plt.title('TVOC Concentration vs Time')
plt.legend()
plt.show()

# eCO2 Concentration vs Time for sgp30 and isgp30
plt.figure()
plt.plot(sgp30.iloc[:, 5], sgp30.iloc[:, 2], linewidth=2, label='Outlet eCO2')
# plt.plot(sgp30.iloc[:, 5], trends[1](sgp30.iloc[:, 5]), label='Outlet Trend Line')
plt.plot(isgp30.iloc[:, 5], isgp30.iloc[:, 2], linewidth=2, label='Inlet eCO2')
# plt.plot(isgp30.iloc[:, 5], trendsin[1](isgp30.iloc[:, 5]), linestyle='--', label='Inlet Trend Line')
plt.xlabel('Time (s)')
plt.ylabel('eCO2 Concentration (ppm)')
plt.title('eCO2 Concentration vs Time')
plt.legend()
```



```
plt.show()

# CO2 Concentration vs Time for scd40 and iscd40
plt.figure()
plt.plot(scd40.iloc[:, 4], scd40.iloc[:, 1], linewidth=2, label='Outlet CO2')
# plt.plot(scd40.iloc[:, 4], trends[4](scd40.iloc[:, 4]), label='Outlet Trend Line')
plt.plot(iscd40.iloc[:, 4], iscd40.iloc[:, 1], linewidth=2, label='Inlet CO2')
# plt.plot(iscd40.iloc[:, 4], trendsin[4](iscd40.iloc[:, 4]), linestyle='--', label='Inlet Trend Line')
plt.xlabel('Time (s)')
plt.ylabel('CO2 Concentration ()')
plt.title('CO2 Concentration vs Time')
plt.legend()
plt.show()

# H2 Concentration vs Time for sgp30 and isgp30
plt.figure()
plt.plot(sgp30.iloc[:, 5], sgp30.iloc[:, 3], linewidth=2, label='Outlet H2')
# plt.plot(sgp30.iloc[:, 5], trends[2](sgp30.iloc[:, 5]), label='Outlet Trend Line')
plt.plot(isgp30.iloc[:, 5], isgp30.iloc[:, 3], linewidth=2, label='Inlet H2')
# plt.plot(isgp30.iloc[:, 5], trendsin[2](isgp30.iloc[:, 5]), linestyle='--', label='Inlet Trend Line')
plt.xlabel('Time (s)')
plt.ylabel('H2 Concentration (ppm)')
plt.title('H2 Concentration vs Time')
plt.legend()
plt.show()

# Ethanol Concentration vs Time for sgp30 and isgp30
plt.figure()
plt.plot(sgp30.iloc[:, 5], sgp30.iloc[:, 4], linewidth=2, label='Outlet Ethanol')
# plt.plot(sgp30.iloc[:, 5], trends[3](sgp30.iloc[:, 5]), label='Outlet Trend Line')
plt.plot(isgp30.iloc[:, 5], isgp30.iloc[:, 4], linewidth=2, label='Inlet Ethanol')
# plt.plot(isgp30.iloc[:, 5], trendsin[3](isgp30.iloc[:, 5]), linestyle='--', label='Inlet Trend Line')
plt.xlabel('Time (s)')
plt.ylabel('Ethanol Concentration ()')
plt.title('Ethanol Concentration vs Time')
plt.legend()
plt.show()

# eCO2 and CO2 Concentration vs Time on the same plot for sgp30, scd40, isgp30, and i
scd40
plt.figure()
plt.plot(sgp30.iloc[:, 5], sgp30.iloc[:, 2], linewidth=2, label='Outlet eCO2 (sgp30)')
plt.plot(scd40.iloc[:, 4], scd40.iloc[:, 1], linewidth=2, label='Outlet CO2 (scd40)')
plt.plot(isgp30.iloc[:, 5], isgp30.iloc[:, 2], linewidth=2, linestyle='--', label='In
let eCO2 (sgp30)')
plt.plot(iscd40.iloc[:, 4], iscd40.iloc[:, 1], linewidth=2, linestyle='--', label='In
let CO2 (scd40)')
plt.xlabel('Time (s)')
plt.ylabel('Concentration ()')
plt.title('eCO2 and CO2 Concentration vs Time')
```



```
plt.legend()  
plt.show()
```